SAND FILTRATION AND CHLORINATION FOR REMOVAL AND INACTIVATION OF *BACILLUS SUBTILIS*

By

Margaret Joan Hernández Vega

A thesis submitted in partial fulfillment of the requirements for the degree of

MASTER IN SCIENCE

in

CIVIL ENGINEERING

(Environmental and Water Resources Engineering)

UNIVERSITY OF PUERTO RICO

MAYAGÜEZ CAMPUS

2015

Approved by:

Sangchul Hwang, PhD President, Graduate Committee	Date
Pedro J. Tarafa, PhD Member, Graduate Committee	Date
Moses Bogere, PhD Member, Graduate Committee	Date
Lillian Ramírez, MS Graduate Studies Representative	Date
Ismael Pagán Trinidad, MSCE Chair, Department of Civil Engineering and Surveying	Date

ABSTRACT

Sustainable water treatment and technology need to be implemented for safe-drinking water. In Puerto Rico, some rural communities do not rely on the central systems operated by the water authority but have their own small treatment systems that do not fully comply with the bacteriological standards. As such, the Río Piedras community, located in San German, Puerto Rico was chosen for the assessment of a sand filtration and chlorination system for the removal of *Bacillus subtilis* as the surrogate microorganisms of *Giardia lamblia* and *Cryptosporidium parvuum*.

The Caín Alto River, the source water of the Río Piedras community water treatment system, was monitored for its physicochemical and bacteriological characteristics for over one year. The results from the statistical analyses showed that conductivity and total dissolved solids were highly positively related (Pearson correlation coefficient = 0.953 and P-value = 0.000) and that *B. subtilis* was highly positively related to turbidity (Pearson correlation coefficient = 0.720 and P-value = 0.001).

Three different lab-scale rapid filtration units were evaluated for the possible packing media of the field-scale filters. Units included two sand filters connected in series, one filter with granular activated carbon incorporating sand and one filter with iron oxide coated sand (IOCS) incorporating sand. Outcomes of the comparison between systems yielded that IOCS filter showed more consistency in the removal of *B. subtilis*, achieving 1.1-log removal. However, IOCS preparation at large scale was neither practical nor economical.

The results from the lab-scale system showed that the sand filtration inactivated 1.5-log removal of *B. subtilis* and disinfection as well. The treatment train achieved 3-log removal of *B.*

subtilis, complying with the USEPA standards of *Cryptosporidium* and *Giardia*. However, further modifications were to be done on the field scale to improve the effectiveness of the system.

The field-scale SEED unit was assessed for *B. subtilis* removal for three days at different configurations. The results showed that the SEED unit under the current hydromechanical and technical properties was not capable of removing *B. subtilis*. Some circumstances could have affected the efficiency of the unit including the initial condition of the system and the actual condition of the community system that made impossible to perform a backwash.

RESUMEN

Tratamiento de agua y tecnología sustentable necesitan ser implementadas para tener agua potable. En Puerto Rico, algunas comunidades rurales no confían en los sistemas centrales operados por la autoridad de agua pero, tienen sus propios pequeños sistemas de tratamiento los cuales no cumplen completamente con los estándares bacteriológicos. Como tal, la comunidad Río Piedras, localizada en San German, Puerto Rico fue escogida para la evaluación de un sistema de filtración de arena y cloración para la remoción de *Bacillus subtilis* como microorganismo sustituto de *Giardia lamblia* y *Cryptosporidium parvuum.*

La fuente de agua del sistema de tratamiento de agua de la comunidad Río Piedras, el Río Caín Alto, fue monitoreada para las características fisicoquímicas y bacteriológicas por más de un año. Los resultados de los análisis estadísticos mostraron que la conductividad y los sólidos disueltos totales fueron alta y positivamente relacionados (coeficiente de correlación Pearson = 0.953 y valor P = 0.000) y que *B. subtilis* fue alta y positivamente relacionado a la turbidez (coeficiente de correlación Pearson = 0.720 y valor P = 0.001).

Tres diferentes unidades de filtración rápida a escala de laboratorio fueron evaluadas para los posibles medios de empaque a utilizar en los filtros a escala de campo. Las unidades incluyeron dos filtros de arena conectados en serie, un filtro con carbón activado granular incorporando arena y un filtro con arena recubierta de óxido de hierro (IOCS por sus siglas en inglés) incorporando arena. Los resultados de la comparación entre sistemas produjeron que el filtro de IOCS mostrara más consistencia en la remoción de *B. subtilis*, logrando una remoción de 1.1-log. Sin embargo, la preparación de IOCS en gran escala no era ni práctico ni económico.

Los resultados del sistema a escala de laboratorio mostraron que la filtración de arena inactivó 1.5-log de remoción de *B. subtilis*, así como la desinfección. El tren de tratamiento logró la remoción de 3-log de *B. subtilis*, cumpliendo con los estándares de la USEPA de *Cryptosporidium* y *Giardia*. Sin embargo, otras modificaciones debían ser realizadas a escala de campo para mejorar la eficiencia del sistema.

La unidad SEED a tamaño de campo fue evaluada durante tres días en diferentes configuraciones para la remoción de *B. subtilis*. Los resultados mostraron que la unidad SEED bajo las propiedades hidromecánicas y técnicas actuales, no fue capaz de remover *B. subtilis*. Algunas circunstancias pudieron haber afectado la eficiencia del sistema incluyendo la condición inicial del sistema y la condición actual del sistema de la comunidad que imposibilitó realizar un lavado contracorriente.

To my dearest family and friends,

"The Lord will fulfill his purpose for me…"

ACKNOWLEDGEMENTS

I would like to extent my appreciation to certain individuals and institutions that played an essential role for the completion of this thesis.

Firstly, I am extremely grateful to my Lord who allowed me, gave me the strength and guidance to achieve this goal.

I would like to expressly thank my advisor, Dr. Sangchul Hwang, for the great opportunities, time, support and advice he has given to me through this degree.

I would also like to thank my committee members and department director, Dr. Moses Bogere, Dr. Pedro Tarafa, and Prof. Ismael Pagán for their time to review my thesis, providing valuable comments and advices.

A special thanks to Norberto Mercado, José Illas, Priscilla Pérez, Tamara Miranda and Karina Rivera. Without their efforts and help this work would not have been possible.

Sincere appreciation extends to the financial support of the United States Geological Survey 104B Program through the Puerto Rico Water Resources and Environmental Research Institute.

I would also like to acknowledge the Rio Piedras community, especially to Esteban, for allowing me to use their system and land for the completion of this work.

My sincere gratitude to my labmates: Isomar Latorre, Keila Pagán, Joann Rodríguez, Linoshka Soto, Norma Torres and Natalia Vázquez for every help during the research, support and friendship. In addition, I extend my thanks to my colleagues of the Environmental Laboratory at the Civil Engineering Department.

Last but not least, I would like to express my sincere gratitude towards my family, especially my parents Francisco Hernández and Elizabeth Vega and sisters Elibeth, Lilliana and Frances, for their encouragement and support.

TABLE OF CONTENTS

LIST OF TABLES

LIST OF FIGURES

LIST OF EQUATIONS

LIST OF ABBREVIATIONS

ATCC = American Type Culture Collection

BFM = Bright Field Microscopy

CSTR = Continuous Flow Reactor

CT = Residual Free Chlorine Concentration x Contact Time

DBP = Disinfection By Products

DI = Deionized

DO = Dissolved Oxygen

F_{sc} = Short-circuiting Factor

GAC = Granulated Activated Carbon

HRT = Hydraulic Retention Time

IOCS = Iron Oxide Coated Sand

MCL = Maximum Contaminant Level

MF = Membrane filtration

MRDL = Maximum Residual Disinfection Level

NTU = Nephelometric Turbidity Unit

OD = Optical Density

PFR = Plug Flow Reactor

PRASA = Puerto Rico Aqueduct and Sewer Authority

SEED = Solar-powered Engineered Experimental Drum

SEM = Scanning Electron Microscopy

SOP = Standard Operating Procedure

SWTR = Surface Water Treatment Rule

TC = Total Coliform

TDS = Total Dissolved Solids

TOC = Total Organic Carbon

USEPA = United States Environmental Protection Agency

USGS = United States Geological Survey

WHO = World Health Organization

XRD = X-ray Diffraction

1. INTRODUCTION

In 2008, 2.5 billions of deaths caused by diarrheal diseases were reported by the World Health Organization (WHO). Among them, the most affected were children. For this reason, the goal of the integrated Global Action Plan for Pneumonia and Diarrhea is to end preventable childhood deaths due to pneumonia and diarrhea by 2025 (WHO/UNICEF, 2013). Some of the causes of the diarrheal disease are the lacking access of safe drinking water, poor sanitation and hygiene (WHO/UNICEF, 2013). Most of the cases, poor water quality is due to contamination of the water resources with human and animal feces which can lead to the growth of microorganisms causing diarrhea.

This scenario is typical of underdeveloped countries. However, some of the rural communities in Puerto Rico do not have access to safe drinking water, which increases their risk in suffering from water-borne diseases. There are approximately 240 systems not served by the Puerto Rico Aqueduct and Sewer Authority, named Non-PRASA. 95% of Non-PRASA systems do not meet the bacteriological standards (Concepción et al., 2010; Herrera, 2009), as reflected in the 93 cases of giardiasis reported by the Centers of Disease Control and Prevention in 2010.

Biological contaminants that are known to be responsible for water-borne diseases include *Giardia lamblia* and *Cryptosporidium parvum.* Both *Giardia* and *Cryptosporidium*, due to their abundance in surface waters and ability to infect humans, represent a major threat for drinking water purposes (Mazoua and Chauveheid, 2005). However, treatment studies for their removal and inactivation are limited since their enumeration techniques are costly and time consuming (Dow et al., 2006). For these reasons, the use of surrogates has been frequently used instead.

Bacillus subtilis has been found to be an effective surrogate of *Giardia lamblia* in drinking water (Facile et al., 2000). Studies for the inactivation of *B. subtilis* by several disinfectants have been performed (Cho et al., 2011 & 2006; Dow et al., 2006; Facile et al., 2000).

1.1 SCOPE AND OBJECTIVES

Several drinking water treatment technologies have been established and implemented in developed countries. Nevertheless, rural communities still do not rely on them and have their own water treatment systems. Rural drinking water supply systems usually have insufficient quantity and poor water quality and hence do not comply with the standards. For these reasons, there is an urge to develop an appropriate technology that can be implemented to rural communities for their water sustainability.

1.1.1 Scope

The goal of this research was to acquire optimum operating parameters for *B. subtilis* removal in the lab-scale and field-scale filtration and disinfection system. The lab-scale system is a scale-down simulation of the field-scale solar-powered engineered experimental drum filtration and disinfection (SEED) unit.

1.1.2 Objectives

The following experiments were conducted to achieve the aforementioned goal:

- Monitor physicochemical and bacteriological parameters of the Caín Alto river water;
- Construct scaled-down lab-scale filtration and disinfection systems;

- Evaluate the removal and inactivation of *B. subtilis* as a surrogate of *G. lamblia* and *Cryptosporidium* in the lab-scale system;
- Apply the optimum operating parameters acquired from the lab-scale systems to the field-scale SEED unit; and
- Provide recommendations for more effective operation of the SEED unit for microbial control.

2. LITERATURE REVIEW

2.1 NON-PRASA SYSTEMS IN PUERTO RICO

Appropriate and sustainable water treatment systems are essential to provide safe drinking water. However, underdeveloped countries and rural communities do not have suitable technologies and hence, fail in providing to their residents good quality water.

In Puerto Rico, the Puerto Rico Aqueduct and Sewer Authority do not serve over 250 communities, or 4% of the residents. Locations of these communities are presented in Figure 1. Moreover, 95% of these communities do not comply with the bacteriological standards of the US Environmental Protection Agency (USEPA) (Herrera, 2009).

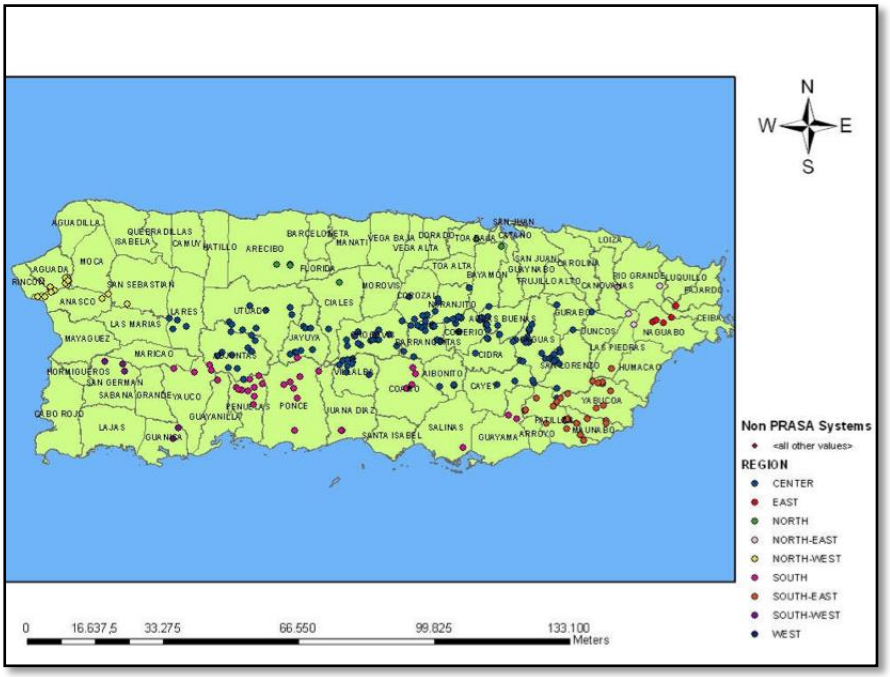

Figure 1 Non PRASA systems in Puerto Rico

Approximately, 40% of Non-PRASA communities have their own water treatment system. An example is the Río Piedras community, located in the municipality of San German, which serves to ~60 families and has its own slow sand filtration and tablet chlorinator (Figure 2).

Figure 2 Río Piedras community location in San German, Puerto Rico.

2.2 RIVER WATER

River water has typically been a source for drinking water, representing approximately 40 % of the sources for Non-PRASA systems (Herrera, 2009). However, an increase of industrial, urban and agricultural activities has affected the quality of these surface waters. Another concern that affects the water quality is the possible biological attack to drinking water. Previous outbreaks of waterborne disease have demonstrated the vulnerability of both the water supply and the public health to contamination of drinking water by jeopardizing the confidence and possibly the economy of communities due to biological threats (Nuzzo, 2006). One of these possible microbial pathogens is *Bacillus anthracis*, a species responsible for causing Anthrax. These two microorganisms, *Bacillus anthracis* and *B. subtilis*, belong to the same genus making them genetically closely related organisms (Waller et al., 2004).

2.3 *BACILLUS SUBTILIS*

Bacillus subtilis is a Gram positive, nonpathogenic and aerobic spore-forming bacteria. *B. subtilis* grows in moderate temperatures and is present in most surface water supplies (Rice et al., 1996). Even though sporulation of aerobic bacteria is correlated to protozoan oocyst due to their ability to survive in harsh environments, yet only serves as an indirect indicator of fecal coliforms and cysts (Facile et al., 2000; Barbeau et al., 1999). *Bacillus* spores' surface properties, i.e. outer layers, allow them to adhere to porous media, biological and non-biological, thus making them highly resistant to killing (Chen et al., 2010). For these reasons, *B. subtilis* serves as a surrogate organism for *B. anthracis*, *Cryptosporidium* oocysts, *Giardia* cysts and enteric viruses (Upadhyayula et al., 2009; Muhammad et al., 2008; Larson and Mariñas, 2003; Nieminski et al, 2000; Rice et al., 1996; Toenniessen and Johnson, 1970). Consequently, as a result of being ubiquitous, it is feasible to achieve a 3-4 log removal by conventional treatment, complying with the 3 log removal of *Giardia* and 2 log removal of *Cryptosporidium*, specified by the Surface Water Treatment Rule (SWTR) (Facile et al., 2000; USEPA, 1989).

2.4 FILTRATION

Typically, filters are stratified with different types and sizes of sand. Several types of filters have been developed with sand as media (Swertfeger et al., 1999). Slow sand filtration has been widely accepted since its development during the 20^{th} century due to its simplicity in operation and cost-effectiveness in microorganism removal in drinking water (Aslan and Cakici, 2007). Although advantageous, slow sand filtration can develop pathogen outbreaks due to clogging when dealing with high-turbidity raw waters (Cleary, 2005). In contrast, rapid sand filtration uses

periodic backwashing to inextricably link the filtration process, dislodging the filter and enhancing its operation (Han et al., 2009).

Even though sand filtration has been effective, different media have been developed in order to comply with the enhanced water quality standards. Granulated activated carbon (GAC) is, for instance, one of the most used packing materials in drinking water treatment since it has properties that effectively remove natural organic matter, micropollutants and microorganisms (Hijnen et al., 2010). Although effluent of filters may be in fulfillment in terms of bacteriological standards, turbidity has to be monitored to comply with the standards of maximum of 5 Nephelometric Turbidity Unit (NTU) at any time and no greater than 1 NTU in at least 95% of the daily samples in any months (USEPA, 2009).

2.5 IRON OXIDE

Several studies have been performed with nanoscale zero-valent iron particle (Shi et al., 2012; Diao et al., 2009) and iron oxide coated sand (Pecson et al., 2012; Bradley et al., 2011) in inactivating viruses, microbes and bacteriophages. However, the use of iron oxide coated sand (IOCS) for the inactivation of *B. subtilis* has not been studied.

IOCS combines physicochemical process with advanced oxidation process, specifically Fenton process. Fenton process can be classified as homogenous, heterogeneous and photo Fenton. In Fenton process the strong oxidants, in particular hydroxyl radicals ($HO\bullet$), are generated from H_2O_2 and dissolved Fe(II) ions.

$$Fe^{3+} + H_2O_2 \longrightarrow Fe^{2+} + HO_2\bullet + H^+$$

$$Fe^{2+} + H_2O_2 \longrightarrow Fe^{3+} + HO^- + HO\bullet$$

At neutral pH under typical water treatment conditions, Fe(II) and Fe(III) exhibit low solubility and stability, limiting the Fenton process. Alternatively, heterogeneous Fenton-like process is effective for water treatment purposes because of its iron (hydr-) oxide particles as the reactive iron source (Nieto, 2012). However, exact mechanism of reaction is still not known.

2.6 DISINFECTION

The majority of the cases, filtration process by itself does not remove the amount of bacteria necessary to comply with the standards. Therefore, disinfection processes are commonly implemented to enhance microbial water quality. Disinfection processes can be divided by their type of disinfectant or by the technique implemented. The most frequently used disinfection processes are: chlorination, ozonation, chloride dioxide, UV irradiation and high pH treatment. In the United States, water disinfection is accomplished mostly by chlorination. Chlorine is the most widely used disinfectant because it is effective at low concentration, is cheap, and forms a residual if applied in sufficient dosage. Chlorine dosage depends on the water quality, but for many drinking water supplies it ranges from 4 to 10 mg/L (Reynolds and Richards, 1996).

Chlorine in water reacts as follows (Reynolds and Richards, 1996):

$$Cl_2 + H_2O \rightarrow HOCl + HCl$$

In dilute solution and at pH greater than 3, the reaction is appreciably displaced to the right. The hypochlorous acid (HOCl) produced then dissociates to yield hypochlorite ion (OCl^-).

$$HOCl \leftrightarrow H^+ + OCl^-$$

Chlorine inactivates all types of microorganisms: protozoa, bacteria and viruses. For example, Jarroll et al. (1981) studied the effect of chlorine on *G. lamblia.* The outcomes of the study are presented in Table 1.

Table 1 Effect of chlorination on inactivating *Giardia lamblia*.

Pathogen	Residual Chlorine Concentration (C, mg/L)	Contact Time (T, min)	Residual Chlorine Concentration x Contact Time (CT, mg-min/L)	% Inactivation	Temp. (°C)	pH
Giardia lamblia	1.5	10	15	99.9	25.0	7.0

The highest matter of concern in disinfection is the possible formation of disinfection by products (DBPs) including trihalomethanes, haloacetic acids, haloacetonitriles and chloral hydrates, which are potential carcinogens, teratogens and mutagens (Hamidin, 2008; Richardson, 2007; Krasner, 2006). The Stage 2 Disinfectants and Disinfection Byproduct Rule of USEPA regulates the DBPs concentration to improve the drinking water quality and provide public health protection.

2.6.1 Models

Inactivation and removal of *Giardia, Cryptosporidium* and aerobic spore-forming bacteria, including *B. subtilis,* by disinfection can be assessed using the modified Chick-Watson, unmodified Chick-Watson, modified Hom and unmodified Hom models (Cho et al., 2011, 2006; Dow et al., 2006; Larson and Mariñas, 2003; Facile et al., 2000; Barbeau et al., 1999; Rennecker et al, 1999).

The Hom model is (Barbeau et al., 1999),

$$\frac{dN}{dt} = -k \cdot m \cdot C^n \cdot t^{m-1} \cdot N$$

Eq. 1 Hom Model

where, C is the disinfectant concentration, N is the concentration of microorganisms, N_0 is the initial concentration, and k, n, m are empirical constants.

By rearranging, deriving and linearizing **Eq. 1**, the Hom equation is converted to

$$\ln\left(-\ln\left(\frac{N}{N_0}\right)\right) = \ln k' + n \ln C + m \ln t$$

Eq. 2 Natural log base Hom Model

3. MATERIALS AND METHODOLOGY

3.1 MATERIALS

3.1.1 River Water

River water was collected from the inlet to the gravel prefilter receiving the Caín Alto River water, located in Río Piedras Community in San German, Puerto Rico (Figure 3). The collected water was then analyzed for physiochemical and biological water quality parameters and utilized for the lab-scale experiments within a 24-h after sampling.

Figure 3 Caín Alto River and sampling location.

3.1.2 *Bacillus subtilis*

3.1.2.1 Enrichment culture

Bacillus subtilis ATCC 6633 was purchased from the American Type Culture Collection (ATCC). The growth medium, the ATCC Media #3 broth: Nutrient Broth (234000), was prepared according to the specification of the Nutrient composition. Materials for the cultivation of the bacteria were: 250 mL Erlenmeyer flasks, venting closures, 1 mL sterilized pipettes, 100 mL graduated cylinders, magnetic bars and stirrer.

3.1.2.2 Spore stain

Schaeffer and Fulton spore stain kit was purchased from Sigma-Aldrich. One Pasteur pipette was used for each stain, malachite green (Schaeffer & Fulton's Spore Stain A), and safranin (Schaeffer & Fulton's Spore Stain B). One microscope slide for each sample, a hot plate, beaker, glass beads and a timer were necessary to perform the stain. The Olympus Toupview Opticam bright field microscopy was used.

3.1.3 Lab-scale Sand Filtration

Three different systems were constructed. Each system consisted of either one or two filters. Each filter was constructed using 3 in. x 6 in. acrylic pipes connected to a NIBCO 4 in x 3 in PVC DWV Closet Flange at the top and bottom. The bottom flange of the filter was jointed with a 4 ¾ in x 4 ¾ in acrylic tap and the top with a 6 in x 6 in acrylic tap. Inside of the filter, a ¼ in tube was connected to a tee, dividing the inflow and increasing the contact with the packing material. All parts were attached with silicone. Figure 4 shows the assembled filter.

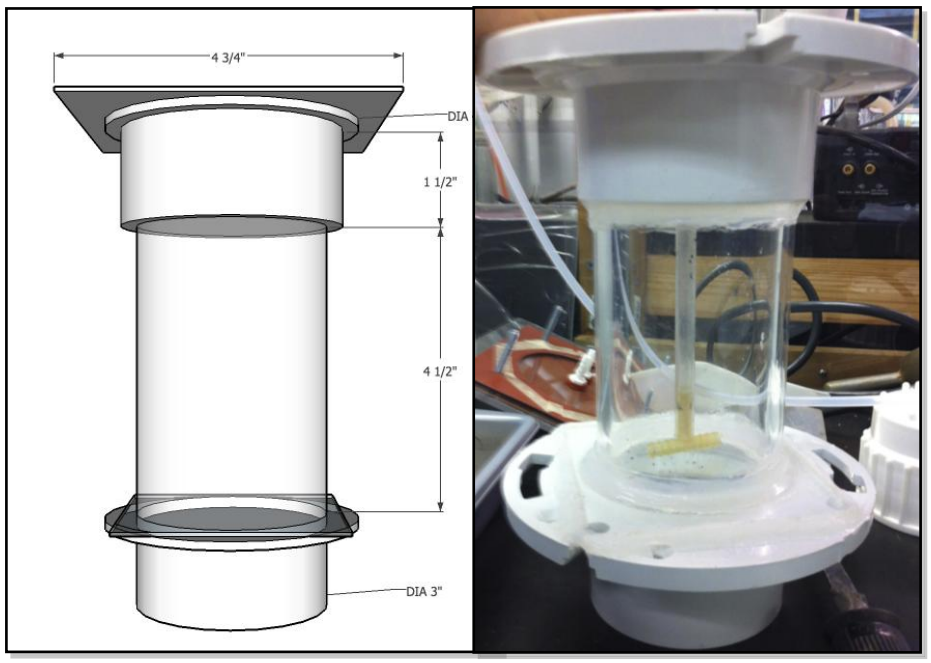

Figure 4 Filter dimensions and picture.

The System 1 consisted of two sand filters connected in series. The specifications and compositions of the packing materials of these filters are shown in Table 2. Sand was purchased from Standard Sand and Silica Corporation.

Table 2 Packing materials used for System 1.

Media	Size	Total Weight (g)
Sand	Global No. SS 30/65, Effective size=0.18mm	230.2
Sand	Global No. SS 20/30, Effective size=0.55mm	460.4
Sand	Global No. SS 6/20, Effective size=1.10mm	230.2

The System 2 consisted of one sand filter incorporating GAC. The specifications and composition of the system are presented in Table 3. Granulated activated carbon was purchased from Calgon Carbon Corporation.

Table 3 Packing materials used for System 2.

Media	Size	Total Weight (g)
GAC	Bituminous, URV, 8 × 30 mesh	230.2
Sand	Global No. SS 20/30, Effective size=0.55mm	460.4
Sand	Global No. SS 6/20, Effective size=1.10mm	230.2

The System 3 consisted of one sand filter incorporating iron-oxide coated sand. The specifications and composition of the system are presented in Table 4.

Table 4 Packing materials to be used for System 3.

Media	Size	Total Weight (g)
Iron oxide/ sand	Global No. SS 30/65, Effective size = 0.18mm, iron oxide coating	230.2
Sand	Global No. SS 20/30, Effective size=0.55mm	460.4
Sand	Global No. SS 6/20, Effective size=1.10mm	230.2

The IOCS was prepared with a ferric chloride solution ($FeCl_3$). In addition to the $FeCl_3$ solution, 10% HNO_3 solution, 5M NaOH solution, beakers, evaporation pan and dry oven were necessary for the process. The IOCS was prepared using the same methodology of Liu et al. (2001). Prior to the coating, the sand was submitted to an acid wash procedure.

Approximately 700 g of sand were washed with 1400 mL of 10% HNO_3 (2mL HNO_3/g sand) for 24 hours. After the 24 hours had been passed, the sand was rinsed with deionized (DI) water until pH 7. After rinse, sand was dried at 105°C for 24 hours and stored in bottles. The bottles used were previously washed with 10% HNO_3 for 24 hours and rinsed with DI water until pH 7.

Acid-washed sand was mixed with the ferric chloride solution (Figure 5) and then dried at 90˚C for 48 hours. The sand was then poured in a glass beaker containing the 5M NaOH solution

and left for 24 hours to assure the completion of neutralization. After neutralization, sand was dried at 90˚C for 24 hours, and then rinsed with DI water until pH 7. After rinse, the sand was dried at room temperature and stored in the previously acid-washed bottles.

Figure 5 IOCS preparation.

IOCS was analyzed for its mineralogical characteristics by X-ray diffraction spectroscopy (XRD) and observed under a scanning electron spectroscopy (SEM). Figure 6 and Figure 7 show the results of XRD analysis whereas Figure 8 and Figure 9 show the SEM images.

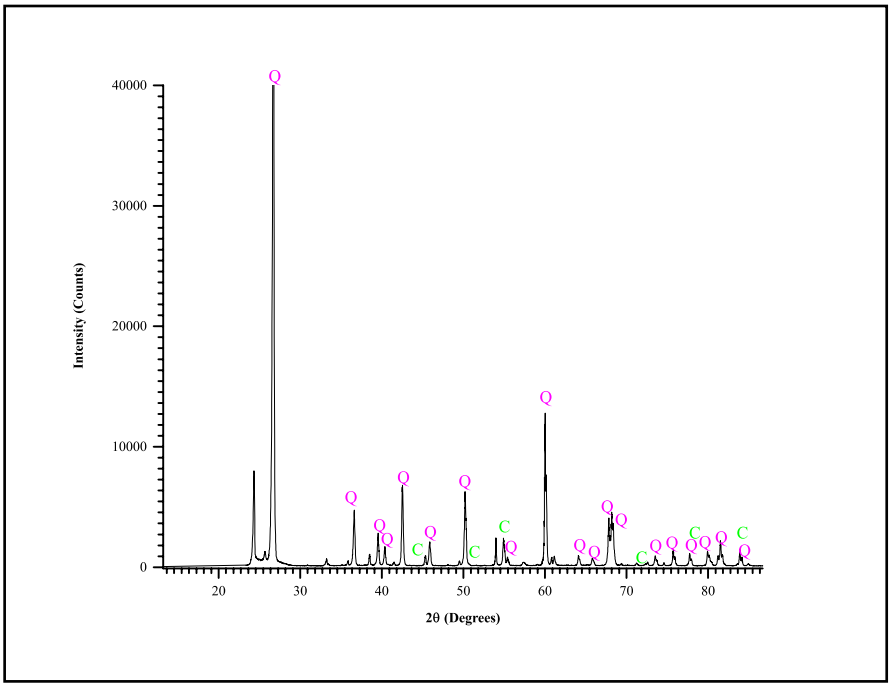

Figure 6 XRD spectra of silica sand*.

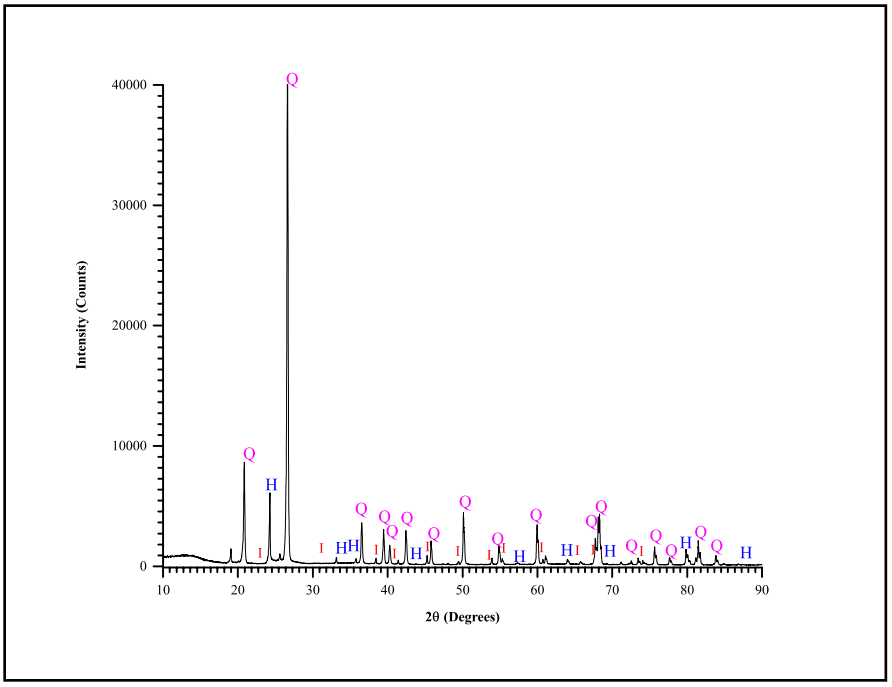

Figure 7 XRD spectra of IOCS†.

* Q stands for quartz and C for graphite.

† Q stands for quartz, I for iron oxide (Fe_2O_3) and H for hematite (Fe_2O_3).

‡ QUANTIFICATION of Protection Agency (2008) Procedure for enumeration of *Bacillus*

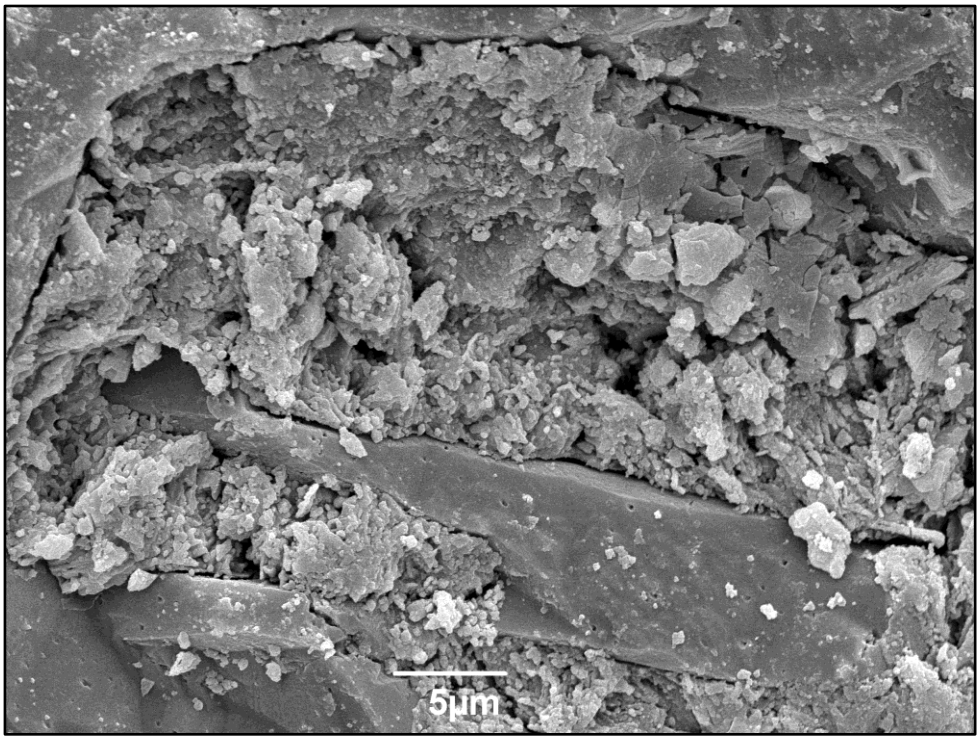

Figure 8 SEM image of silica sand.

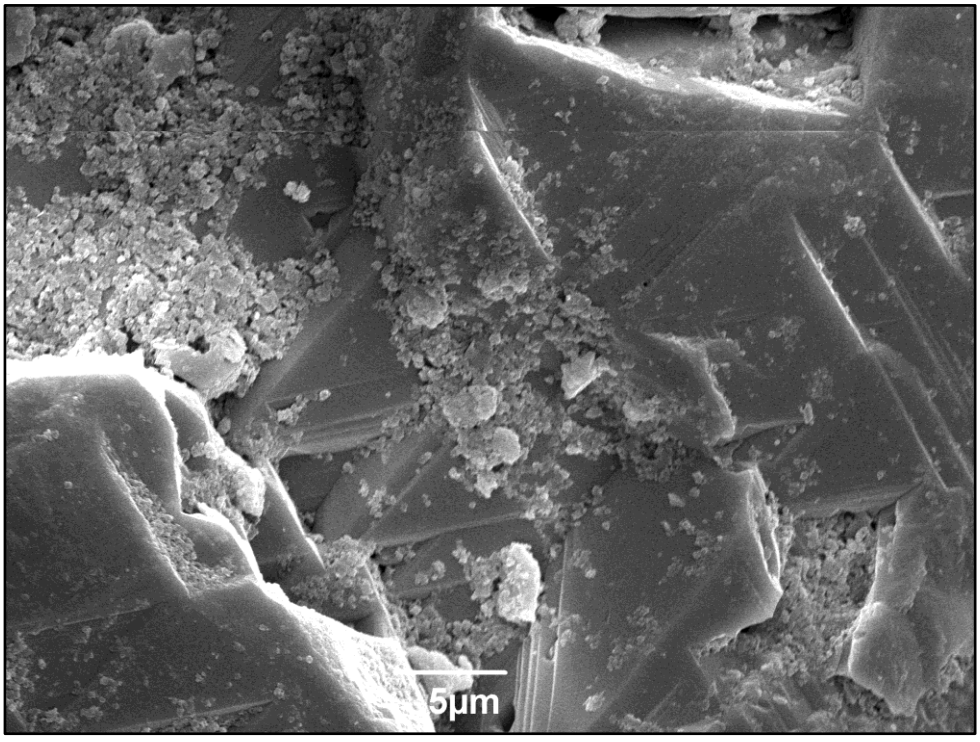

Figure 9 SEM image of IOCS.

3.1.4 Lab-scale Disinfection

An 11” x 6” acrylic disinfection basin was constructed using silicone to bond the walls. The basin contained one baffle to increase the contact time of the disinfectant with the water to be treated and one triangular section at the end that provided a Venturi effect. The total volume of the basin just before the water started flowing through the Venturi section was 3.674 L. Schematics of the basin with their dimensions are presented in Figure 10.

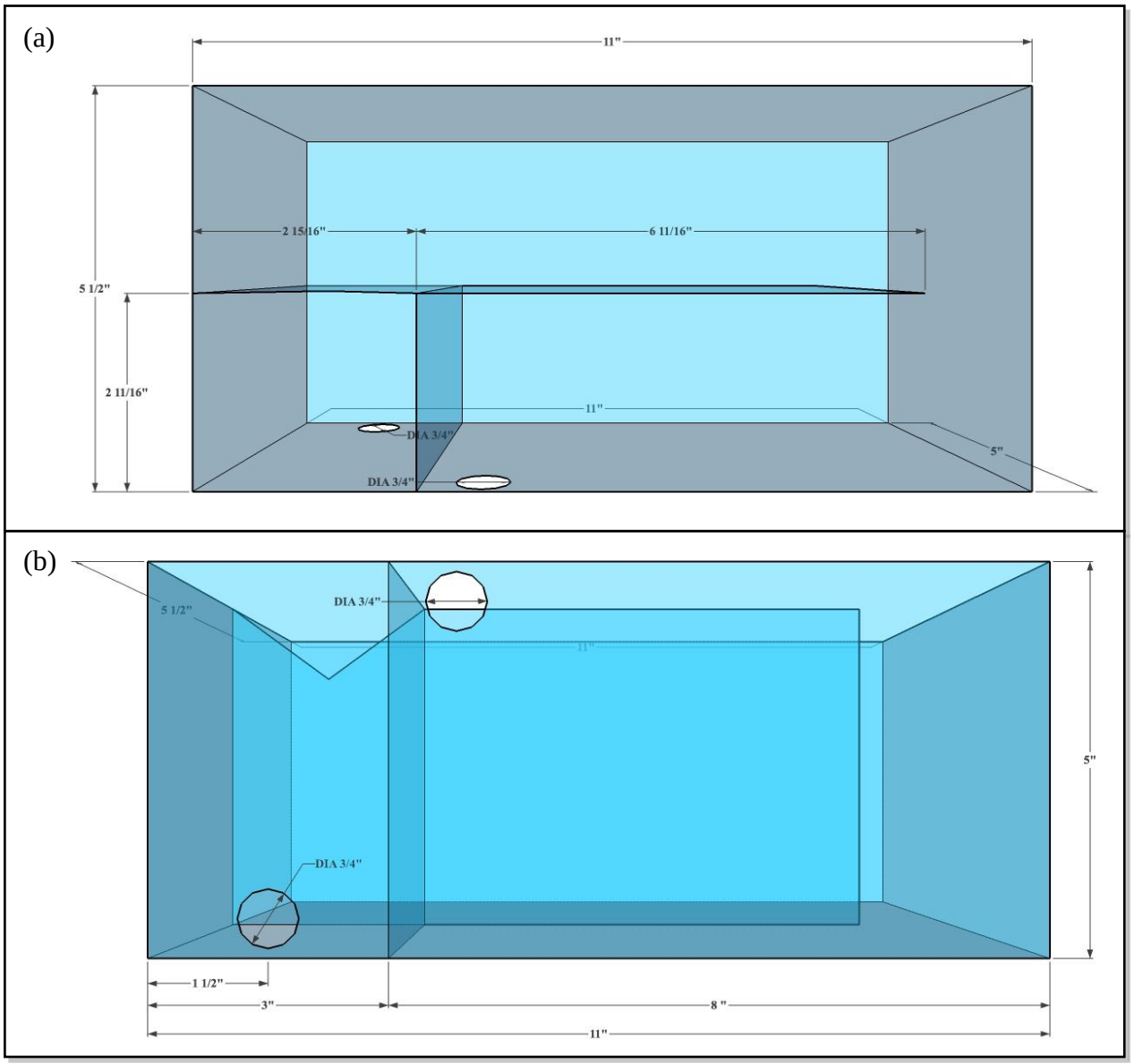

Figure 10 Disinfection basin dimensions (a) top view and (b) front view.

3.1.5 Field-scale Sand Filtration

Three 55-gallon polyethylene open head drums were connected. The drums had three different sand sizes and quantity. The composition and specification of the sand are shown in Table 5. The sand used was also purchased from Standard Sand and Silica Corporation.

Table 5 Packing materials to be used for SEED unit.

Media	Size	Total Weight (g)
Sand	Global No. SS 30/65, Effective size=0.18mm	67.8
Sand	Global No. SS 20/30, Effective size=0.55mm	135.6
Sand	Global No. SS 6/20, Effective size=1.10mm	67.8

3.1.6 Field-scale Disinfection

A tablet chlorinator, Exceltec EIC Tablet Feeder Model 200, was connected to the effluent from the filters. Aqua Chem 3-inch Chlorine Tablets were used as the disinfectant with PVC rings as the spacers. Whirl-Paks of 100 mL with sodium thiosulfate ($Na_2S_2O_3$) to stop the chlorination were used to take the samples.

3.2 METHODOLOGY

3.2.1 Water Quality Analysis

Water quality of the Caín Alto River was evaluated for the field and the laboratory experiments. Laboratory analysis was performed within a 24-h of sampling to determine its physicochemical and bacteriological characteristics. Table 6 presents the physicochemical parameters, equipment and methodology used for water quality assessment in the field and the laboratory.

Table 6 Physicochemical parameters evaluated in the field and the laboratory.

Location	Parameter	Model Equipment	Methodology
Field	pH	OAKTON Multi-parameter PCS Testr 35	Insert pH meter into sample
	Total dissolved solids (TDS)	OAKTON Multi-parameter PCS Testr 35	Insert TDS meter into sample
	Conductivity	OAKTON Multi-parameter PCS Testr 35	Insert conductivity meter into sample
	Temperature	OAKTON Multi-parameter PCS Testr 35	Insert temperature meter into sample
Laboratory	Turbidity	HACH 2100P TURBIDIMETER	Insert 10 mL of sample into vial
	Total organic carbon	HACH DR2800	HACH Method 10129 Low Range (0.3-20.0 mg/L C)

In terms of bacteriological characteristics, membrane filtration (MF) was performed within 24-h of sampling to quantify the presence of *Escherichia coli*, total coliforms (TC) and *B. subtilis*. The USEPA T&E Facility Technical Standard Operating Procedure (SOP) No. 301[‡] was used for the proper enumeration of *B. subtilis*. MF was also performed after the 30-min contact time of disinfection for the quantification of *B. subtilis*. The membrane used had a pore diameter of 0.45 μm and the analysis was performed under sterile conditions. Filtered membranes were incubated at 35˚C for 24-h, using m-ColiBlue24® from HACH for the total coliforms and *E. coli*, and prepared nutrient broth for *B. subtilis*. Figure 11 shows incubated membranes with

[‡] US Environmental Protection Agency (2008). Procedure for the enumeration of *Bacillus subtilis* water samples T&E SOP No. 301. Shaw Environmental & Infrastructure, Inc.

grown colonies. Quantification of bacteria was based on their color, red colonies were total coliforms, blue colonies *E. coli* and ivory were *B. subtilis*.

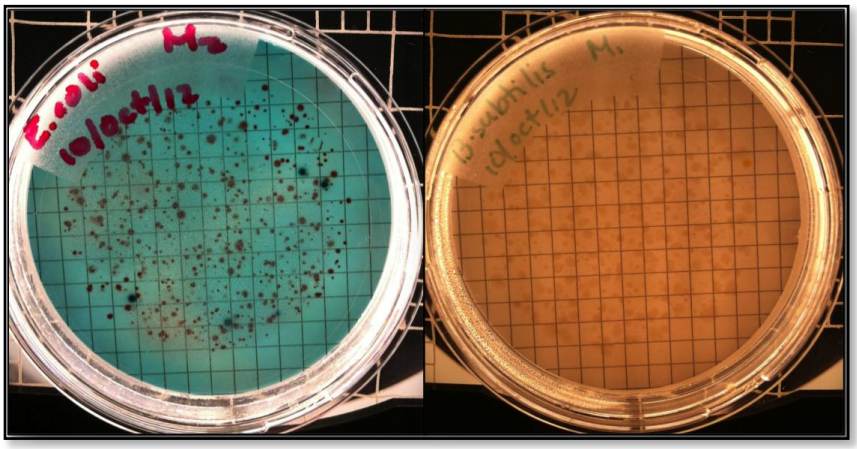

Figure 11 Incubated membranes with grown TC, *E. coli* and *B. subtilis*.

3.2.2 *B. subtilis*

3.2.2.1 Enrichment culture

The growth medium broth for *B. subtilis* reactors was prepared with 1.5 g of Beef Extract, 2.5 g of Peptone and 500 mL of DI water. The broth prepared was sterilized in the autoclave at 121 ˚C and 20 psi for 25 minutes. 100 mL of the broth were transferred to a 250 mL Erlenmeyer flask (reactor) with a magnetic bar on a stirrer. Then, 1 mL of *B. subtilis* stock solution was added to the 250 mL reactor. A total of two reactors were used for the *B. subtilis* culturing. After two weeks, 1 mL of grown *B. subtilis* in each reactor were transferred to newly prepared enrichment reactor. Figure 12 shows a schematic of the process. In addition, acclimation and growth of the *B. subtilis* was studied by performing optical density (OD) measurements every 48 hours for two weeks.

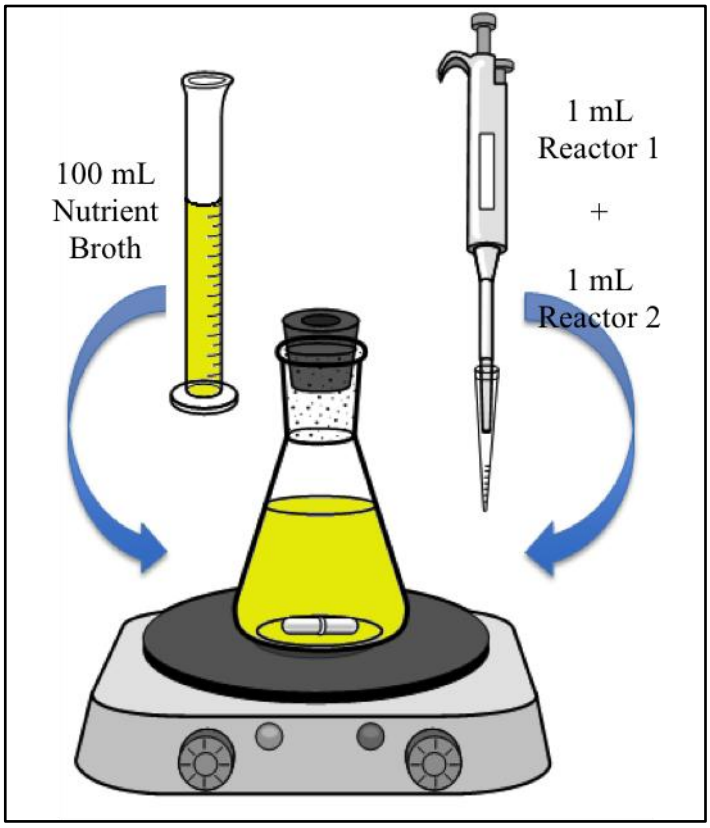

Figure 12 *B. subtilis* enrichment culture process.

3.2.2.2 Sporulation

Schaeffer Fulton technique was employed for the visualization of the sporulation of *B. subtilis*. 100 mL of the Caín Alto river water and 1 mL of cultured *B. subtilis* were added to an Erlenmeyer flask. This reactor was then submitted to a wet heat at 90 ˚C, according to the USEPA SOP No. 301. One drop of treated water was placed, let air dried and fixed to a slide. After fixation, the slide was flooded with malachite green for 5 minutes, which was receiving steam (Figure 13). Finally, rinsed slide was then flooded with safranin for 30 seconds and visualized under a Bright Field Microscopy (BFM). Water samples for stain were taken at 3, 10, 15 and 30 minutes of hot water treatment.

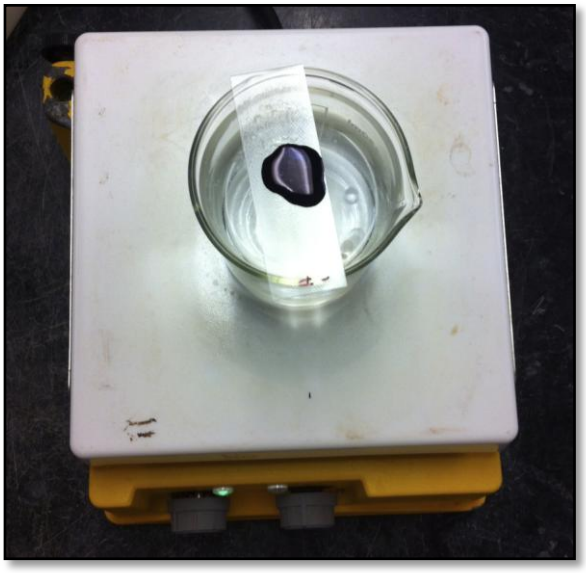

Figure 13 Schaeffer Fulton spore stain technique.

3.2.3 Laboratory-scale Systems

The laboratory-scale systems consisted of a filter, or two filters connected in series, connected to a disinfection basin. The laboratory-scale filters were scaled down by 60 times from the field SEED unit. Disinfection basin was built corresponding to the effluent flow rate of the sand filters.

3.2.3.1 Iron leaching from IOCS

Two different experiments were performed to assess the IOCS for leaching. The first experiment was performed by agitating in duplicates five different quantities of IOCS, 1, 2, 3, 4 and 5 grams, with 20 mL of DI water for 24 hours in a tumbler. After 24 hours, iron leaching from IOCS was measured at pH 8.6. The second experiment was done by agitating in duplicates 3 grams of IOCS with 20 mL of DI water in a tumbler. Samples were taken at 1, 4, 8, 20, 24, 48 and 72 hours of agitation. After sampling, a 0.20 μm filter was used for each sample and experiment. Iron concentration was then measured for each sample.

3.2.3.2 Filtration

Tracer studies were performed for each filter system. Filters were rinsed with DI water until water effluent conductivity reached the value of DI water. NaCl solutions were prepared to be used as the tracer for the study and were pumped to the systems at different flowrates. Conductivity measurements at the filters effluent were taken every 3 minutes until saturation was achieved or the normalized conductivity reached at least 95% of the solution conductivity. Systems 1 and 2 were run at 60.6, 11.6 and 1.4 mL/min. System 3 was run at 134, 98 and 60 mL/min. Difference in flowrates between systems was because the two pumps used (System 1 and 2 used the same pump) had different speed capacities and could not run at the same flowrates.

The influent water to be treated was prepared by adding 100 mL of cultured *B. subtilis* for every 20 L of the Caín Alto river water. The prepared water was pumped to the system at 60 mL per minute. For the sand filters, samples at the effluent were taken at 7.6, 15.2, 22.8 and 30.4 minutes. For the GAC sand filter, samples at the effluent of the filter were taken at 7.3, 14.5, 21.8 and 29 minutes. For the IOCS filter, samples at the effluent were taken at 3.8, 7.6, 11.4 and 15.2 minutes. These sampling times and intervals were determined based on the results from the previous tracer study. Figure 14 shows a set up of three different lab-scale filters. MF was then performed to each sample with appropriate dilutions. Iron concentration was measured to each sample taken from the IOCS filter.

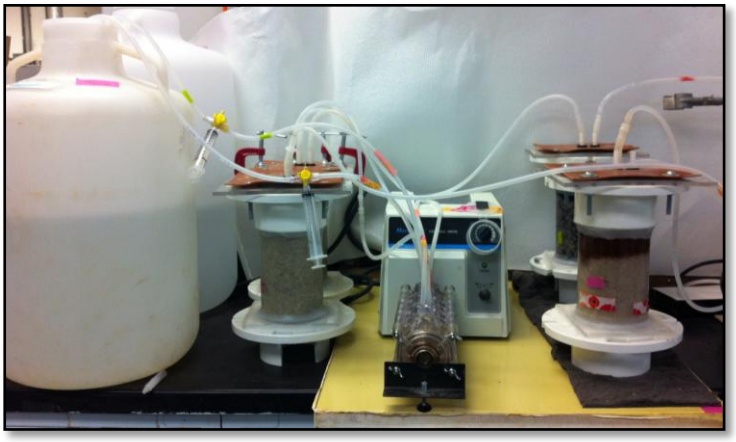

Figure 14 Filters set up.

3.2.3.3 Hom model

The Hom Model assessed the inactivation and removal of *B. subtilis*. For this assessment, four different reactors were used with 100 mL of the Caín Alto river water, 0.5 mL of *B. subtilis* solution with an initial concentration of 200,000 CFU/100 mL of *B. subtilis*, and the initial chlorine concentrations of 2, 5, 10 and 20 mg/L. Two chlorine stock solutions at the concentrations of 7,830 and 6,400 mg/L were prepared and used for the reactors. Samples were taken at times shown in Table 7. Residual chlorine concentration and *B. subtilis* concentrations were measured for each sample taken which were immediately quenched with 1 gram of sodium thiosulfate per 100 mL of sample.

Table 7 Sampling times for the Chick-Watson Model assessment.

Initial free [Cl_2] (mg/L)	Time (min)
2	0
	17
	40
	57
10	0
	10
	20
	29
5	0
	15
	30
	40
20	0
	5
	10
	20

The logarithmic removal and inactivation of *B. subtilis* were evaluated by using a simple logarithmic ratio between the numbers of *B. subtilis* at the initial and specific times in the test.

$$-\log_{10}\frac{C}{C_0} = \log\left(removal\ efficiency\right)$$

Eq. 3 Log Removal Efficiency

The disinfection kinetics of *B. subtilis* was evaluated by the use of the disinfection concentration decay on a first order reaction: (Tchobanoglous et al., 2003)

$$C = C_0 exp^{-kt}$$

Eq. 4 First order rate equation

where, C is the concentration of chlorine at time (t), C_0 is the initial concentration of chlorine, and k is the rate constant.

3.2.3.4 Disinfection

Disinfection was assessed by injecting a chlorine stock solution at 1,620 mg/L at 0.75 mL/min to the prepared river water. In such a way, the initial Cl_2 concentration was achieved at 13 mg/L. Effluent samples were taken at 17.7, 61.2, 122.4 and 183.2 minutes, free residual chlorine concentrations were measured and samples were immediately quenched with 1 gram of sodium thiosulfate per 100 mL of sample. MF was performed with their appropriate dilution to each sample to quantify the presence of *B. subtilis* in the samples and hence determine the efficiency of the system. Figure 15 shows the disinfection basin set up.

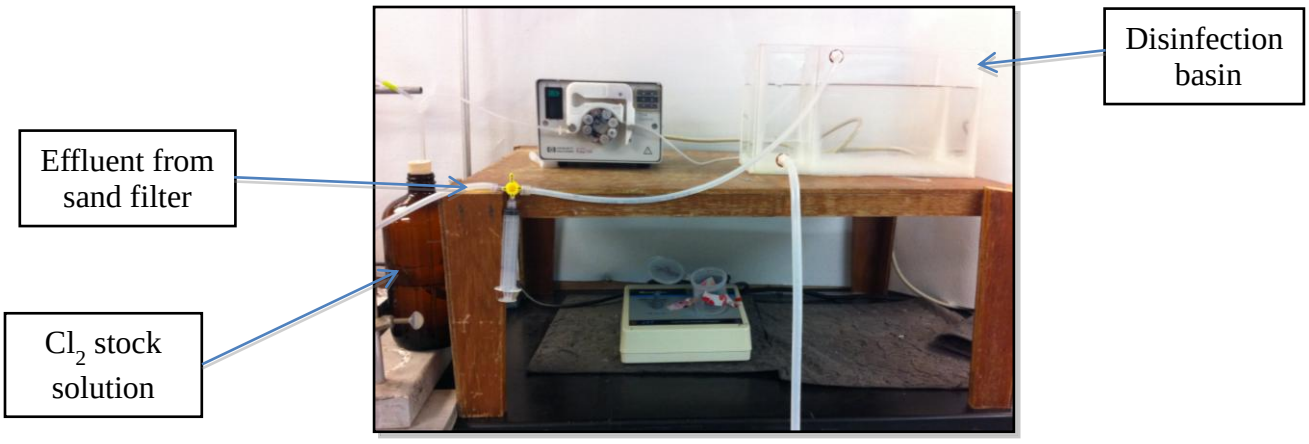

Figure 15 Disinfection basin system.

3.2.3.4.1 *B. subtilis* spores in disinfection

Batch experiments were performed to visualize the effect of disinfection on *B. subtilis* sporulation. 1 mL of cultured bacteria was rinsed with 10 mL of phosphate buffer solution and centrifuged 3 times for 15 minutes at 3,000 rpm. After rinse, the bacteria were added to 100 mL of river water. Four reactors were assessed with chlorine doses of 0, 2, 5, and 10 mg/L with a

contact time of 30 minutes. 1 gram of sodium thiosulfate was added to each reactor in order to stop the effect of chlorine after the 30 minutes and then reactors were submitted to the wet heat at 80˚C for 10 minutes. In parallel, samples that were not heat-treated were also prepared for a comparison purpose. Finally, the Schaeffer Fulton technique was employed for the visualization of spores and observed under the microscope. A schematic of this process is presented in Figure 16.

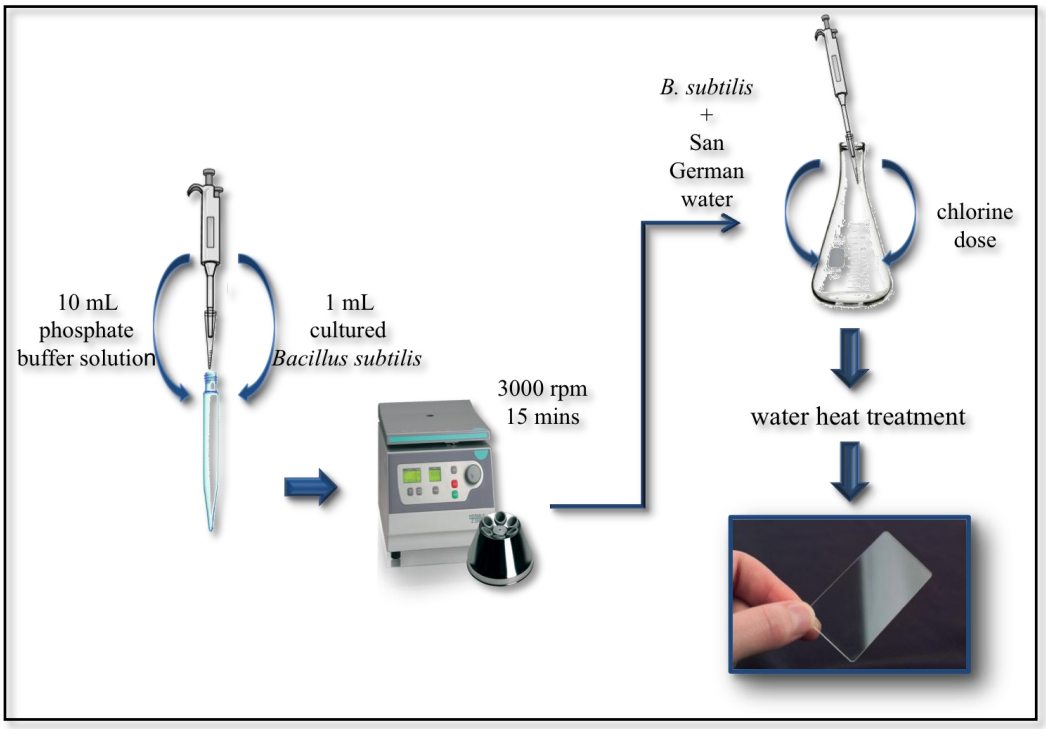

Figure 16 Disinfection effect on spores batch experiment sketch.

A second batch experiment was performed to assess the effect of disinfection on spores at different times of the heat treatment. The process performed was similar to the previous method except for the rinse of the cultured bacteria. Chlorine doses used in this experiment were 10 and 20 mg/L and the wet heat times were 3, 10, 15 and 30 minutes.

A third batch was assessed to visualize the bacteria using a scanning electron microscopy (SEM) of model JEOL JSM-6390 in the Chemical Engineering Department of the University of Puerto Rico at Mayagüez. Two Erlenmeyer flasks (reactors) were used for the assessment with 80 mL of the Caín Alto river water and 20 mL of *B. subtilis* solution in each reactor. The first reactor was the control whereas the second was exposed to 10 mg/L Cl_2 for 30 minutes. After 30 minutes, 1 gram of sodium thiosulfate was added to the reactor to stop the chlorination effect. After 30 minutes, both reactors were then submitted to wet heat to eliminate any source of microbial contamination. 10 mL of samples were then centrifuged for 15 minutes at 4000 rpm and repeated until samples were consumed and bacteria were concentrated. The pellets were rinsed three times with phosphate buffer solution. Each pellet was fixed by immersing them into 5% gluteraldehyde (5% v/v 0.1M phosphate buffer solution) for 3 hours. Gluteraldehyde was decanted from the vials and pellets were rinsed twice with phosphate buffer solution. Then pellets were sequentially dehydrated with 70% (70% v/v 0.1M phosphate buffer solution), 90% (90% v/v 0.1M phosphate buffer solution) and 100% acetone for 20 minutes in each acetone solution. In order to preserve the stability of the fixed structure, samples were dried in a Critical Point Dryer in the Biology Department of the University of Puerto Rico at Mayagüez. Fixation method used was taken from the study of Law et al. (2001).

3.2.3.5 Treatment train

After performing the filters and disinfection basin experiments individually, the sand filters were connected to the disinfection basin as shown in Figure 17. Two treatment trains were run for this study. The first experiment was a short-term treatment and was run for 184 minutes. Sampling times and ports are presented in Table 8. Port 1 represents the influent of the filters, port 2 is the effluent of the filters and influent for the disinfection basin and the port 3 is the

effluent of the disinfection basin. Flowrate of filters was set at 60 mL/min. Chlorine stock solution concentration was 1,470 mg/L and injected at 0.75 mL/min. Quantification of *B. subtilis* was performed of each sample with their appropriate dilutions. Chlorine residual was measured in the samples from port 3 which were immediately quenched with 1 gram of sodium thiosulfate per 100 mL of sample.

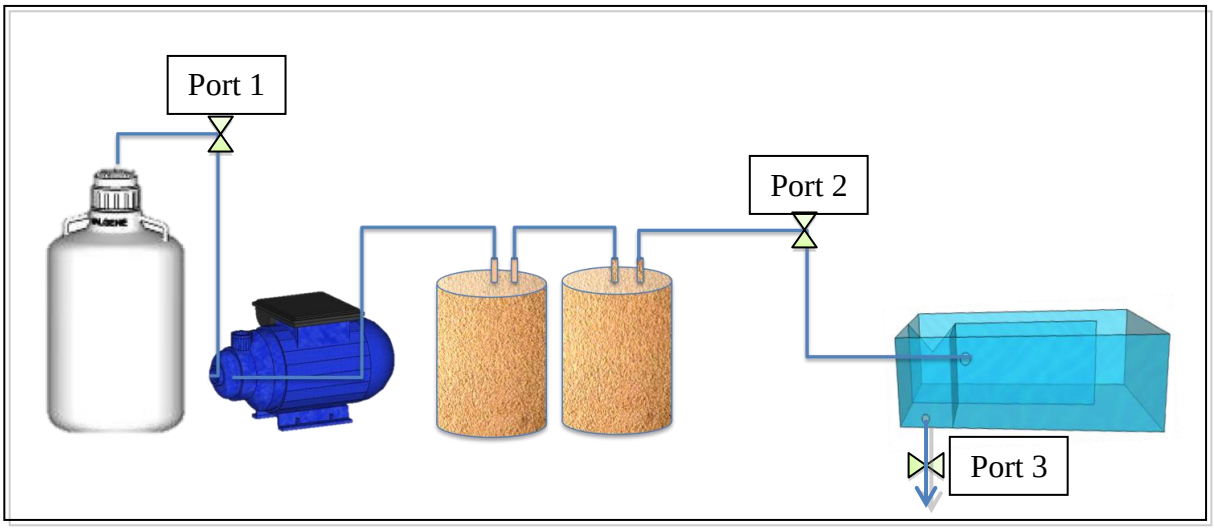

Figure 17 Laboratory scale System 1.

Table 8 Sampling times and ports for treatment train 1

	Contact time (min)		
Sample	Port 1	Port 2	Port 3
1	7.6	7.6	
2	15.2	15.2	
3		17.7	17.7
4	38	38	
5		61	61
6	76	76	
7		122	122
8	184	184	184

The second experiment, as a long-term treatment train, was run for > 27 hours (i.e., longer than 1 day). This was run to assess the service life of the filters. Table 9 contains the sampling times at the respective ports. Ports represent the same as in the first short-term treatment train. Flowrate of the filters was also set at 60 mL/min with a first chlorine stock solution concentration of 1,520 mg/L and injected at 0.75 mL/min to the disinfection basin. A second chlorine stock solution with a concentration of 1,590 mg/L was prepared at 20.5 hours. Enumeration of *B. subtilis* was performed by MF with appropriate dilutions. Residual chlorine was measured in the samples from port 3 and quenched with 1 gram of sodium thiosulfate per 100 mL of sample. Samples #1 - #8 in Table 9 served as replicates of the short-term treatment train as well.

Table 9 Sampling times and ports for long term treatment train.

	Contact time (min)		
Sample	Port 1	Port 2	Port 3
1	7.6	7.6	
2	15.2	15.2	
3		17.7	17.7
4	38	38	
5		61	61
6	76	76	
7		122	122
8	184	184	184
9	421	421	421
10	900	900	900
11	1279.5	1279.5	1279.5
12	1659	1659.5	1659.5

3.2.3.6 Backwash

Backwash was performed using the effluent from the disinfection basin at 60 mL/min for > 5 hours. Free chlorine was measured every three minutes until the chlorine demand at both ports 1 and 2 reached a steady state.

3.2.4 Field-scale System

The optimum operating parameters for removal of *B. subtilis* in the lab-scale system were tested for the field-scale SEED unit. The SEED unit consisted of two phases: 3-Drums Filtration and Post-Chlorination.

3.2.4.1 Filtration

Three different combinations of two drums connected in series were used for this phase. Each combination of two drums was run for 7 hours. The first combination of drums (C-A) was performed with a Caín Alto river flowrate of 0.9 gpm. The influent to the drum filtration was spiked with a 5.33-time diluted *B. subtilis* solution, which was injected at 18 mL/min. The second combination of drums (A-B) was run with an influent with a spike of an 8-time diluted *B. subtilis* solution injected at 18 mL/min and a Caín Alto river flowrate of 1.1 gpm. For the third combination (B-C), the influent to the filters was the same as the second combination but with a Caín Alto river water flowrate of 1.15 gpm.

3.2.4.2 Post-Chlorination

The sand-filtration effluent was fed into the Post-Chlorinator and a tablet chlorinator was used for this phase (Figure 18). In order to comply with the USEPA Maximum Residual Disinfection Level (MRDL) for chlorine of the National Primary Drinking Water Regulations, the Post-Chlorinator was modulated to have a residual chlorine concentration lower than 4 mg/L (USEPA, 2009).

Figure 18 Tablet chlorinator.

3.2.4.3 SEED unit

A solar-powered logic controller and electromechanical pumps and valves operated the SEED filtration and disinfection unit (Figure 19). Filtration and backwash were the operation mode of the unit. The quantity and operation of valves were distributed as follows: 4 motorized valves for each drum and two valves per drum operation mode (Figure 20). Two drums were run in series, being the first the lead drum and the second the lag drum. The third drum was stayed in a stand-by state. The Caín Alto river water was the influent of the unit. The unit was run for each combination described in 3.2.4.1. Samples were taken at times 0, 2, 4, 6 and 7 hours at the ports P1 (influent of the drums), P2 (effluent of the drums) and P3 (effluent of the chlorinator). The sampled water was tested for its physicochemical and bacteriological characteristics.

Figure 19 SEED unit.

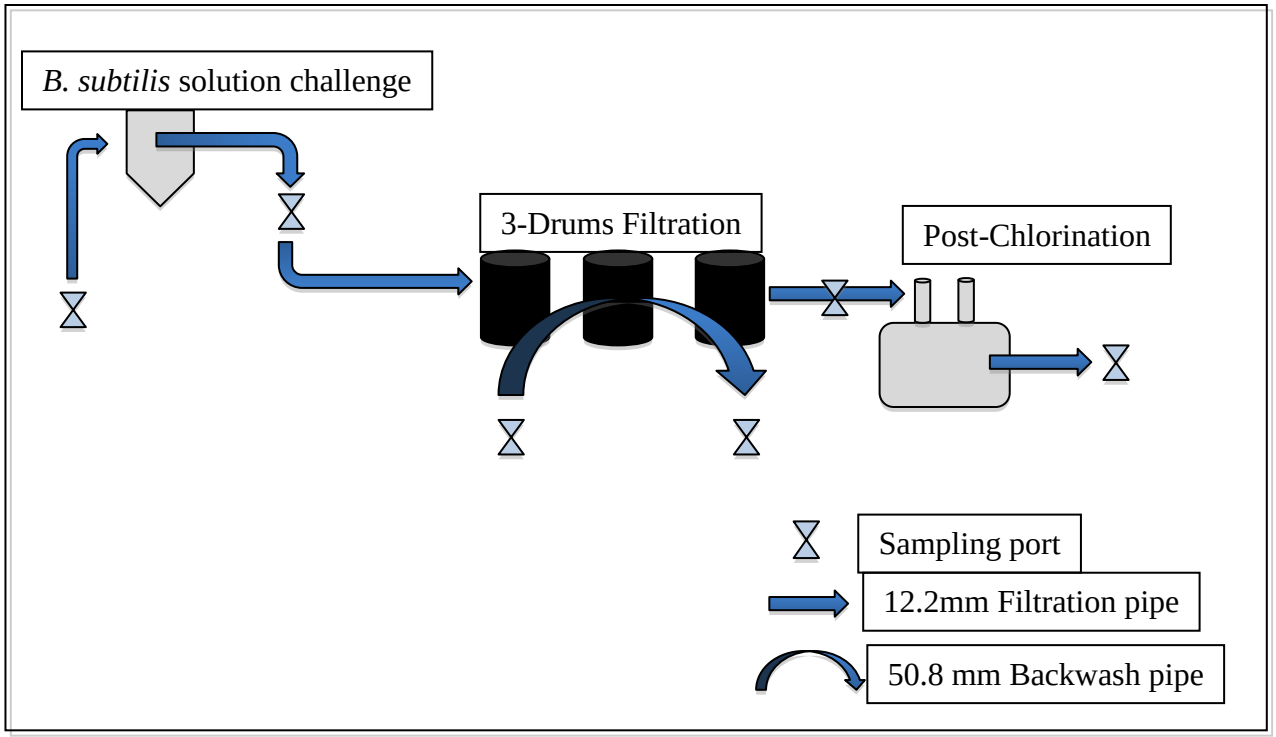

Figure 20 Schematic of SEED unit.

4. RESULTS AND DISCUSSION

4.1 WATER QUALITY

Water quality of the Caín Alto River was monitored for 1 year and 4 months for physicochemical and biological characteristics. In terms of pH (Figure 21 and Figure 22), sampling was done 25 times. pH values ranged from 8.43 in March 2013 to 8.74 in December 2012, with a mean of 8.62 and standard deviation of 0.10. Statistics shows that the mean was smaller than the median (8.64), making the distribution asymmetric with increasing values from April to December and then decreasing. This behavior made the distribution to slightly skew to the left.

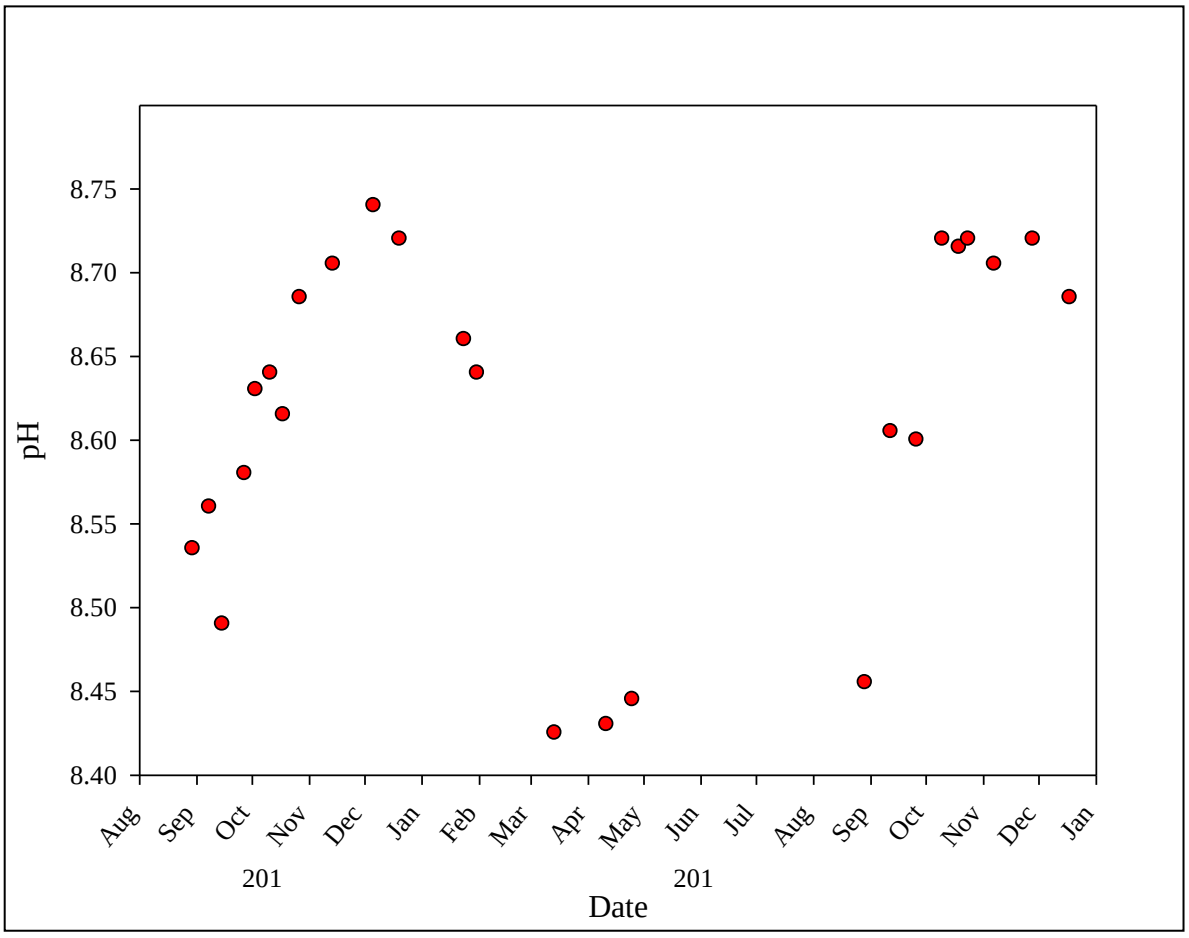

Figure 21 pH values during monitoring period.

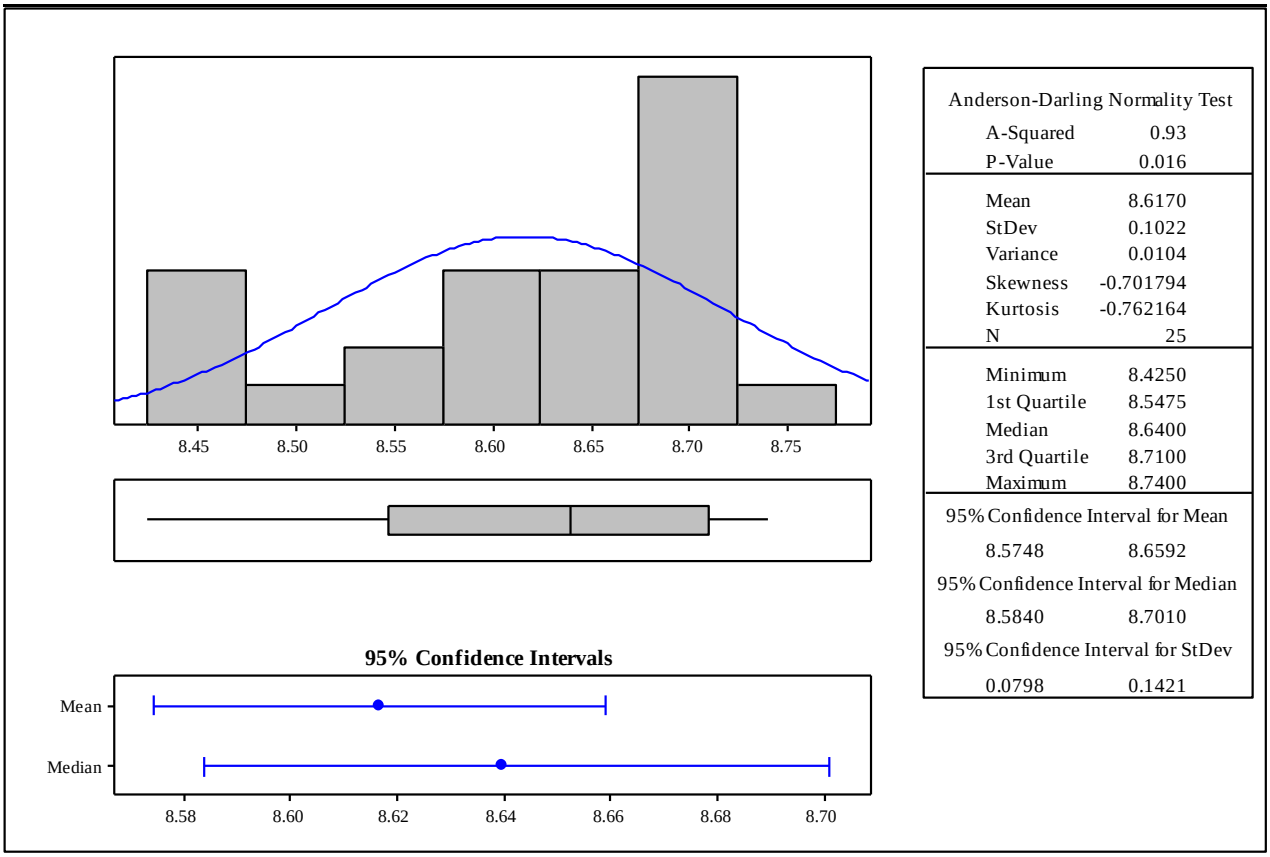

Figure 22 Summary statistics for pH of Caín Alto river water.

According to the Water Data Report of 2012 of the United States Geological Survey (USGS) station 50133600 Río Guanajibo near San German, values ranged between 7.9 and 8.1 (Table 10). Values of pH in our study were higher compared to the values monitored by the USGS. Fluctuation in the data might be due to difference in sampling location, temperature and equipment. In our study, the samples were taken from the effluent of the gravel filter of the actual system. Because gravel is mostly composed of calcium carbonate, which is basic in nature, passage of the river water through the gravel might have increased the pH of the sampled water. Moreover, according to the Le Châtelier's Principle, an increase of temperature causes a decrease in pH due to the tendency in reaching equilibrium. Temperatures of the sampled water

in our study were lower than the values reported by the USGS in 2012, as will be discussed later. This difference might also explain the higher pH values in our study.

Table 10 pH data of the 50133600 Rio Guanajibo near San German, PR (USGS, 2012).

Date	pH, water, unfiltered, field, standard units
11-03-2011	7.9
02-02-2012	7.9
05-16-2012	8.1
08-08-2012	7.9

Conductivity gives an idea of the dissolved solid concentration present in the water (Reynolds and Richards, 1996). In terms of conductivity (Figure 23 and Figure 24), 25 samples were measured having values from 230 in November 2013 to 361 μS/cm in March 2013. The mean and standard deviation were 301.4 and 36.1 μS/cm. The mean, 301.4 μS/cm, was similar to the median, 307.5 μS/cm, but was not the same. For this reason, the distribution of the data was asymmetric with high values from January to April. Hence, the distribution was slightly skewed to the left.

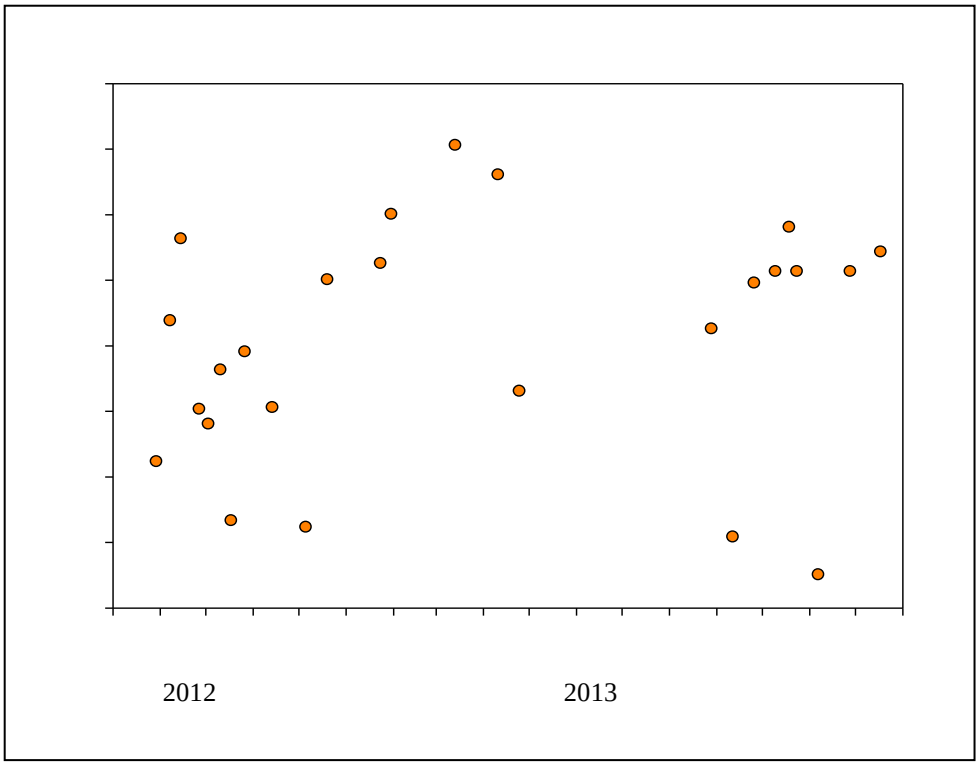

Figure 23 Conductivity values during monitoring period.

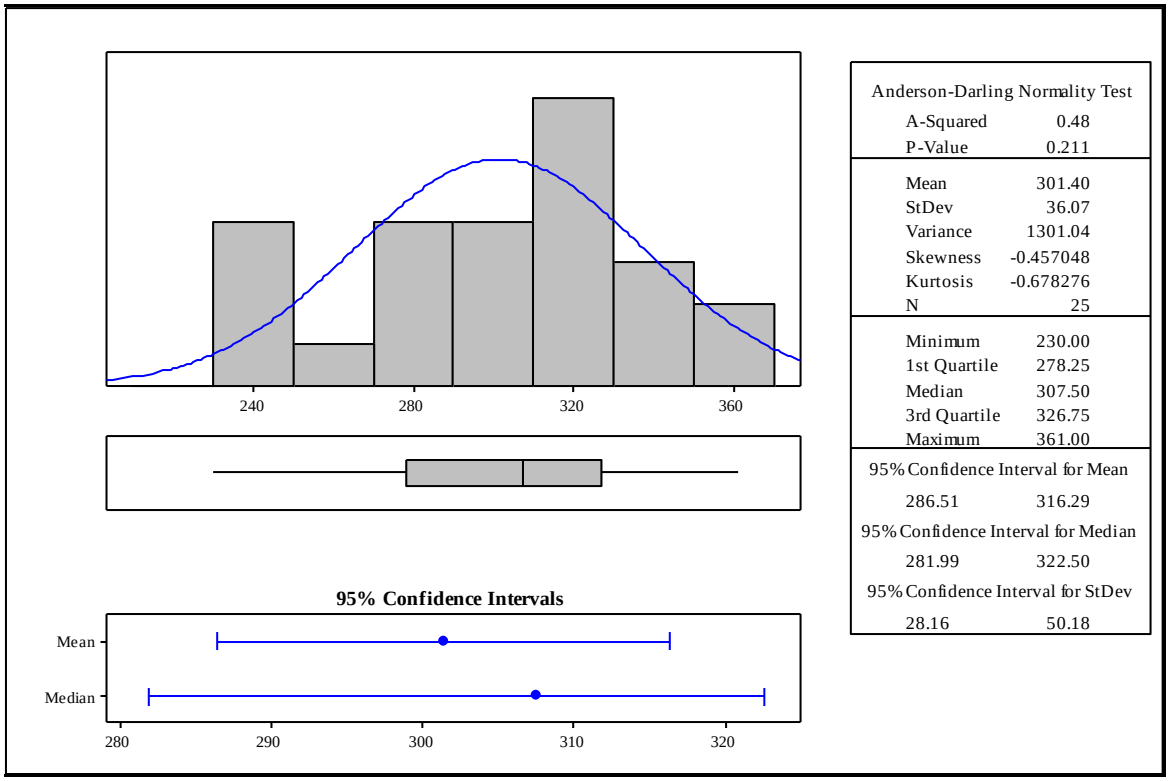

Figure 24 Summary statistics for conductivity of Caín Alto river water.

USGS reported in the Water Data Report 2012 the specific conductance of the Guanajibo River near San German (Table 11). Reported values ranged from 401 to 590 µS/cm at 25˚C, being considerably higher than those from our study. However, historically, specific conductance fluctuated significantly, showing that there is no specific range. Please refer to the Appendix for historical data (Table 42).

Table 11 Specific conductance data of 50133600 Rio Guanajibo near San German (USGS, 2012)

Date	Specific conductance, water, unfiltered, µS/cm at 25˚C
11-03-2011	421
02-02-2012	590
05-16-2012	401
08-08-2012	455

In terms of turbidity (Figure 25 and Figure 26), 24 samples were taken and measured. The values ranged from low 0.38 NTU in April 2013 to high 2.45 NTU in November 2013. These values correspond to discharge values presented in Guanajibo River, which had low discharge value on April 2013 and high value on November 2013 (Figure 27) (USGS, 2014). Since discharge depends on the rainfall captured on the drainage area and the Caín Alto River is in the drainage area of the Guanajibo River (Figure 28), turbidity values monitored might be due to rainfall events presented in the drainage area, causing the fluctuations in the values. The mean and standard deviation during the monitoring period were 0.83 NTU and 0.48 NTU, respectively. Distribution of the data was asymmetric and right skewed since the mean was greater than the median, 0.68 NTU. Nevertheless, during the monitoring period, turbidity measurements did not exceed 5 NTU in any measurements. But, only 75 % of samples had turbidity below 1 NTU. Therefore, turbidity did not satisfy the Surface Water Treatment Rule (SWTR) requirements.

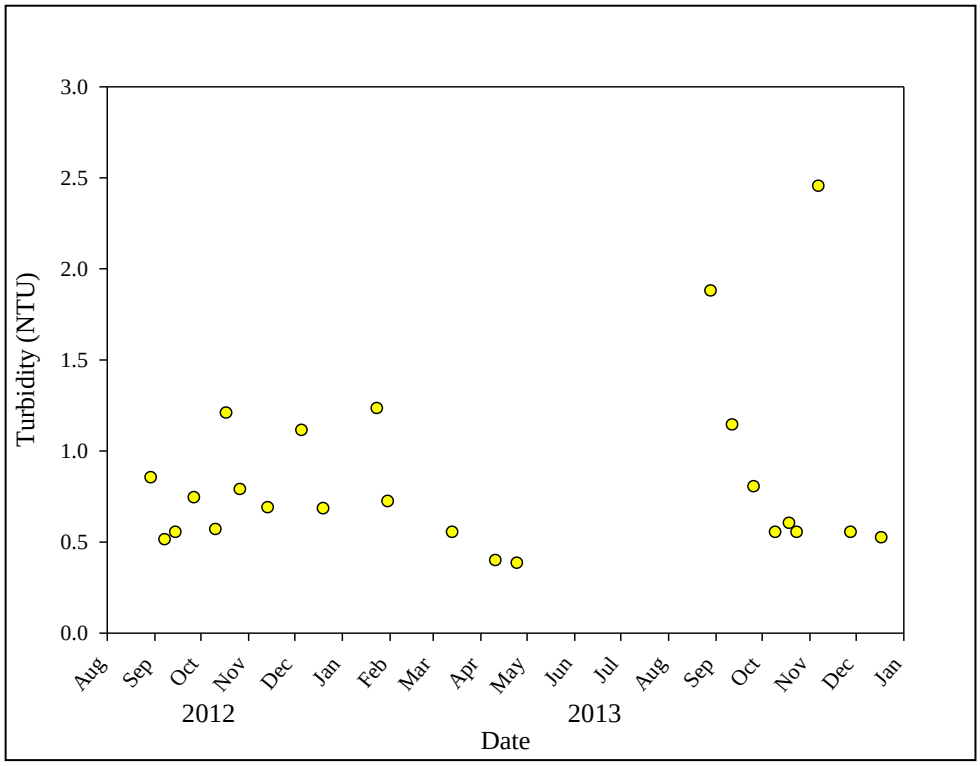

Figure 25 Turbidity values during monitoring period.

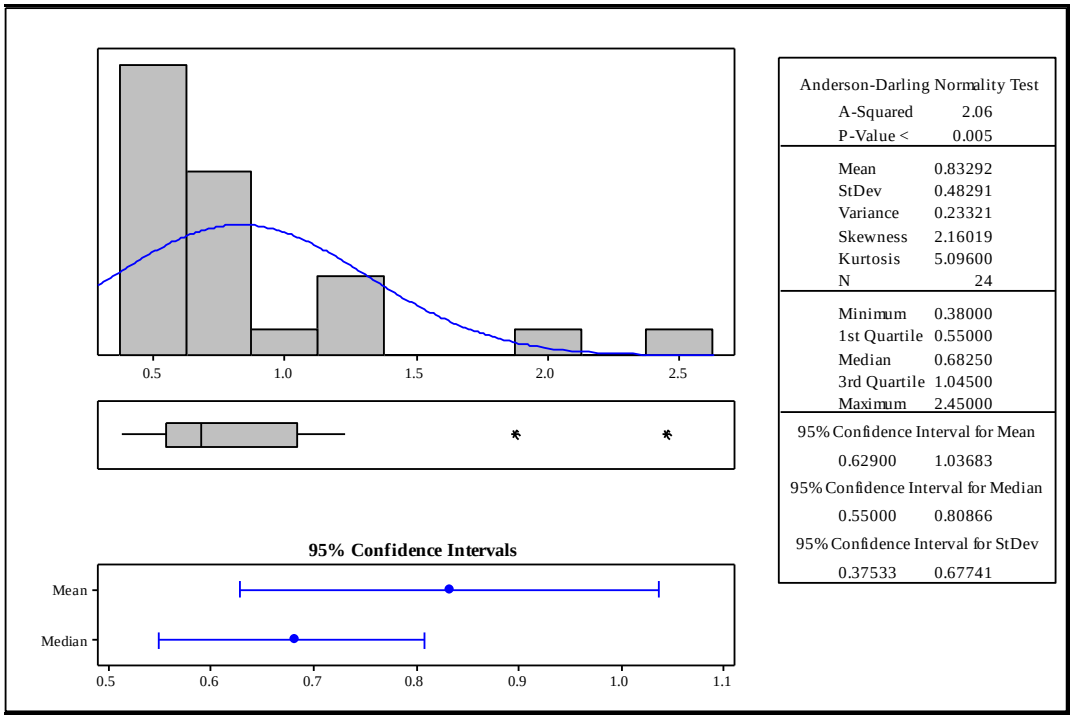

Figure 26 Summary statistics for turbidity of Caín Alto river water.

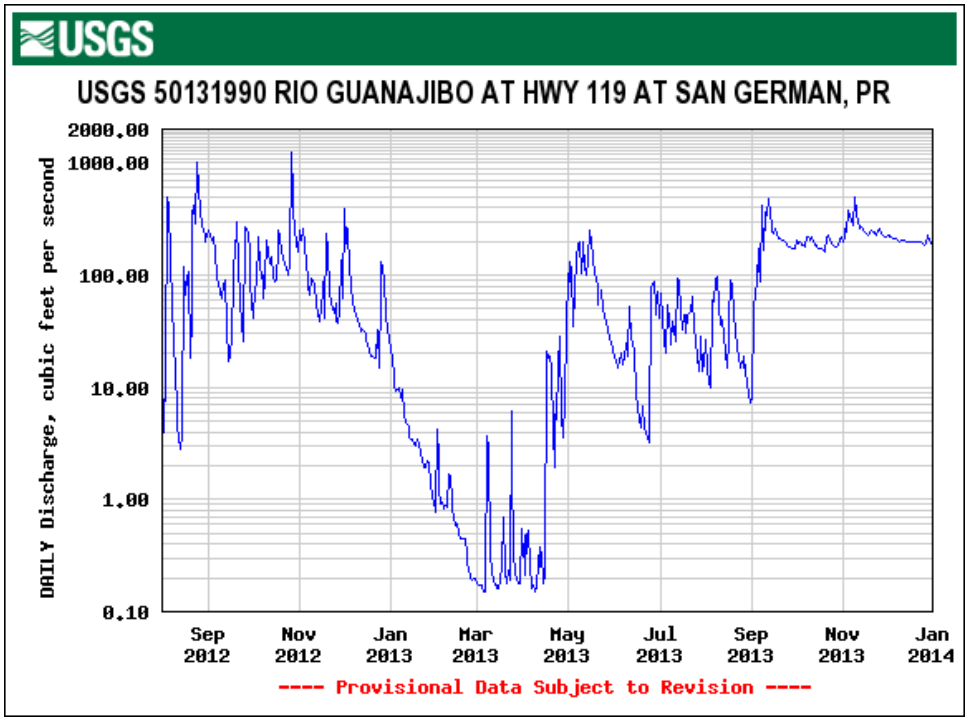

Figure 27 Daily discharge of the Guanajibo River during the monitoring period (USGS, 2014).

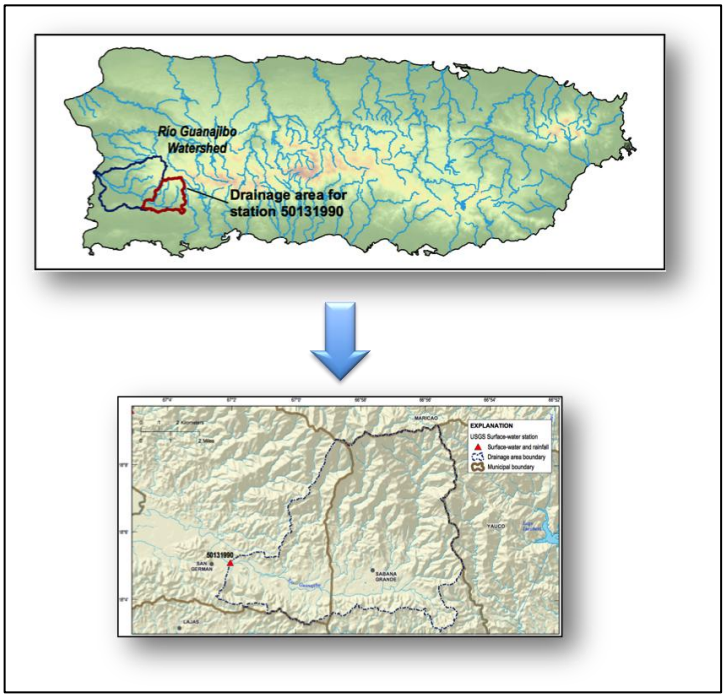

Figure 28 Guanajibo River drainage area.

In 2012, turbidity measurements (Table 12) of the Guanajibo River fluctuated from 3.3 to 18 NTRU (USGS, 2012). In our study, the values of turbidity were lower since turbidity was measured in the effluent of the gravel filter, as mentioned previously. However, in both cases the maximum values were reported on November.

Table 12 Turbidity measurements of the USGS 50133600 Rio Guanajibo near San German (USGS, 2012).

Date	Turbidity, water, unfiltered, ratiometric correction, NTRU
11-03-2011	18
02-02-2012	3.3
05-16-2012	17
08-08-2012	3.9

25 samples were measured for the total dissolved solids (TDS) assessment (Figure 29 and Figure 30). Values of this parameter were between 156 ppm in August 2012 and 258.5 ppm in March 2013. The mean and standard deviation were 212.3 and 28.0 ppm, respectively. Inequality of the mean and median (220.5 ppm) showed that the distribution of the data was asymmetric with highest values from December to March. These variations made the distribution skewed to the left.

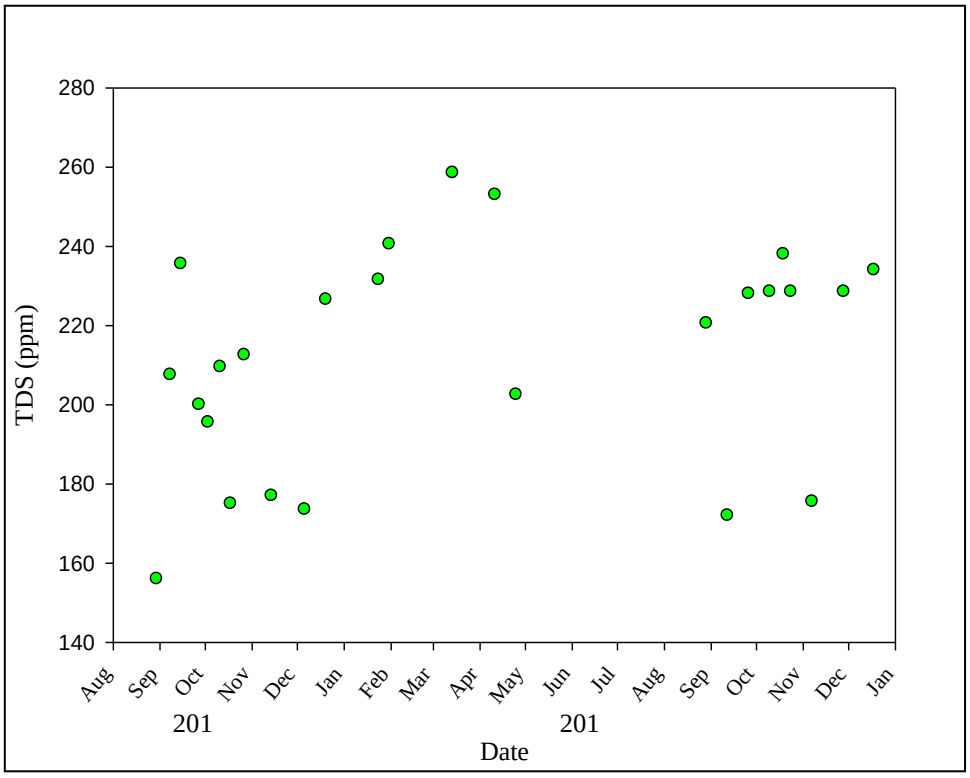

Figure 29 TDS values during monitoring period.

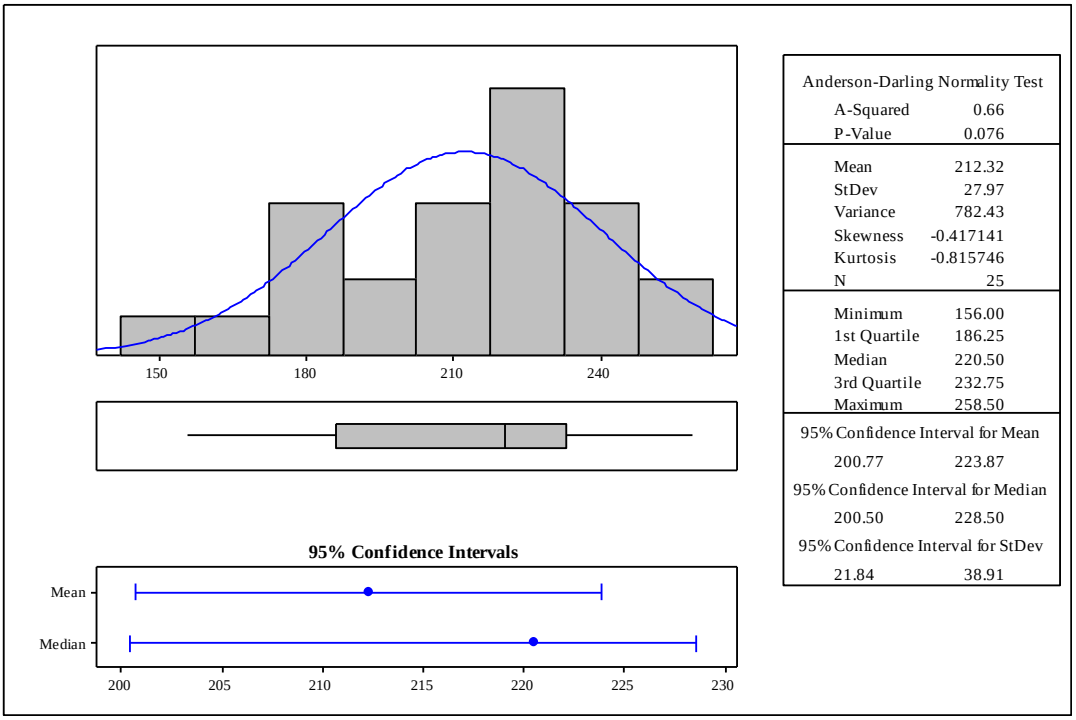

Figure 30 Summary statistics for TDS of Caín Alto river water

None of the TDS measurements was over 600 ppm. Therefore, it could be classified as "good in terms of palatability of the water" (WHO, 2011). Due to its low concentration of TDS, it would not present a matter of concern for health, scaling in distribution lines, or in house appliances.

TOC measurements were performed for 24 samples during the monitoring period (Figure 31 and Figure 32). Values of this parameter were between 0.3 mg/L in January 2013 and 19.6 mg/L in September 2012. The mean and standard deviation were 4.5 and 5.8 mg/L, respectively. Data distribution is asymmetrical and right skewed due to inequality of mean (4.5 mg/L) and median (1.7 mg/L). However, TOC from September 2013 to December 2013 were mostly constant at 1.6 mg/L.

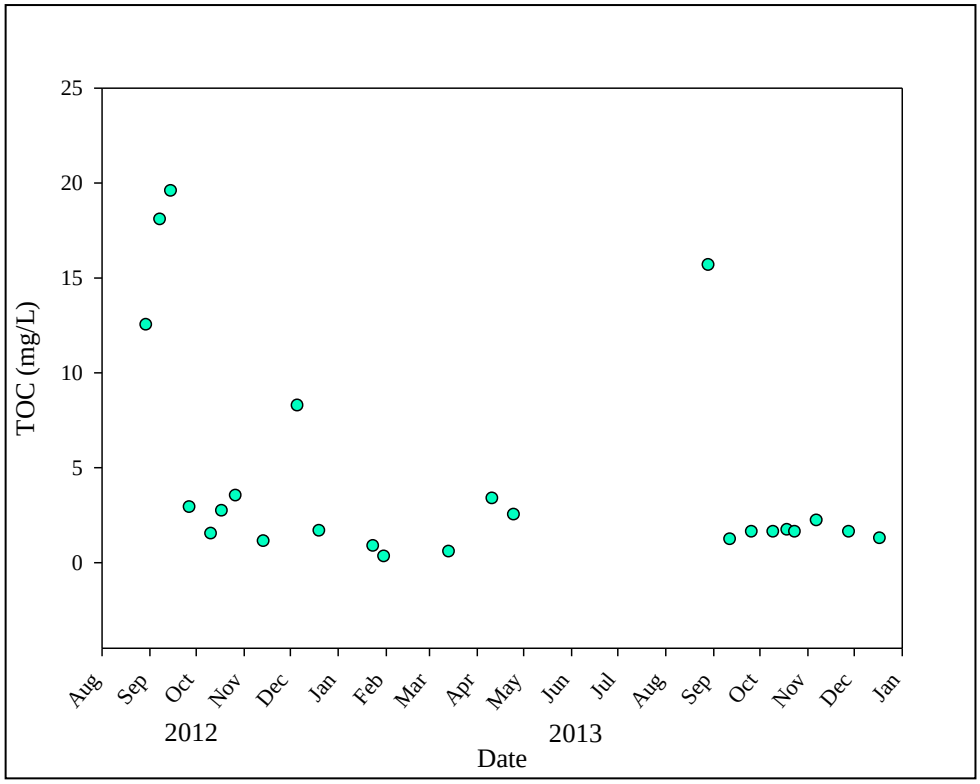

Figure 31 TOC values during monitoring period.

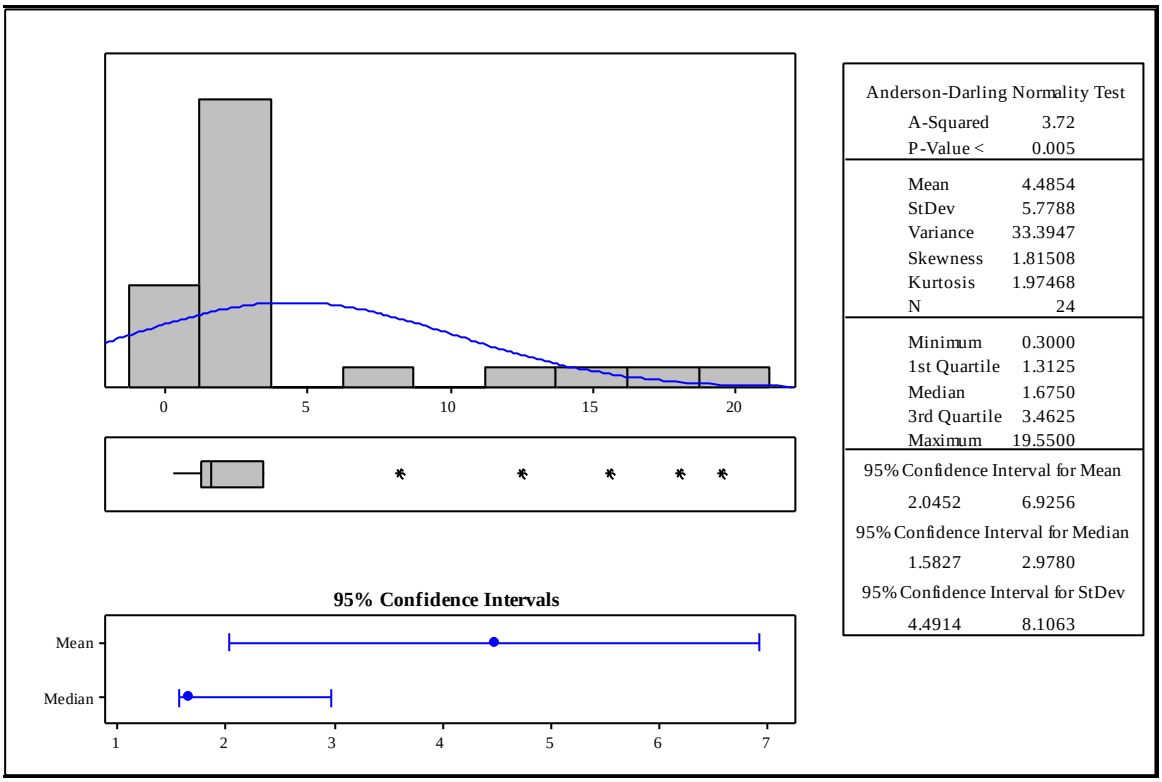

Figure 32 Summary statistics for TOC of Caín Alto river water.

Temperature during monitoring ranged from 21.7 ˚C in January 2013 to 27.8 ˚C in August 2012 on the 25 samples measured (Figure 33 and Figure 34). These values corresponded to the seasons of winter and summer in Puerto Rico. The mean, median and standard deviation were 24.3, 24.6 and 1.3˚C, respectively. Data distribution was almost symmetrical (slightly left skewed) with the lowest values during the winter period, from the middle of December to the end of January.

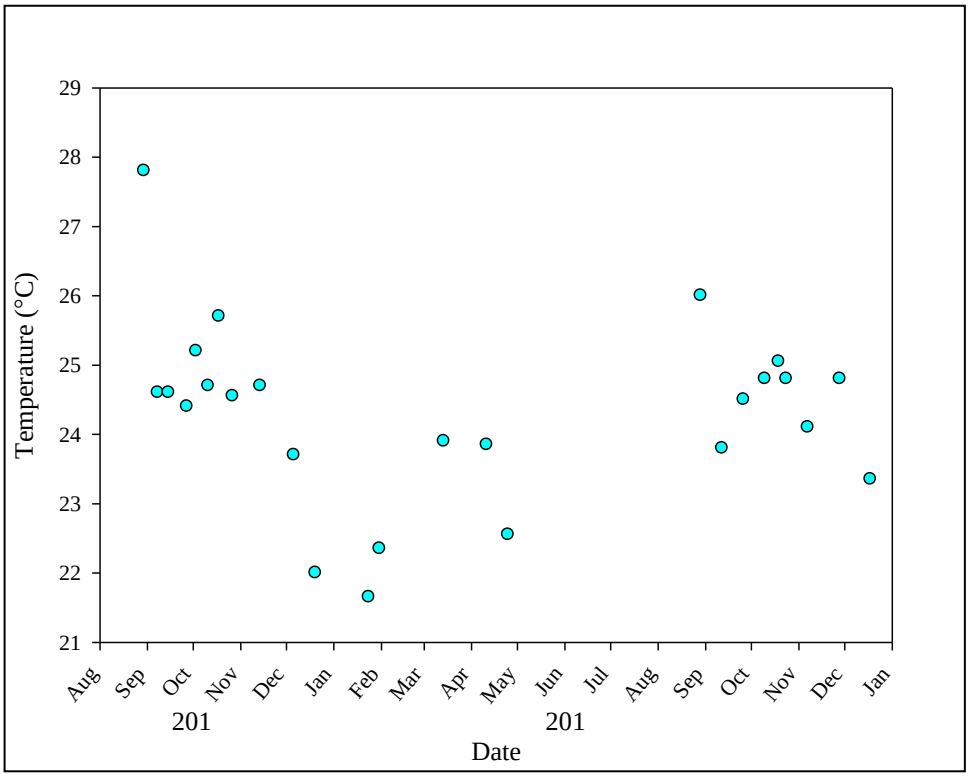

Figure 33 Temperature values during monitoring period.

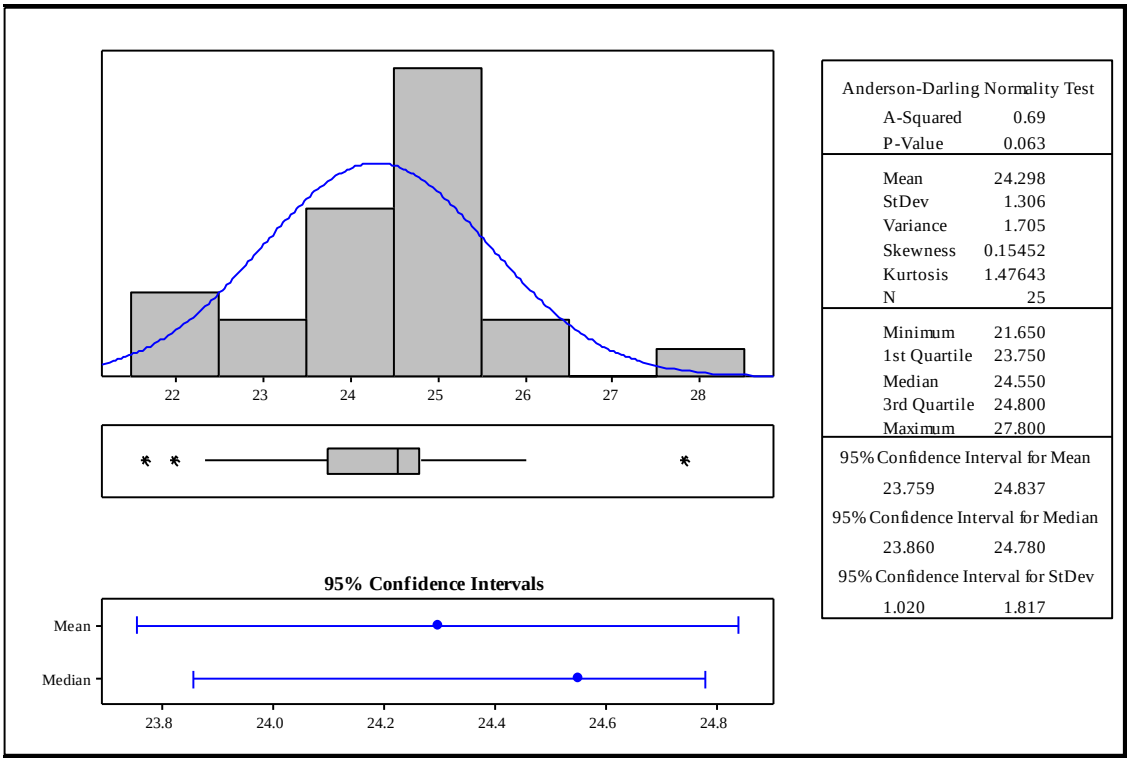

Figure 34 Summary statistics for temperature of Caín Alto river water.

Temperatures measured in our study were similar to those by USGS station 50133600 in 2012 (Table 13). However, the same minimum and maximum values were not found in the same months of monitoring. Temperature can be correlated with the concentration of dissolved oxygen (DO) in water. Results indicated that in January 2013 river water sample had the highest DO concentration while in August 2012 the lowest.

Table 13 Temperature data of USGS 50133600 Rio Guanajibo near San German (USGS, 2012).

Date	Temperature, water, ˚C
11-03-2011	24.3
02-02-2012	21.8
05-16-2012	27.9
08-08-2012	26.9

14 samples were evaluated in terms of *E. coli* (Figure 35 and Figure 36). The minimum numbers of bacteria were 0 CFU/100 mL in February and April 2013 and the maximum of 50 CFU/100 mL in September 2013. The mean, median and standard deviation were 13.6, 12.5 and 11.8 CFU/100 mL, respectively. Data distribution was asymmetrical with the lowest *E. coli* number during the winter season, and skewed to the right. According to the SWTR, 12 out of the 14 samples were in acute Maximum Contaminant Level (MCL) violation if source water was not submitted to an appropriate treatment.

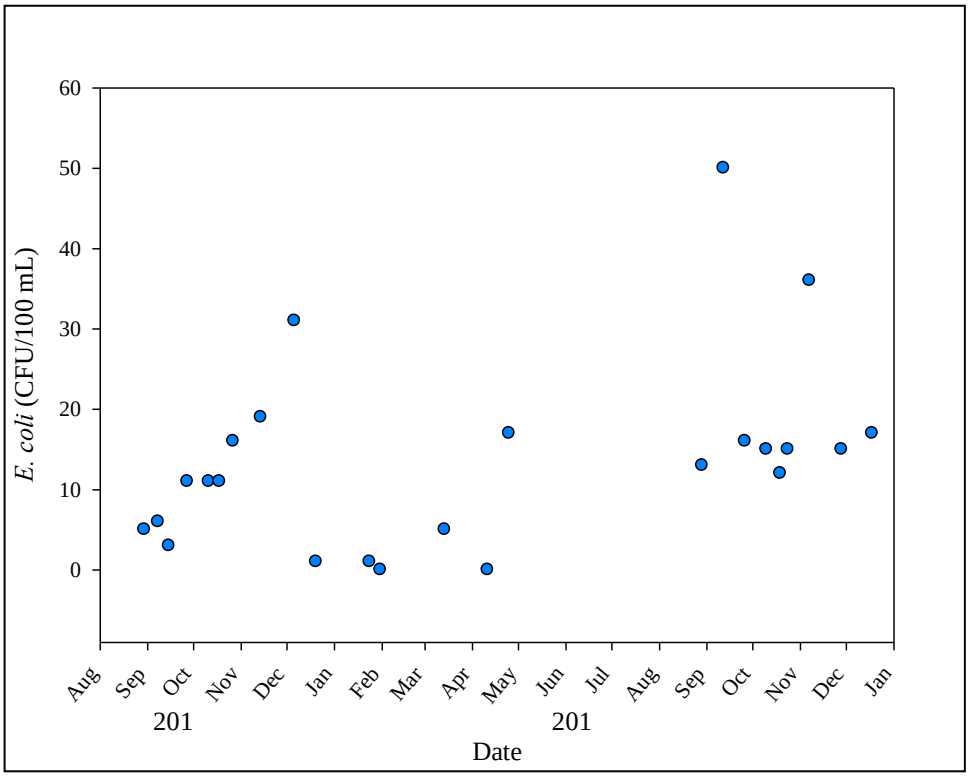

Figure 35 *E. coli* numbers during monitoring period.

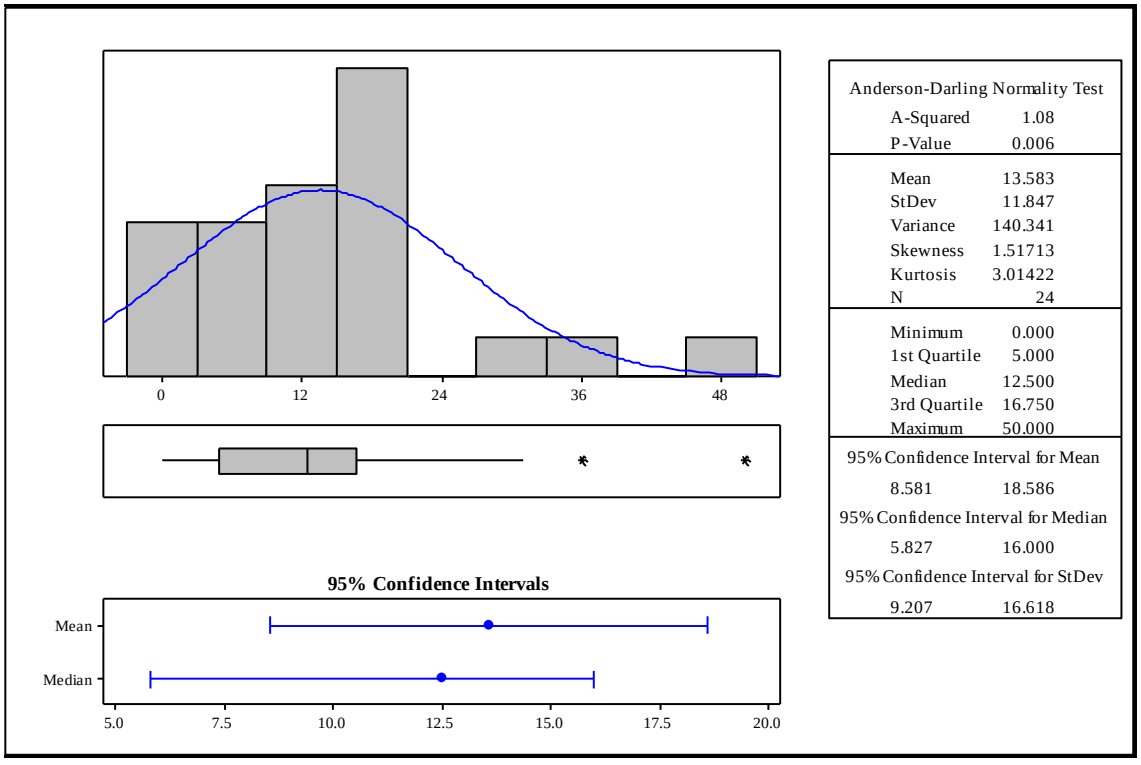

Figure 36 Summary statistics for *E. coli* of Caín Alto river water.

Total coliforms were quantified in 22 samples during the monitoring period (Figure 37 and Figure 38). A wide range of total coliforms was found in the monitoring period. The minimum counted coliforms were 11 CFU/100 mL in January 2013 whereas the maximum value, 2080 CFU/100 mL was measured in September 2012. The distribution of the data was found to be asymmetrical and right skewed. The mean value and standard deviation were found to be 843.8 ± 693.3 CFU/100 mL and the median 775 CFU/100 mL. All samples were found to be TC positive and their corresponding measurement of *E. coli* was also positive, making the source water in acute MCL violation if no further treatment was to be performed.

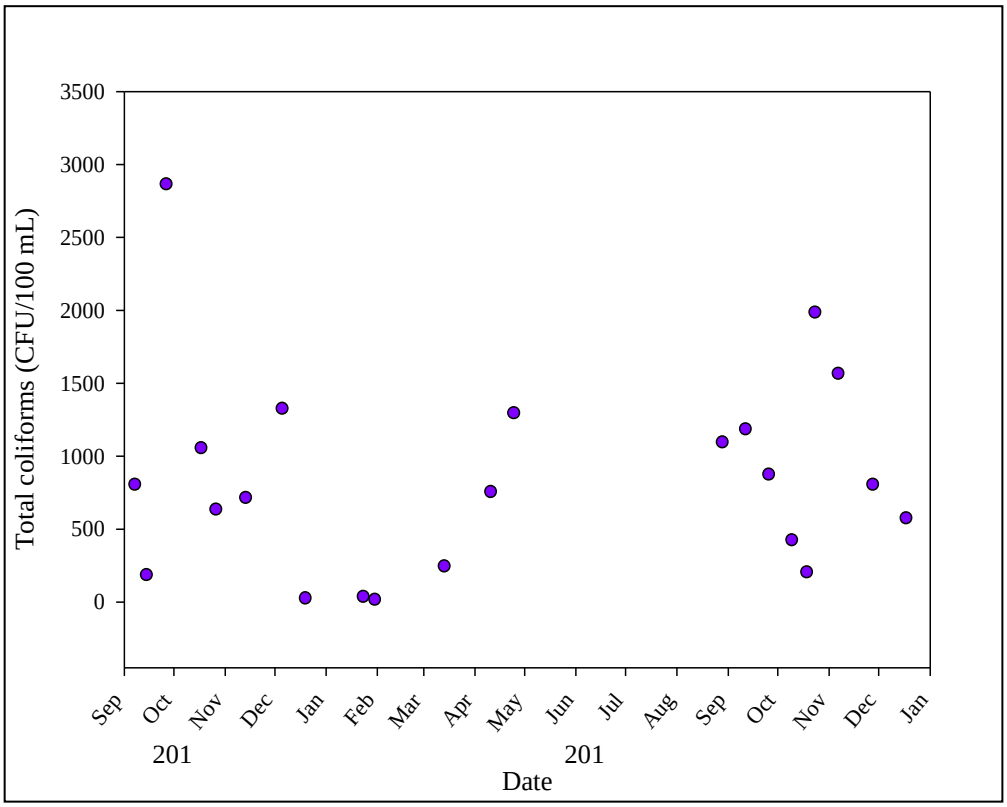

Figure 37 Total coliform numbers during monitoring period.

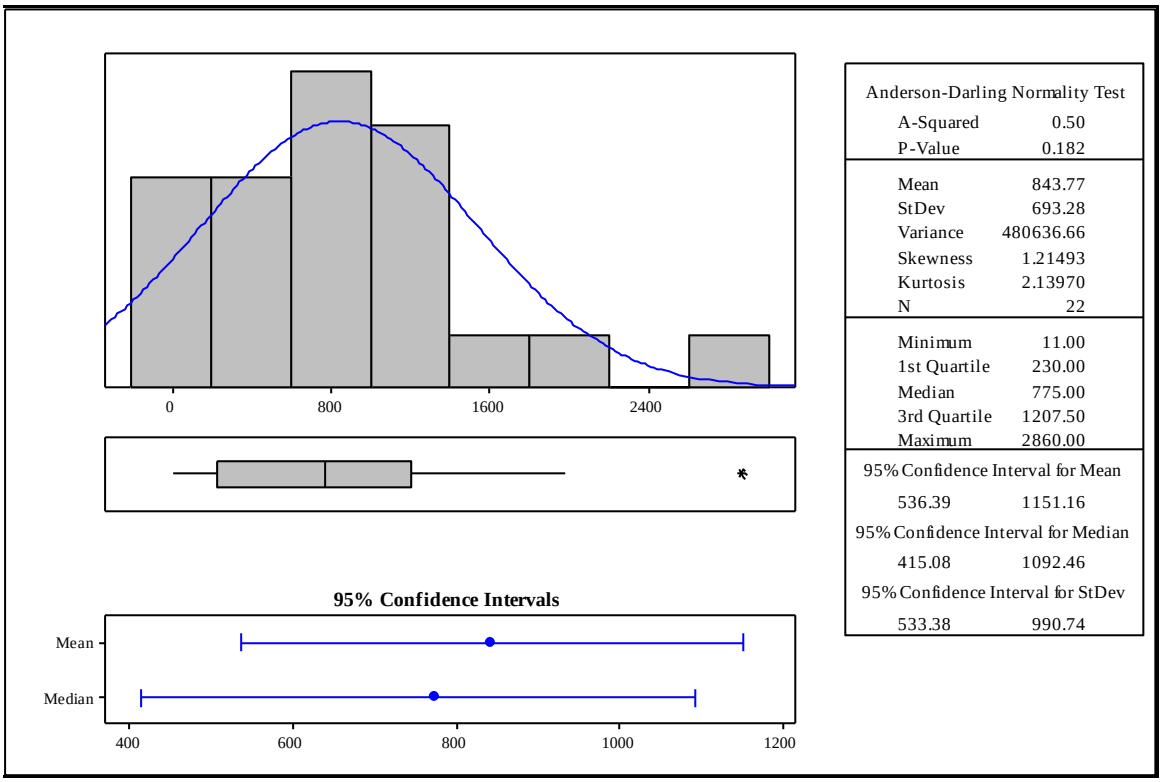

Figure 38 Summary statistics for total coliforms of Caín Alto river water.

Higher numbers of the total coliforms were quantified in USGS station 50133600 (Table 14) (USGS, 2012). The minimum and maximum numbers of coliforms were not found in the same months as with our study.

Table 14 Total coliform enumeration of USGS 50133600 Rio Guanajibo near San German (USGS, 2012).

Date	Total coliform, col/100 mL
11-03-2011	10,000
02-02-2012	3,000
05-16-2012	64,000
08-08-2012	20,000

Quantification of *B. subtilis* was performed for 18 samples during the monitoring period (Figure 39 and Figure 40). *B. subtilis* enumeration was found to range from 105 CFU/100 mL in January 2013 to 10200 CFU/100 mL in November 2013, with November and December being

the months with the highest number of counted colonies. These values corresponded with the high values of the discharge of the Rio Guanajibo as discussed previously. Because *B. subtilis* are ubiquitous aerobic bacteria and commonly present in soil, surface runoff due to rainfall events might have caused the increment in *B. subtilis* count in the river water. The collected data had an asymmetric distribution, being right skewed. The mean and standard deviation were found to be 1,014 ± 2,327 CFU/100 mL and median was 270 CFU/100 mL.

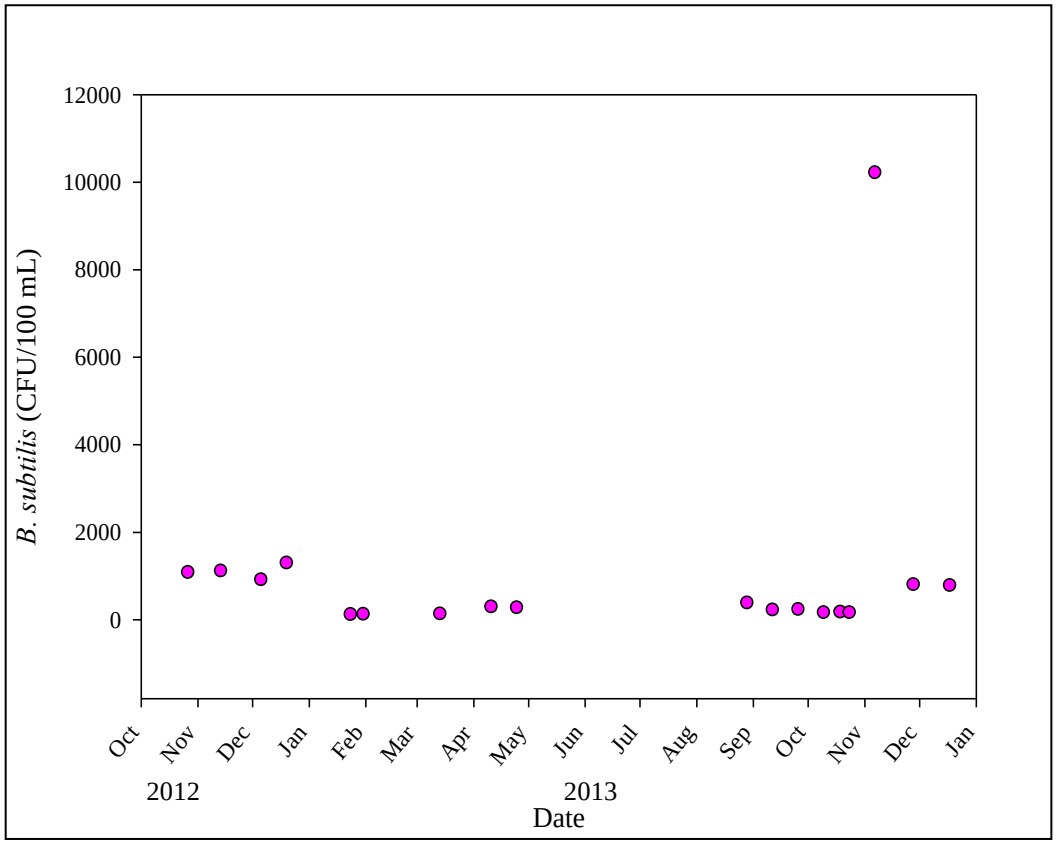

Figure 39 *B. subtilis* number during monitoring period.

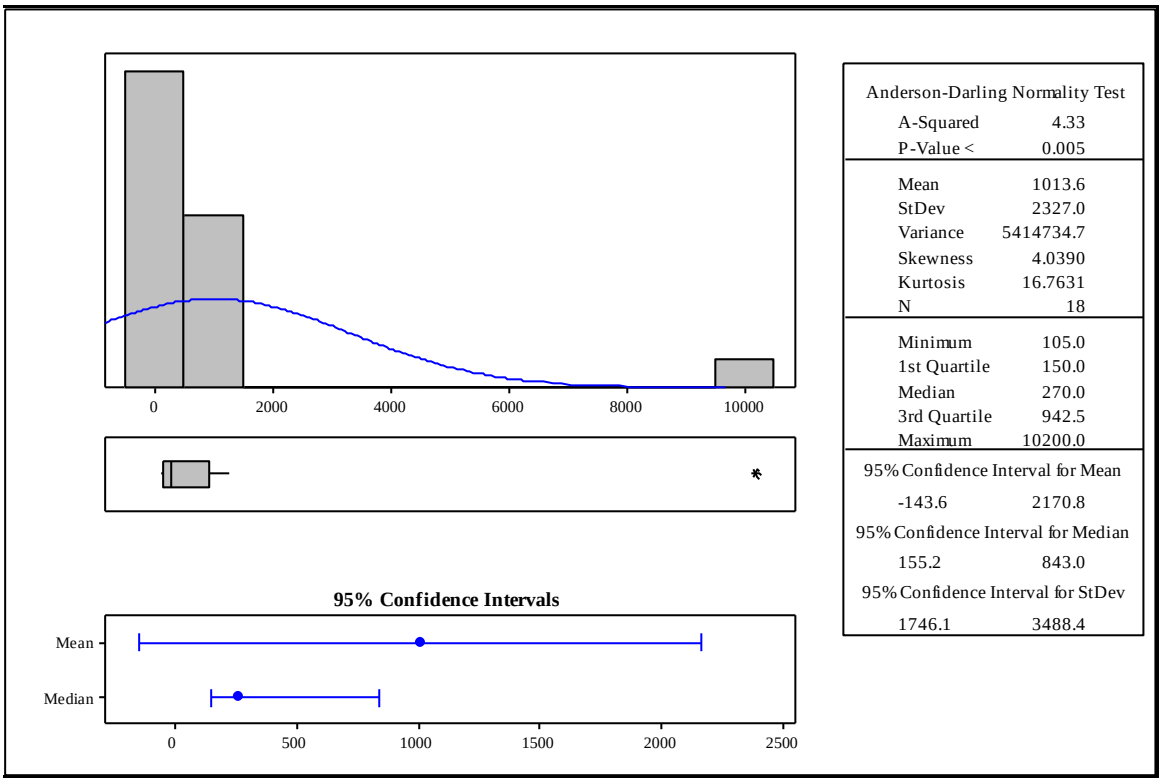

Figure 40 Summary statistics for *B. subtilis* of Caín Alto river water.

A summary of the water quality for Caín Alto River can be found on Table 15. Additional efforts were made to assess any correlations among the measured water quality parameters. Figure 41 shows a matrix plot of the parameters pH, conductivity, turbidity, TDS, TOC, temperature, *E. coli*, total coliforms and *B. subtilis*.

Table 15 Summary of water quality parameters for Caín Alto River.

Parameter	Mean	Standard Deviation
pH	8.62	0.10
Conductivity	301.50 µS/cm	36.07 µS/cm
Turbidity	0.83 NTU	0.48 NTU
TDS	212.32 ppm	27.97 ppm
TOC	4.89 mg/L	5.78 mg/L
Temperature	24.30 ˚C	1.31 ˚C
E. coli	13.58 CFU/100 mL	11.85 CFU/100 mL
TC	843.77 CFU/ 100 mL	693.28 CFU/ 100 mL
B. subtilis	1013.6 CFU/100 mL	2327 CFU/100 mL

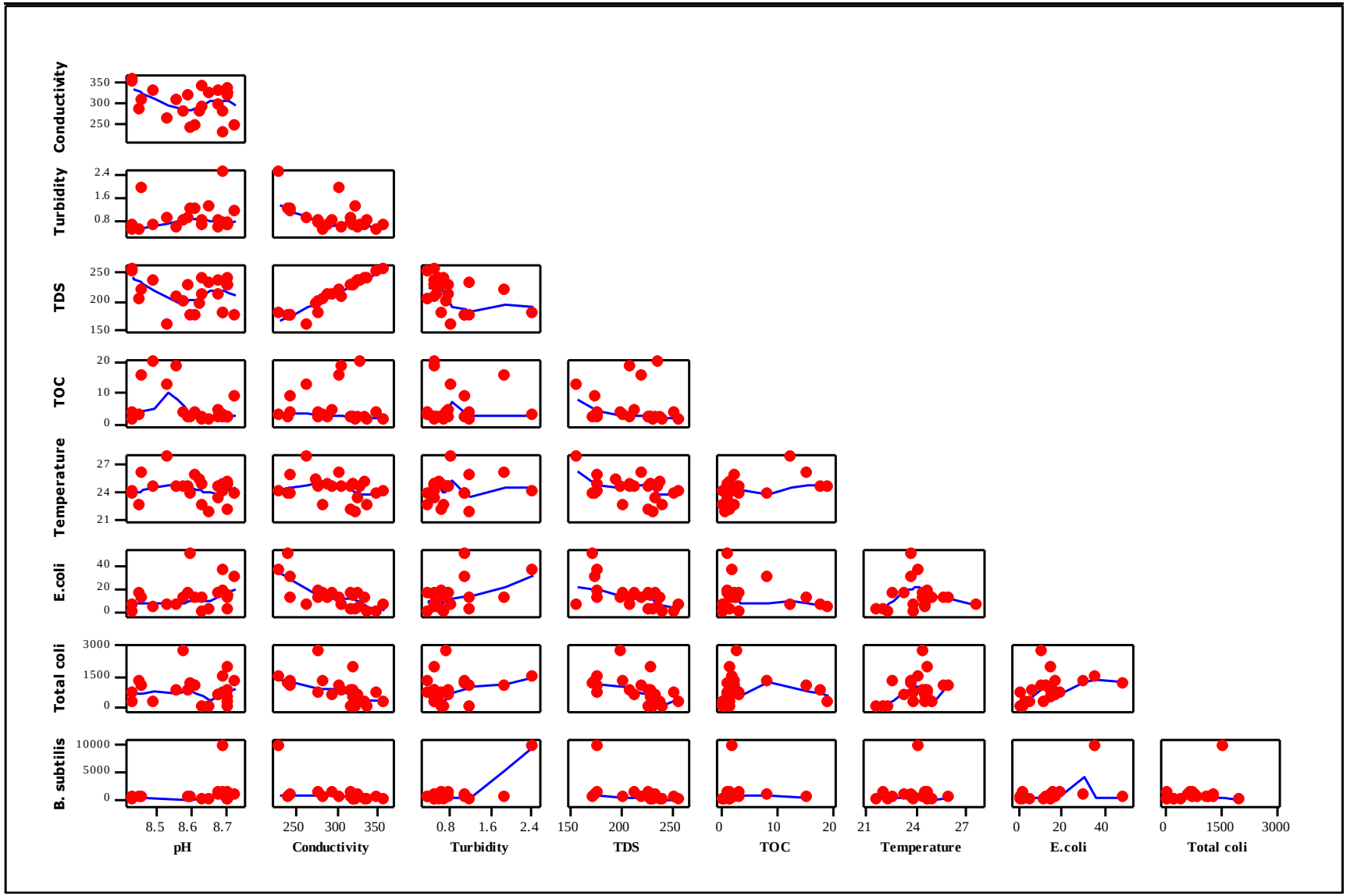

Figure 41 Matrix plot of pH, conductivity, turbidity, TDS, TOC, temperature, *E. coli*, total coliforms and *B. subtilis*.

From the matrix plot, it can be seen a good relationship between conductivity and TDS. However, for a proper analysis of the parameters the Pearson correlation and P-values were calculated using the Minitab. Table 16 presents the output of this statistical analysis.

Table 16 Pearson correlation and P-values of the water quality parameters monitored.

	pH	Conductivity	Turbidity	TDS	TOC	Temperature	*E. coli*	Total coliforms
Conductivity	-0.216							
	0.3							
Turbidity	0.103	-0.581						
	0.633	0.003						
TDS	-0.188	**0.953**	-0.438					
	0.369	**0**	0.032					
TOC	-0.418	-0.063	0.101	-0.147				
	0.042	0.768	0.639	0.492				
Temperature	-0.128	-0.277	0.113	-0.391	0.433			
	0.542	0.181	0.6	0.053	0.035			
E. coli	0.312	**-0.692**	0.451	-0.57	-0.186	0.052		
	0.138	**0**	0.027	0.004	-0.385	0.809		
Total coliforms	-0.021	-0.551	0.236	-0.507	-0.008	0.322	**0.437**	
	0.927	0.008	0.29	0.016	0.973	0.144	**0.042**	
B. subtilis	0.232	**-0.556**	**0.72**	-0.45	-0.021	0.035	**0.401**	0.341
	0.355	**0.017**	**0.001**	0.061	0.934	0.89	**0.099**	0.167
Cell contents:	Pearson correlation							
	P-value							

The statistical analysis clearly showed a positive relation between conductivity and TDS. The Pearson correlation and P-value for these two parameters were 0.953 and 0.000 respectively. In terms of the bacteriological parameters, it was found that *B. subtilis* was highly positively correlated with turbidity, having Pearson correlation and P-values of 0.720 and 0.001 respectively. In contrast, *B. subtilis* was highly negatively correlated with conductivity, presenting values of -0.556 and 0.017 of Pearson, covariance and P-value respectively. *B. subtilis*

might be positively correlated with *E. coli* for the Pearson correlation of 0.401. However, the P-value, 0.099, was greater than 0.05 indicating a weak evidence. In terms of *E. coli*, the Pearson correlation of 0.437 indicated that it might be positively correlated to the presence of total coliforms. The small P-value, 0.042, implied a strong evidence of this correlation.

4.2 *B. SUBTILIS*

Enrichment of *B. subtilis* culture was successfully performed. However, special attention was given to the nutrient broth temperature. When the nutrient broth was submitted to a harsh change in temperature (i.e. from hot to cold) and the transfer was performed, it was noticed that the color of *B. subtilis* enrichment culture changed from yellow to black pigmented (Figure 42). According to Hecker et al. (2009) and Höper et al. (2006), *B. subtilis* can change genetically when submitted to harsh environments including, temperature, stress and starvation. Moreover, Nakamura (1989) made a study for the differentiation of bluish and brownish black pigmented *B. subtilis* and found that the brownish-black pigment *B. subtilis* were a new species. Therefore, in order to prevent further genetic changes, during the preparation and autoclaving of the nutrient broth, it was allowed to cool down to ambient temperature by natural convection.

Figure 42 Improper *B. subtilis* enrichment culture.

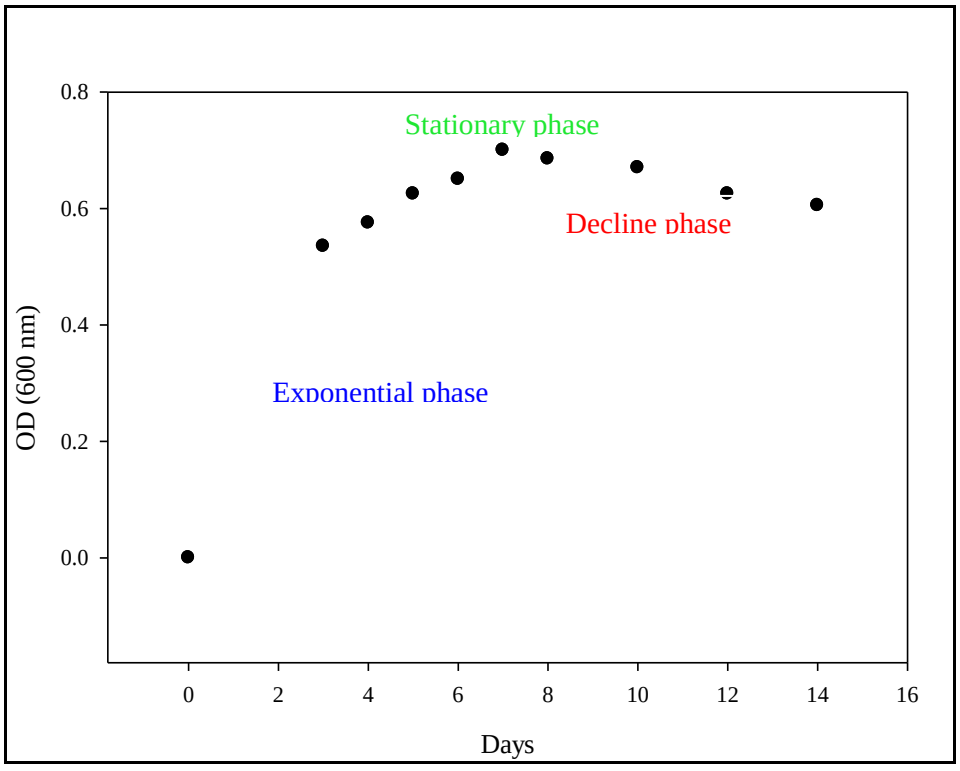

Figure 43 *B. subtilis* growth curve.

A growth curve of *B. subtilis* obtained during enrichment is presented in Figure 43. The OD measurements showed that *B. subtilis* was fully acclimated since a lag phase was not present. After 1 week of transfer (exponential phase), the *B. subtilis* growth reached the stationary phase with an OD of 0.7. However, it did not have a long stationary phase and started decline phase on the 8^{th} day until the 14^{th} day when the new transfer was performed. The rate of decline phase was slower than the exponential phase, behaving like a typical cell growth curve (Carcano, 2010).

4.2.1 *B. subtilis* Sporulation

B. subtilis spores were visualized at four different times of wet heat (3, 10, 15 and 30 minutes). As shown in Figure 44, the sizes of spores increased with time. This swelling of the *Bacillus* spores might be due to the water permeability of the cortex and coat which enables diffusion of water into the spore. Similarly, Westphal et al. (2002) found this behavior in *Bacillus thuringiensis* caused by relative humidity. Moreover, Driks (1999) made a study of the assembly of the *B. subtilis* spore coat by genetic modifications and showed that the coat did not play an important role for its survival. Hence, it can be said that the presence of diffused water in the spore might not represent a threat for itself. It is important to recall that the studies of Wrestphal et al. (2002) and Driks (1999) were performed using only cultured bacteria and their findings had not been proved with wild bacteria. Considering the above explanation and Figure 44, some of the spores did not swell. This mixture of swelled and non-swelled spores might be due to the mixture of wild and cultured *B. subtilis*. However, because the technique used for this experiment did not allow differentiating between wild and cultured bacteria it cannot be certain that this was the cause.

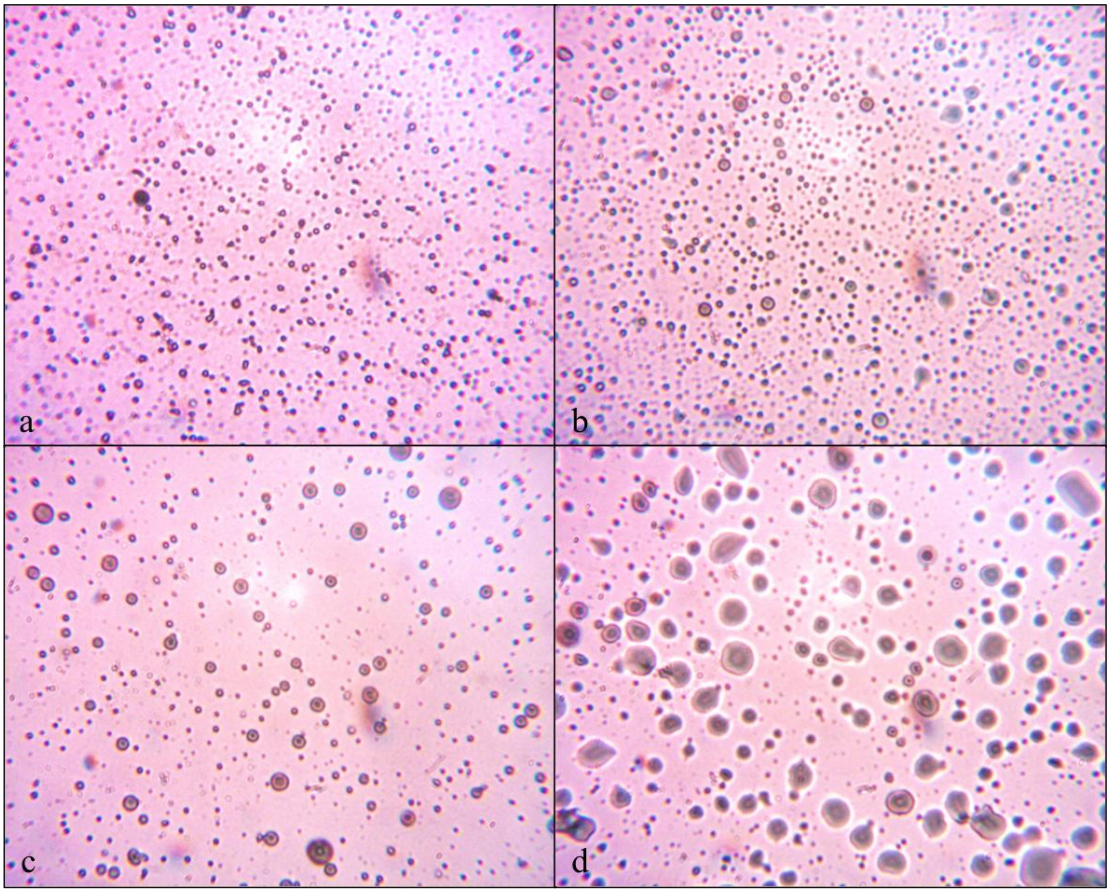

Figure 44 *B. subtilis* spores at (a) 3 minutes, (b) 10 minutes, (c) 15 minutes and (d) 30 minutes of wet heat observed at 100x magnification.

4.3 LABORATORY-SCALE SYSTEMS

4.3.1 Iron leaching

Figure 45 shows the aqueous iron concentration leached out of the five different quantities of IOCS. All the cases produced an iron concentration greater than the maximum concentration, 0.3 mg/L, of the Secondary Standards (National Archives and Records Administration, 2011). In general, the more the IOCS was present in the system, the higher iron concentration was found in the liquid phase.

Figure 46 shows the aqueous iron concentration during the 72 hours of reaction time with a fixed quantity of IOCS at 3 grams. As shown, iron concentration increased with increasing time. Additional data of iron leaching at pH 10 can be found in the Appendix.

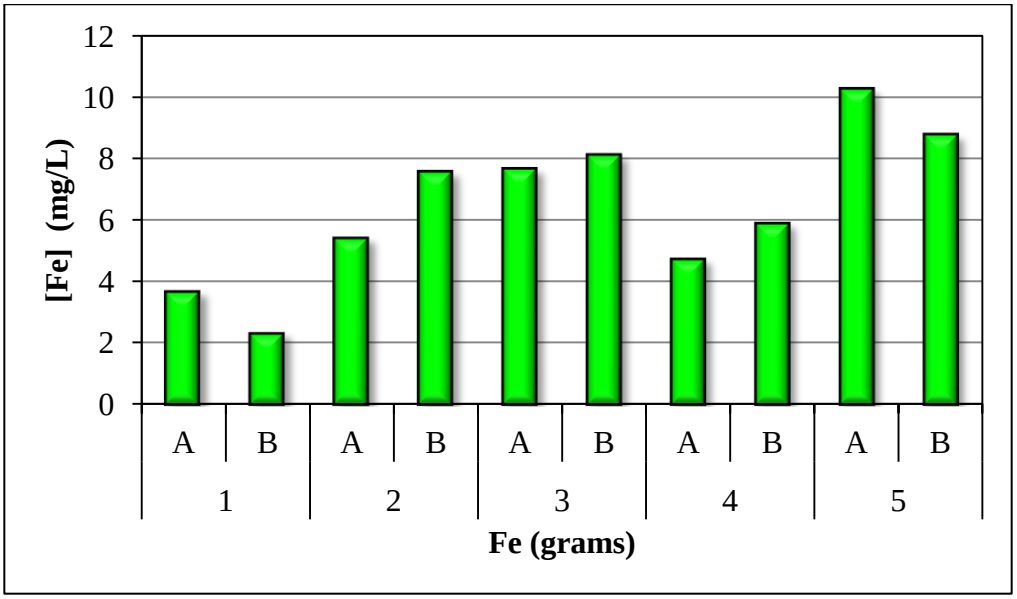

Figure 45 24-hour iron leaching from IOCS at pH 8.6.

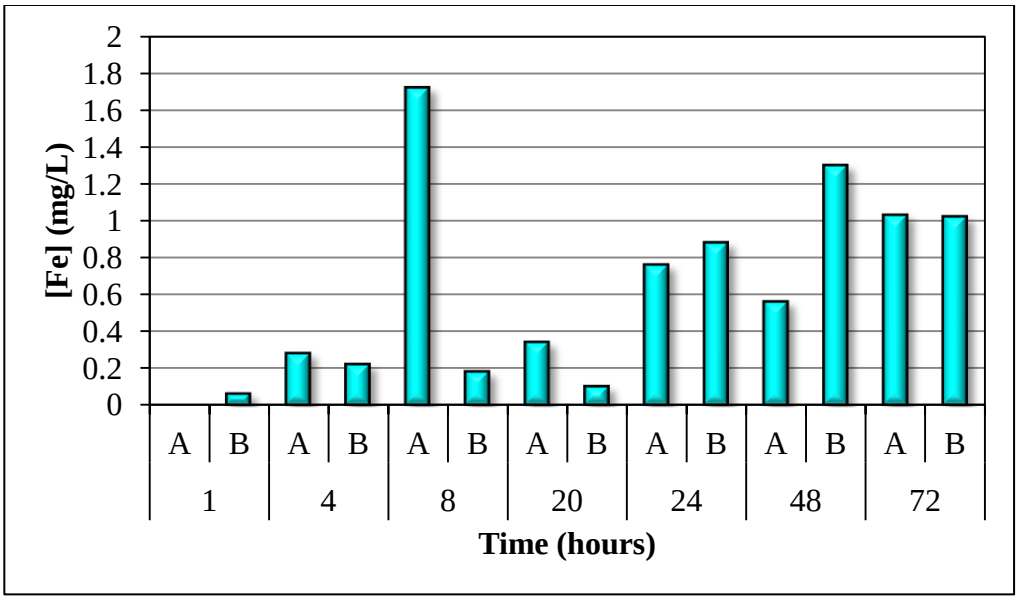

Figure 46 Iron leaching from 3 grams of IOCS at pH 8.6.

4.3.2 Filtration

As mentioned previously, *B. subtilis* inactivation and removal were assessed by using three different packed filters. The hydraulic characteristics of the filters were evaluated with tracer studies and the sampling times for each filter system were determined.

4.3.2.1 Tracer studies

Tracer studies for the filters of System 1 and 2 were performed in replicates at flowrates of 60.6, 11.6 and 1.4 mL/min. Results of System 1 are shown in Figure 47.

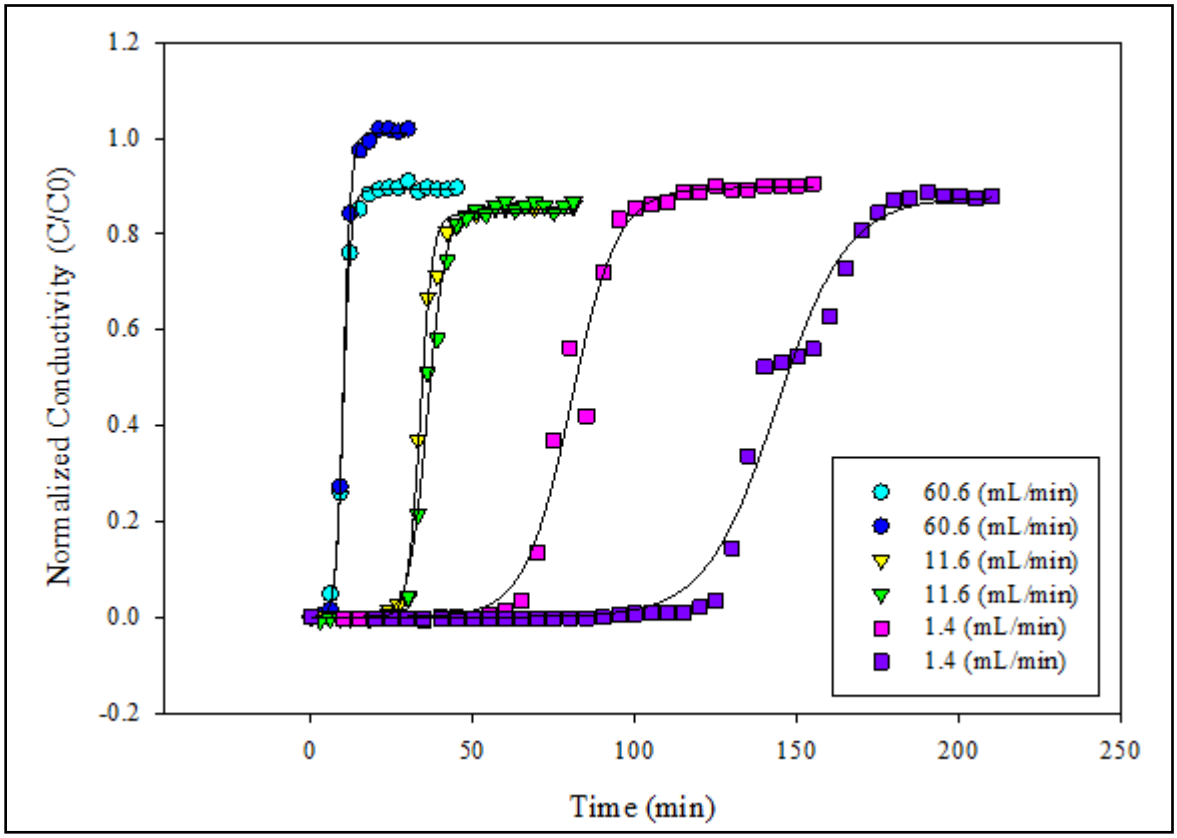

Figure 47 Tracer study results for System 1.

System 1 showed a sigmoidal behavior. Sigmoidal regression was performed using the Sigmaplot with the following equation:

$$f = \frac{a}{1 + e^{-\frac{x - x_0}{b}}}$$

Eq. 5 3-parameter Sigmoidal regression

Where, a is the maximum asymptote, b is the Hill's slope (steepness of the curve) and x_0 is the time of inflection point $(minutes)$.

Regression outputs and their statistical analysis are presented in Table 17. Statistics showed that the Sigmoidal regression effectively described the filter, all values of R^2 were greater than 0.98 and the P-values were less than 0.0001.

Table 17 Equation parameters and statistical results of tracer study for System 1.

Flowrate (mL/min)	Coefficient	Value	Std. Error	P	R^2
60.6	a	1.0096	0.0047	<0.0001	0.9995
	b	1.1557	0.0426	<0.0001	
	x_0	10.155	0.0566	<0.0001	
60.6 (replicate)	a	0.8929	0.0035	<0.0001	0.9991
	b	1.1957	0.0507	<0.0001	
	x_0	10.0179	0.0635	<0.0001	
11.6	a	0.8429	0.0065	<0.0001	0.9966
	b	1.8871	0.1525	<0.0001	
	x_0	33.7594	0.1745	<0.0001	
11.6 (replicate)	a	0.8538	0.0069	<0.0001	0.9968
	b	2.8269	0.1843	<0.0001	
	x_0	35.9585	0.2118	<0.0001	
1.4	a	0.8965	0.0147	<0.0001	0.9882
	b	7.1849	0.7344	<0.0001	
	x_0	80.2843	0.8455	<0.0001	
1.4 (replicate)	a	0.877	0.0184	<0.0001	0.9864
	b	10.8944	0.9654	<0.0001	
	x_0	143.6931	1.1501	<0.0001	

t_{10} values were obtained from Figure 47 and plotted for each flowrate run as shown in Figure 48. An exponential regression of the data gave the equation for the sampling times at different flowrates for System 1 with an R^2 of 0.9604. The equation obtained was

$$t_{10} = 99.26Q^{-0.591}$$

Eq. 6 t_{10} for System 1

where,

t_{10} is the time that takes 10% of the water to pass through the filter, $(minutes)$; and Q is the flowrate $\left(\frac{mL}{min}\right)$.

The hydraulic parameters at flowrates of 60.6, 11.6 and 1.4 mL/min using the previous **Eq. 6** to calculate the t_{10} are presented in Table 18. These values showed that at a very low flowrate (1.4 mL/min), filter had dispersion through all the media. At approximately 10 mL/min the filter behaved as an ideal plug flow reactor (PFR) since the hydraulic retention time (HRT) and t_{10} were practically the same. However, at the highest flowrate, HRT was lower than the t_{10}, indicating short-circuiting. Moreover, the calculated short-circuiting factor (F_{sc}) values indicated that at very low flowrate there was mixed flow, i.e. water passed through the filter media, since F_{sc} was lower than 0.3. In contrast, at higher flowrates, F_{sc} overpassed 1 indicating no mixed flow, i.e. no water contacted with the filter media. Therefore, tracer study showed that water dispersion in the filter was not fully efficient, meaning that its design would work better at very low flowrates. Nevertheless, the flowrate of 60.6 mL/min was chosen for further experiments in order to keep the filtration rate the same between the lab-scale filters and the field scale SEED unit. In such a way, the filtration rate of the lab-scale filters (in 3" diameter) was 1.33

mL/min/cm^2 at 60.6 mL/min, whereas the field-scale SEED filters (in 24" diameter) had the filtration rate of 1.30 mL/min/cm^2 at 1 gpm.

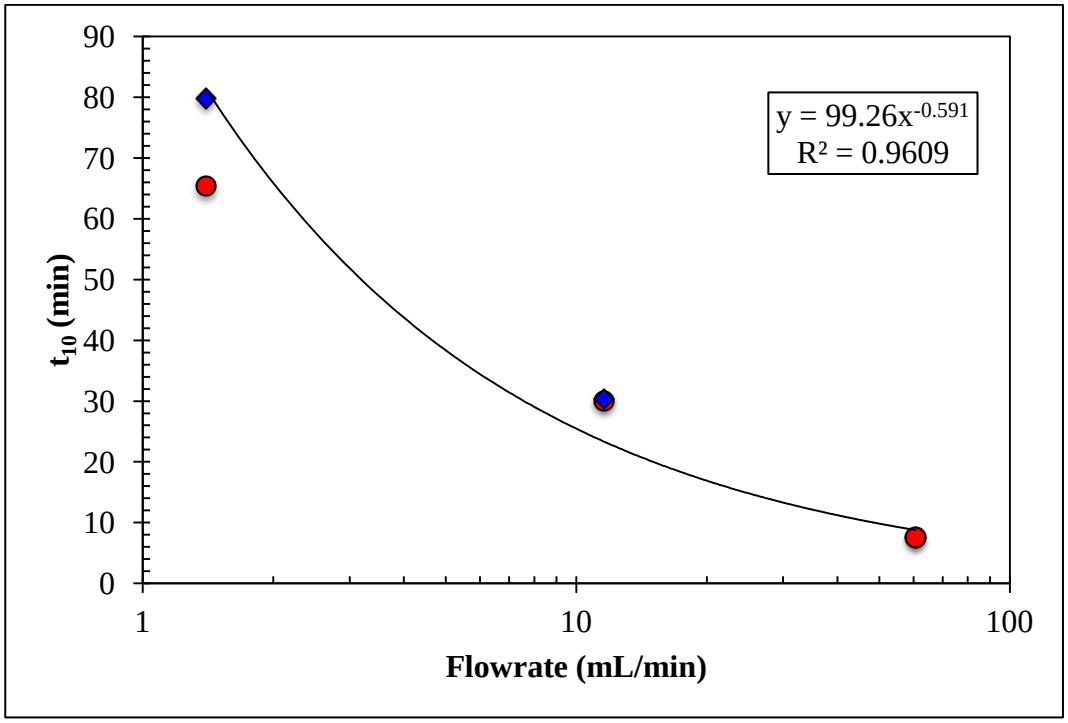

Figure 48 t_{10} values by flowrate for System 1.

Table 18 Hydraulic parameters of System 1.

Parameter	Flowrate (mL/min)		
	60.6	11.6	1.4
t_{10}	7.59	30.22	72.61
HRT	5.74	29.99	248.47
F_{sc}	1.32	1.01	0.292

System 2 (GAC incorporated sand filter) was also submitted to a tracer study and showed the similar results that System 1 did (Figure 49). The data were also fitted using the sigmoidal equation (Eq. 5).

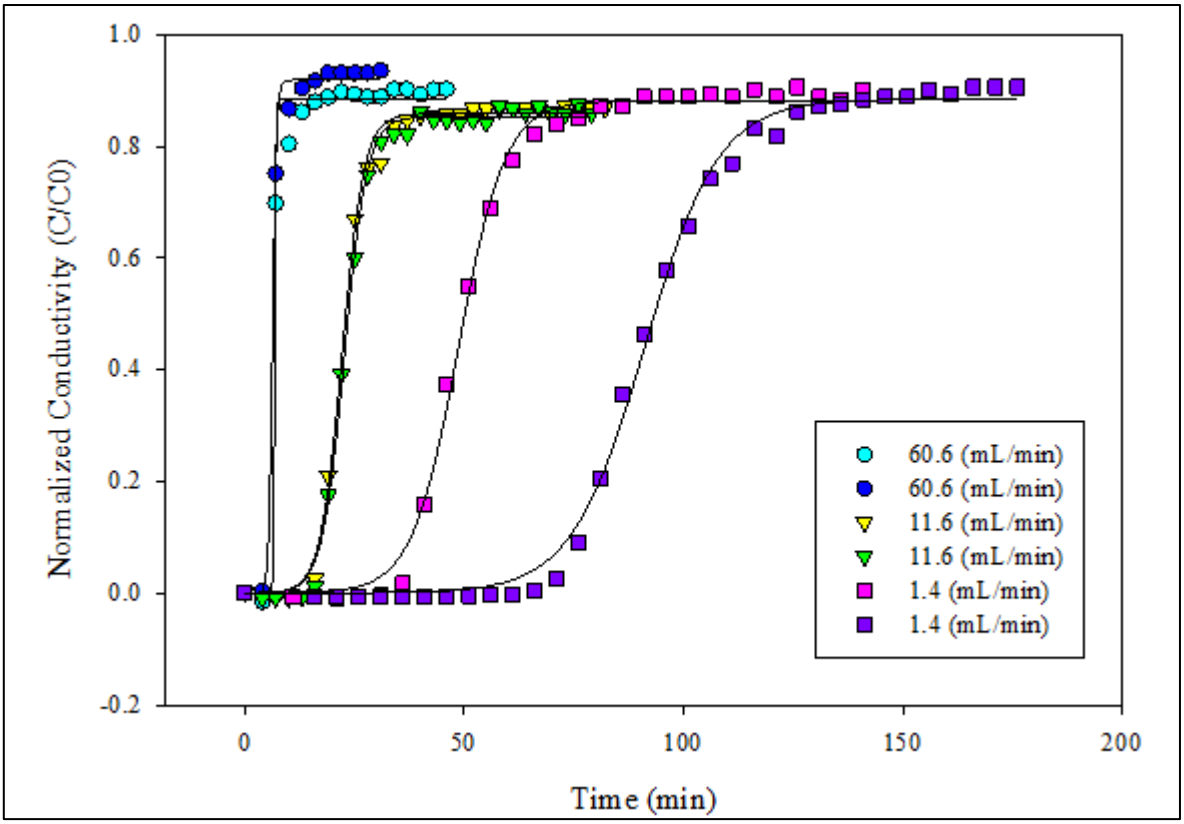

Figure 49 Tracer study results for System 2.

Equation coefficients and statistical analysis for System 2 are presented in Table 19. All values of R^2 were greater than 0.99. However, in case of the run performed at 60.06 mL/min, the P-value for the coefficient b was 0.1201 showing weak evidence of the regression. A high P-value (1) was also obtained from the replicate at this flowrate. In addition, the P-value for the coefficient of x_0 was 0.9999 in the replicate. Based on the results, the sigmoidal three-parameter equation at a flowrate of 60.6 mL/min did not fully fit the data.

Table 19 Equation parameters and statistical results of tracer study for System 2.

Flowrate (mL/min)		Coefficient	Std. Error	P	R^2
60.6	a	0.9185	0.0076	<0.0001	0.9972
	b	0.457	0.2627	0.1201	
	x_0	6.3152	0.3971	<0.0001	
60.6 (replicate)	a	0.8842	0.0072	<0.0001	0.9937
	b	0.1447	54104.8188	1	
	x_0	6.809	71400.7956	0.9999	
11.6	a	0.8583	0.0049	<0.0001	0.9972
	b	2.5092	0.1437	<0.0001	
	x_0	22.1789	0.2201	<0.0001	
11.6 (replicate)	a	0.8527	0.0045	<0.0001	0.9978
	b	2.5588	0.13	<0.0001	
	x_0	22.6816	0.1488	<0.0001	
1.4	a	0.8812	0.0058	<0.0001	0.9969
	b	5.3102	0.2957	<0.0001	
	x_0	48.6944	0.3395	<0.0001	
1.4 (replicate)	a	0.884	0.0066	<0.0001	0.9972
	b	8.3977	0.381	<0.0001	
	x_0	91.1609	0.4419	<0.0001	

Nevertheless, t_{10} was obtained by the sigmoidal equation obtained in Figure 49. The relationship between t_{10} and flowrate Q was as follows (Figure 50):

$$t_{10} = 50.656Q^{-0.464}$$

Eq. 7 t_{10} for System 2

With the above **Eq. 7** and selected flowrate, the first sampling time for the filtration in System 2 was obtained. The t_{10} at a flowrate of 60.6 mL/min was calculated to be 7.52 minutes.

The hydraulic parameters at flowrates of 60.6, 11.6 and 1.4 mL/min are presented in Table 20. Similarly to System 1, at a very low flowrate (1.4 mL/min), filter had dispersion through all

the media as the hydraulic parameters values showed. In contrast to System 1 at a medium flowrate of~10 mL/min, the filter did not behave exactly as an ideal PFR due to inequality of the HRT and t_{10} which performed likewise to the highest flowrate with HRT lower than the t_{10}, also indicating short-circuiting. F_{sc} values at the highest flowrate showed the same behavior as System 1. At very low flow conditions there was mixed flow by indicating with F_{sc} of ~0.3. At the other higher flowrate, F_{sc} overpassed 1 indicating no mixed flow. Likewise, tracer study revealed that water dispersion in the filter was not completely efficient, working better at very low flowrates. Still, the 60.6 mL/min flowrate was chosen for further experiments in order to keep the most similar filtration conditions to the field-scale SEED unit.

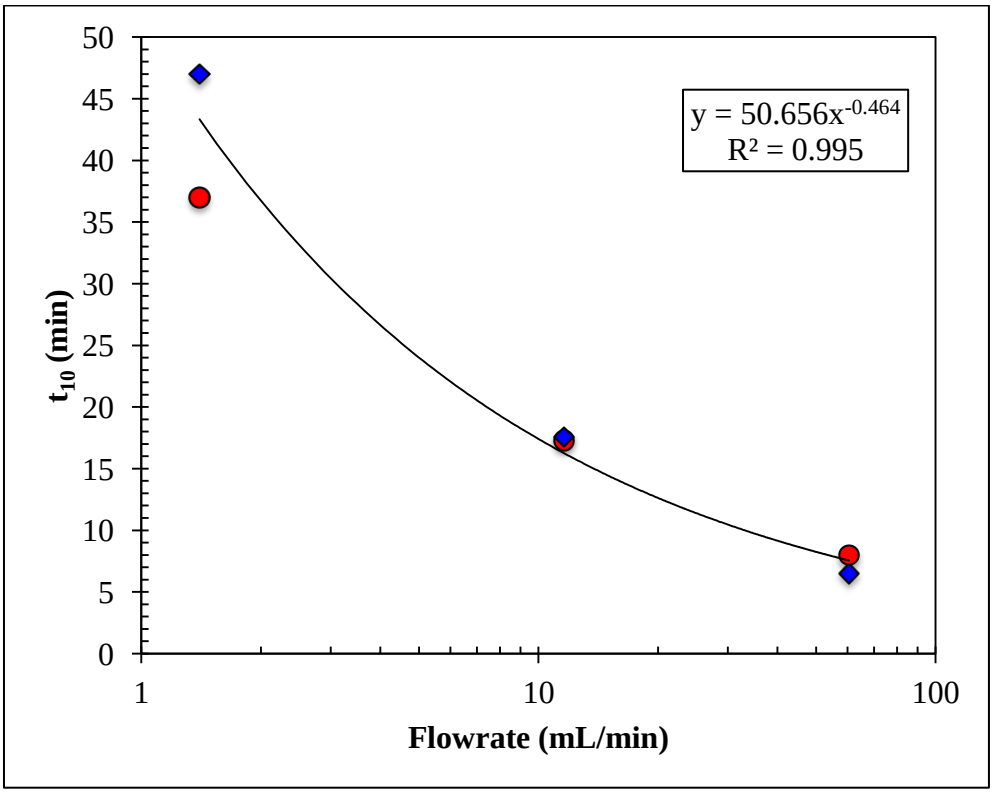

Figure 50 t_{10} values by flowrate for System 2.

Table 20 Hydraulic parameters of System 2.

Parameter	Flowrate (mL/min)		
	60.6	11.6	1.4
t_{10}	7.25	17.45	42
HRT	3.05	15.96	132.24
F_{sc}	2.37	1.09	0.32

System 3 was also submitted to a tracer study and described by the sigmoidal three-parameter equation (Figure 51). Statistical coefficients obtained from the regressions are presented in Table 21. P-values from regression performed at a flowrate of 61 mL/min were as high as 1, indicating that for this flowrate the coefficients obtained might not describe well the water path in the filter, although the R^2 value was as high as 0.9932.

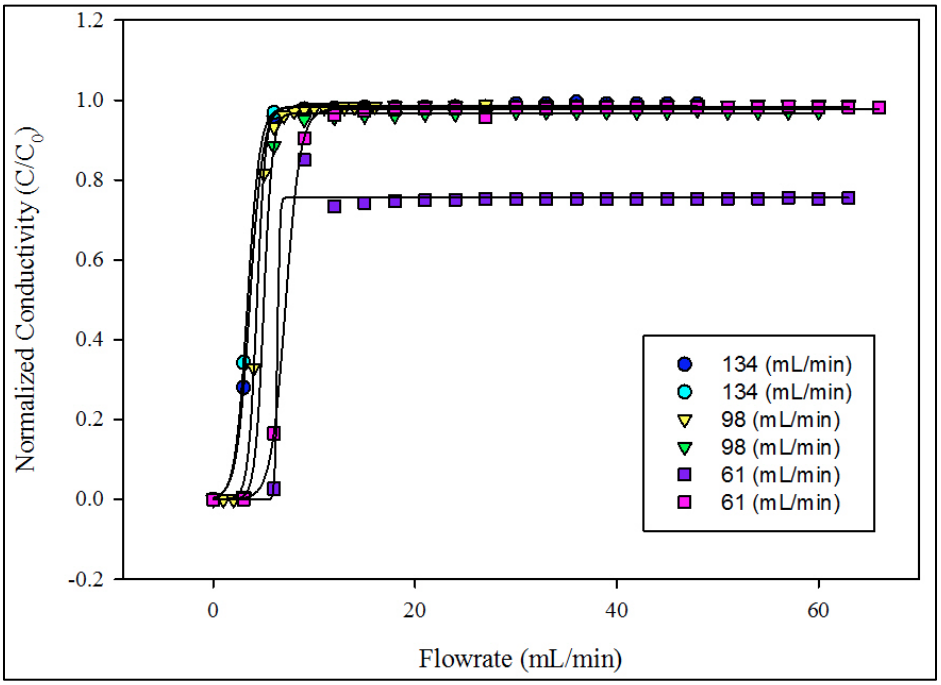

Figure 51 Tracer study for System 3.

Table 21 Equation parameters and statistical results of tracer study for System 3.

Flowrate (mL/min)		Coefficient	Std. Error	P	R^2
134	a	0.9852	0.0016	<0.0001	0.9996
	b	0.6598	0.0365	<0.0001	
	x_0	3.6098	0.0376	<0.0001	
134 (replicate)	a	0.9819	0.0005	<0.0001	1
	b	0.6068	0.018	<0.0001	
	x_0	3.3789	0.0122	<0.0001	
98	a	0.9827	0.0021	<0.0001	0.999
	b	0.4259	0.0152	<0.0001	
	x_0	4.3155	0.0182	<0.0001	
98 (replicate)	a	0.967	0.0014	<0.0001	0.9996
	b	0.424	0.0412	<0.0001	
	x_0	4.9931	0.0996	<0.0001	
61	a	0.7558	0.0052	<0.0001	0.9932
	b	0.1041	6652979.479	1	
	x_0	6.3424	21887091.45	1	
61 (replicate)	a	0.9781	0.0015	<0.0001	0.9996
	b	0.7306	0.0191	<0.0001	
	x_0	7.164	0.0347	<0.0001	

The t_{10} values were obtained (Figure 51) for each run and were plotted against the flowrate (Figure 52). The equation obtained was:

$$t_{10} = 1121.7Q^{-1.268}$$

Eq. 8 t_{10} for System 3

Having obtained the equation for t_{10}, the sampling times were then determined for the experiment. The t_{10} at a flowrate of 61 mL/min for System 3 was 6.11 minutes (calculated from **Eq. 8**). For each flowrate, its respective hydraulics parameters are obtained as shown in Table 22. Differing from Systems 1 and 2, none of the three flowrates assessed achieved an HRT greater than their corresponding t_{10}, hence F_{sc} values were greater than 1. This was not a surprise since

the plots of the tracer study (Figure 51) showed a step input (PFR) behavior. Difference in flowrate was quite high and did not allow to make a more detailed comparison with System 3.

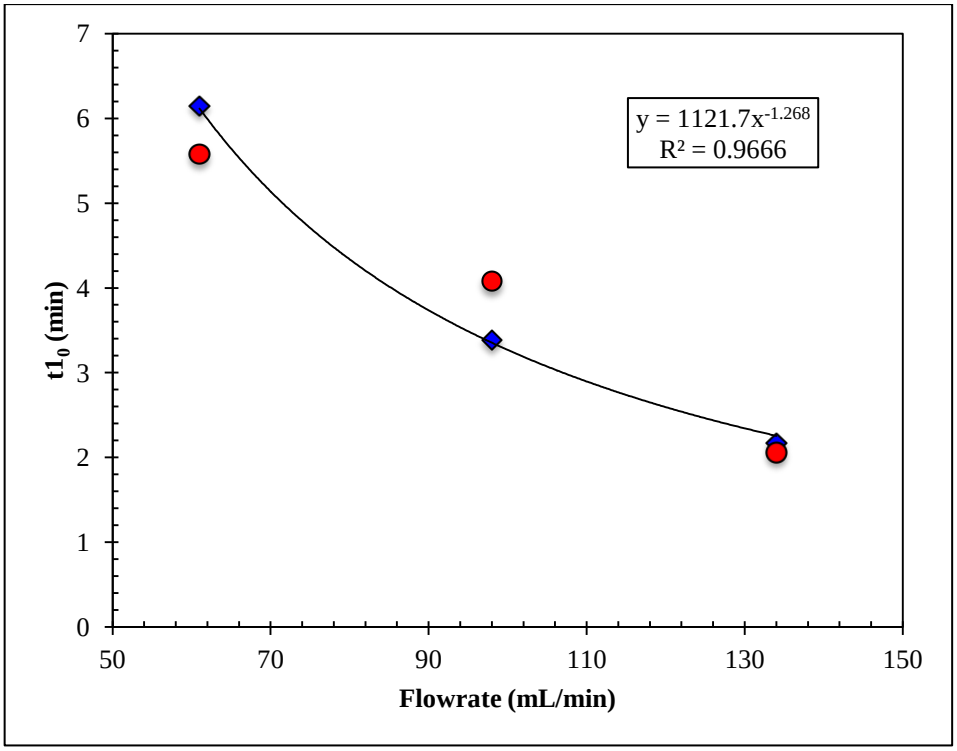

Figure 52 t_{10} values by flowrate for System 3.

Table 22 Hydraulic parameters of System 3.

Parameter	Flowrate (mL/min)		
	134	98	68
t_{10}	2.11	3.73	5.86
HRT	1.16	2.13	3.08
F_{sc}	1.82	1.75	1.90

4.3.2.2 *B. subtilis* removal by filtration

The three filter systems were run using the sampling times determined by the tracer studies. The first filter system assessed was System 1 and the results are presented in Figure 53. *B. subtilis* numbers at the influent of the filter were fluctuated from 800 to 12,400 CFU/100 mL. At the

effluent of such system, the numbers of bacteria were from 100 to 8,700 CFU/100 mL over filtration equivalent to 10 pore volumes. Therefore, performance of filters (i.e., *B. subtilis* removals) fluctuated between a minimum negative value of -948 % and a maximum of 98 % *B. subtilis* removal. Negative values of removals might be due to adhesion of spores to the water-air interface caused by pores of smaller size than the diameter of the spores rather than to the attachment of the spores to the silica sand (Chen et al., 2010).

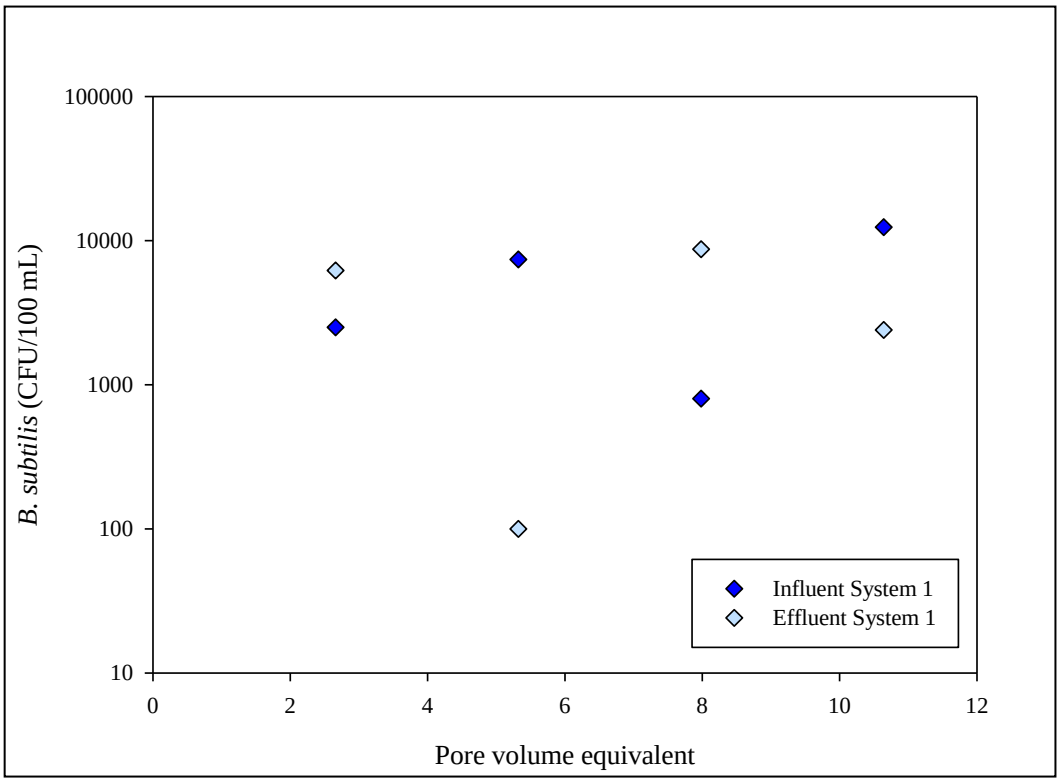

Figure 53 Influent and effluent *B. subtilis* number from System 1.

GAC filter (System 2) efficiency was assessed over 10 pore volumes equivalent and the numbers of *B. subtilis* at the influent and effluent of filtration are shown in Figure 54. The numbers of bacteria ranged between 4,000 and 12,600 CFU/100 mL at the influent of the filter, whereas at the effluent from 6,900 to 35,300 CFU/100mL. All *B. subtilis* percent removals from

System 2 showed negatives values, from -17% to -1,581%, obtaining the highest negative percent removal at 10.2 pore volume equivalent. This behavior might be due to the ability of GAC to attach microorganisms on its surface area, limiting the performance of the filter. A similar result was obtained but for the removal of *E. coli*, MS 2 bacteriophage and anaerobic spores by GAC filters (Highnen et al., 2010). In contrast, the removal of *Giardia* and *Cryptosporidium* by GAC filters (Highnen et al., 2010) (1.3-2.7 log removal) was opposite to the results obtained in this study.

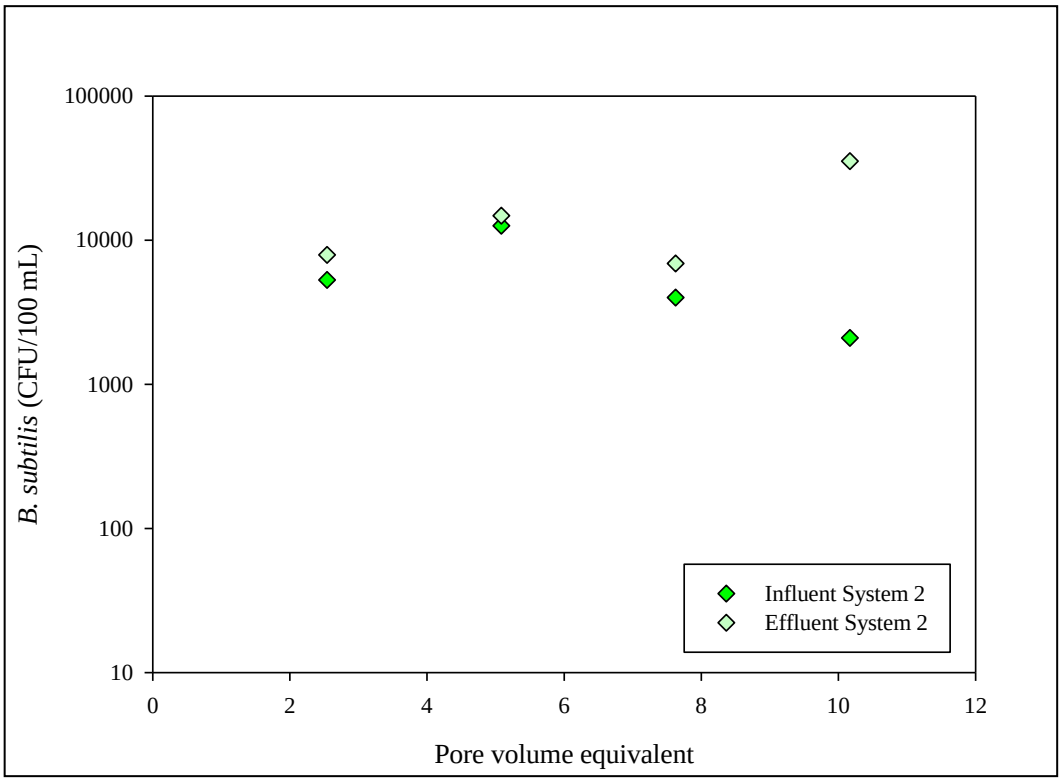

Figure 54 Influent and effluent *B. subtilis* number from System 2.

IOCS filter (System 3) performed much better than Systems 1 and 2 (Figure 55) showing 2,400 to 17,000 CFU/100 mL at the influent and 1,000 to 9,600 CFU/100 mL at the effluent. Effectiveness of the IOCS filter was assessed by calculating the percent removal (Table 23) and a maximum of 92.1 % (~1.1 log removal) was achieved. In contrast with other Systems (1 and 2),

percent removal obtained in this System 3 were decreasing with increasing pore volume equivalent which might indicate saturation of the filter. Likewise, Diao and Yao (2009) obtained a 95% inactivation of *B. subtilis var. niger* using 1 mg/L of zero-valent iron nanoparticles and 100% inactivation when treated with 10mg/L of the nanoparticles. Higher removals by the use of an IOCS had been obtained when inactivating viruses. Bradley et al., (2011) tested biofilters packed with iron oxide amended sand and obtained 5 log removal of MS2 bacteriophages compared to 0.5 log removal with the sand biofilter. However, Pecson et al. (2012) showed that MS2 adsorbed onto IOCS could be released again to the filtrate.

Samples of System 3 were also evaluated for possible iron leaching in the effluent. Table 23 shows the iron concetration from the samples taken and assessed. Results showed that iron concentration throughout the experiment was lower than 0.3 mg/L, the maximum concentration of the Secondary Standards (National Archives and Records Administration, 2011).

Among the three filter systems, System 3 showed more consistency in the removal of *B. subtilis* since sustained positive values. However, the good of this study was for the optimization of small water treatment for rural communities with scarce economical resources. IOCS preparation in a large scale was neither practical nor economical for such communities. Hence, System 1, which was the second best with *B. subtilis* removal, was the most appropriate system and was, therefore, chosen for further assessment.

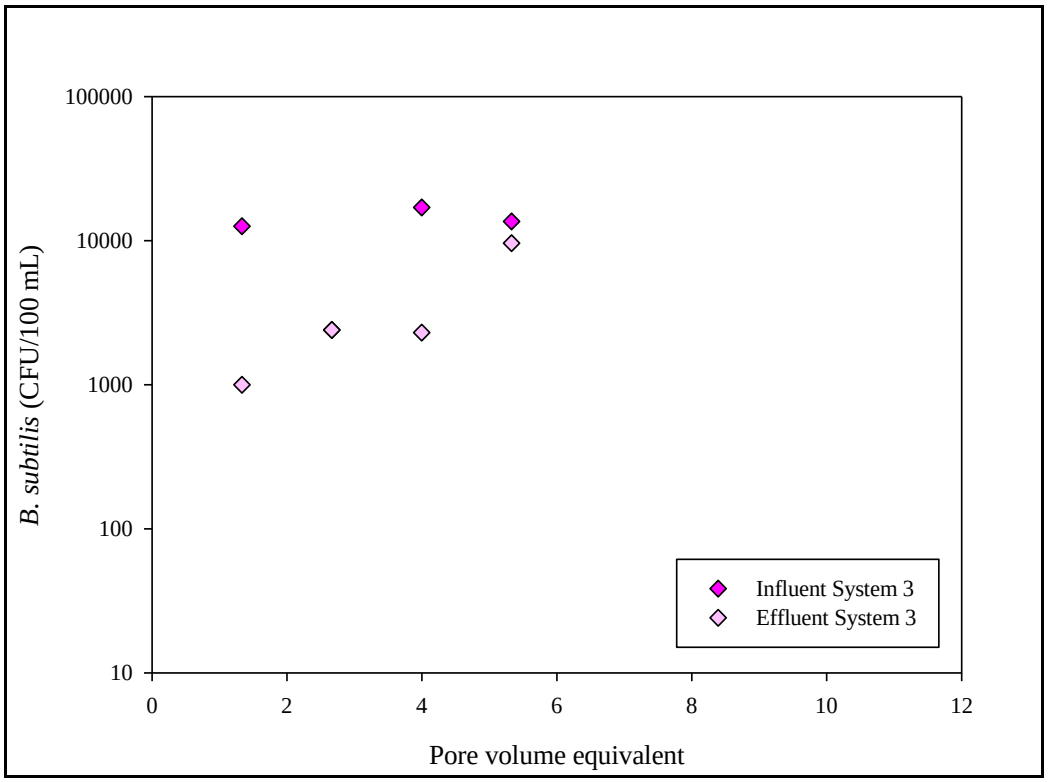

Figure 55 Influent and effluent *B. subtilis* number from System 3.

Table 23 Percent of *B. subtilis* removal and Fe leachate from filter of System 3.

Sampling time (min)	Pore volume equivalent	% *B. subtilis* removal	Fe (mg/L)
3.8	1.332	92.1	0.06
7.6	2.664	0	0.01
11.4	3.997	86.5	0
15.2	5.329	29.4	0

4.3.3 Hom model

After performing a series of batch experiments at the initial Cl_2 concentrations of 2, 5, 10 and 20 mg/L, and contact times, the Cl_2 residual and *B. subtilis* concentrations were obtained (Table 24) and the percent removal were calculated (Figure 56).

Table 24 Cl_2 and *B. subtilis* concentration at varying contact time for Hom equation.

Initial [Cl_2]	Residual [Cl_2]	t	N_0	N_f
2	0.08	17	2000000	500
	0.07	40	2000000	400
	0.06	57	2000000	400
5	0.33	15	2000000	300
	0.25	30	2000000	500
	0.27	40	2000000	100
10	0.32	10	2000000	800
	0.25	20	2000000	200
	0.23	29	2000000	200
20	0.88	5	2000000	700
	0.79	10	2000000	300
	0.69	20	2000000	100

Note: Initial and Residual [Cl_2] in mg/L, t is the contact time in minutes and N_f is the final *B. subtilis* concentration in CFU/100 mL

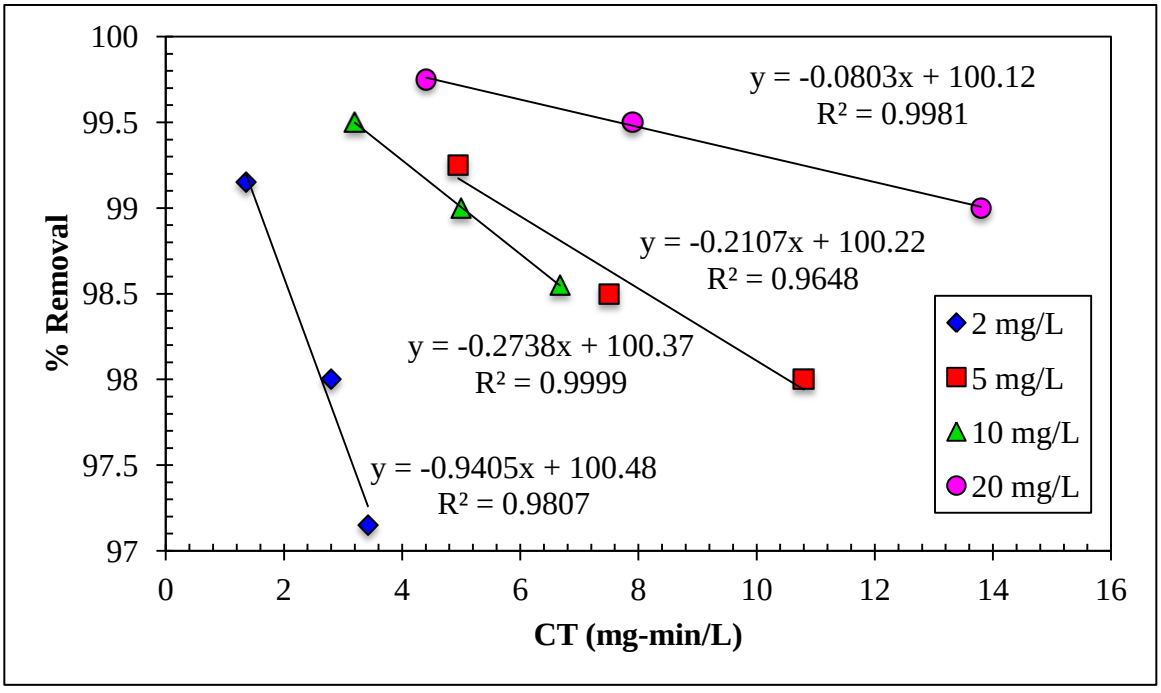

Figure 56 *B. subtilis* percent removal by disinfection in batch experiment.

All percent removals were between 97 and 99.75 %. These percent removals were high enough to suggest that inactivation of *B. subtilis* could be obtained only by chlorination (highest

removal was 2.6 log) as *G. lamblia* inactivation studies had achieved (Jarroll et al., 1981). Subsequently, the data (Table 24) were then fitted with a Multiple Linear Regression to obtain the parameters of the equation of the *B. subtilis* removal with disinfection. The final equation was as follows:

$$\ln\left(-\ln\frac{N}{N_0}\right) = 1.521 + 0.108\ \ln C + 0.163\ \ln t$$

Eq. 9 Empirical Hom Model

Using the above equation, the residual Cl_2 concentration was calculated in such a way to comply with the 3-log removal of *Giardia*, standard of the USEPA. Substituting 3 log in the $-\ln\frac{N}{N_0}$ term and 17.7 minutes as the t_{10} of the disinfection chamber in **Eq. 9** gives:

$$\ln(3) = 1.521 + 0.108\ \ln C + 0.163\ \ln(17.7)$$

$$C = 0.000262\ \text{mg/L}$$

In the case of the USEPA standard for *Cryptosporidium*, 2-log removal, substitution of 2 log and 17.7 minutes in **Eq. 9** gives:

$$\ln(2) = 1.521 + 0.108\ \ln C + 0.163\ \ln(17.7)$$

$$C = 6.13\ \text{x}10^{-6}\ \text{mg/L}$$

Yet the residual Cl_2 concentrations were found to be lower than the MRDL and still were lower than the range proposed by the WHO Guideline of Drinking Water Quality (>0.5mg/L) (WHO, 2011). This indicates that chlorination by itself would inactivate *B. subtilis* in a 3 log removal as required by the SWTR of the USEPA but will not yield an optimum residual chlorine

to prevent microbial contamination in the distribution lines. On the contrary, *G. lamblia* inactivation parameters (Table 1) yielded a higher residual Cl_2 (1.5 mg/L) that was within the WHO guidelines and the MRDL.

4.3.4 Disinfection

4.3.4.1 Disinfection chambers tracer studies

The disinfection basin constructed was also submitted to a tracer study to determine the hydraulic characteristics, by which sampling times were to be chosen. Results are shown in Figure 57.

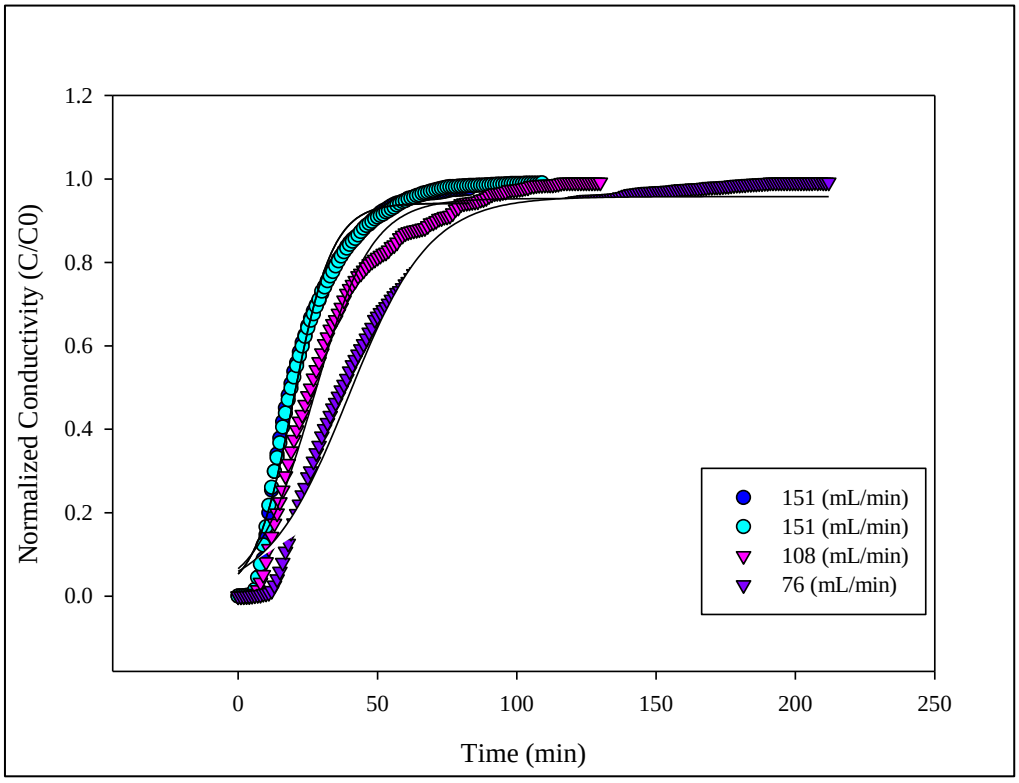

Figure 57 Tracer study results of disinfection basin.

The 3-parameter sigmoidal equation fitted the tracer curves (Eq. 5).

Table 25 provides the coefficients of the aforementioned equation. As shown, very good P-values (<0.0001) and R^2 (0.98) were obtained. t_{10} values were obtained as well and plotted for each flowrate (Figure 58). These data were further submitted to a linear regression to obtain the equation of the line:

$$t_{10} = -0.1039Q + 23.922$$

Eq. 10 t_{10} for disinfection basin

where, t_{10} is the time that takes 10% of the water to pass through the filter, $(minutes)$; and Q is the flowrate $\left(\frac{mL}{min}\right)$.

Using the above equation (**Eq. 10**), the t_{10} at 60 mL/min was calculated to be 17.7 minutes and the HRT was 61.2 minutes. These times were the first two sampling times used. Hydraulic parameters for the disinfection basin verified the baffling condition of the chamber (Table 26). Outcomes of the tracer study showed that the disinfection basin behave as a typical continuous input tracer reactor with a dead volume (stagnant region). Therefore, in the stagnant region the tracer, which in this study was NaCl, did not react with the basin water (no mixing of flow) (Figure 57) (Fogler, 2006). The best time in which this behavior was noticed was during the t_{10} of the basin. Thus, this study also served to verify if the basin constructed would comply with the establishment of the USEPA Enhanced Surface Water Treatment Rule in using the t_{10} as the time for CT determination (USEPA, 2006). Moreover, all flowrates indicated a poor condition of baffling in terms of F_{sc} ($0.32 < F_{sc} < 0.37$).

Table 25 Equation parameters and statistical results from tracer study of disinfection chamber.

Flowrate (mL/min)	Coefficient	Value	Std. Error	P	R^2
151	a	0.9417	0.0075	<0.0001	0.9807
	b	7.0336	0.3194	<0.0001	
	x_0	19.823	0.3566	<0.0001	
151 (replicate)	a	0.9417	0.0075	<0.0001	0.9807
	b	7.0336	0.3194	<0.0001	
	x_0	19.823	0.3566	<0.0001	
108	a	0.9533	0.0054	<0.0001	0.981
	b	10.4117	0.3624	<0.0001	
	x_0	27.0918	0.3976	<0.0001	
76	a	0.9577	0.0037	<0.0001	0.9822
	b	14.583	0.3941	<0.0001	
	x_0	39.5584	0.4339	<0.0001	

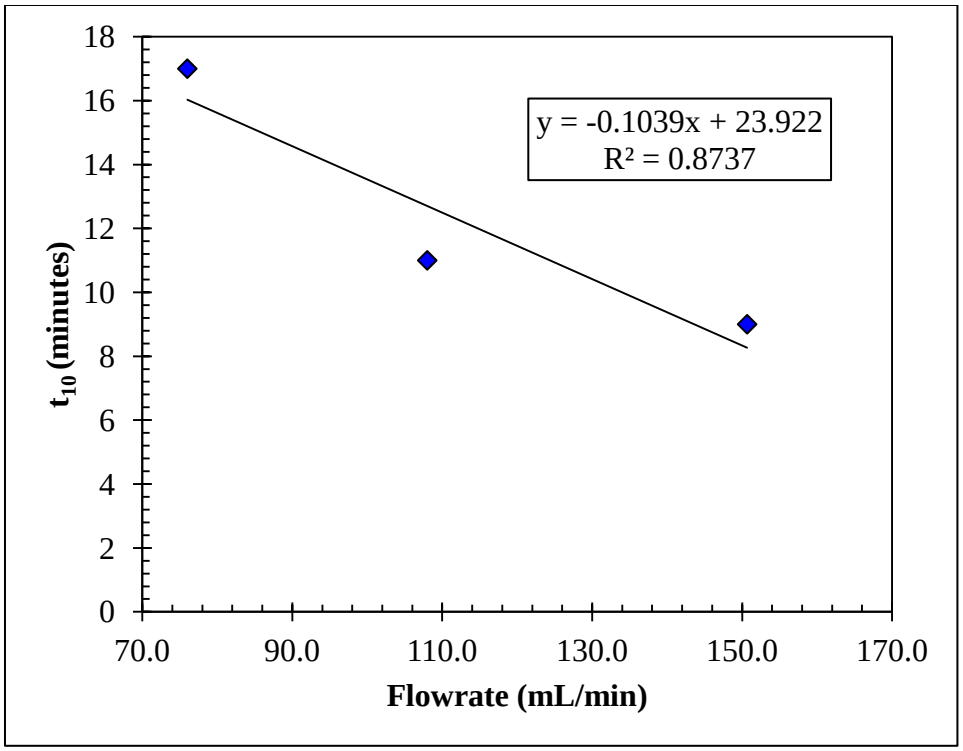

Figure 58 t_{10} values by flowrate for disinfection basin.

Table 26 Hydraulic parameters for the disinfection basin.

Parameter	Flowrate (mL/min)		
	150.7	108.3	76
t_{10}	9	11	17
HRT	24.38	34.02	48.34
F_{sc}	0.37	0.32	0.35

4.3.4.2 *B. subtilis* removal by disinfection

B. subtilis removal and inactivation by disinfection were successfully performed over 60 CT (Figure 59). A three-parameter Exponential Rise to Maximum regression was performed using the Sigmaplot with the following equation with coefficients' values of **Eq. 11** and statistical parameters presented in Table 27.

$$f = y_0 + a(1 - e^{-bx})$$

Eq. 11 B. subtilis percent removal by disinfection basin

Where, y_0 is the y-intercept; a is the amplitude of the curve; and b is the rise factor.

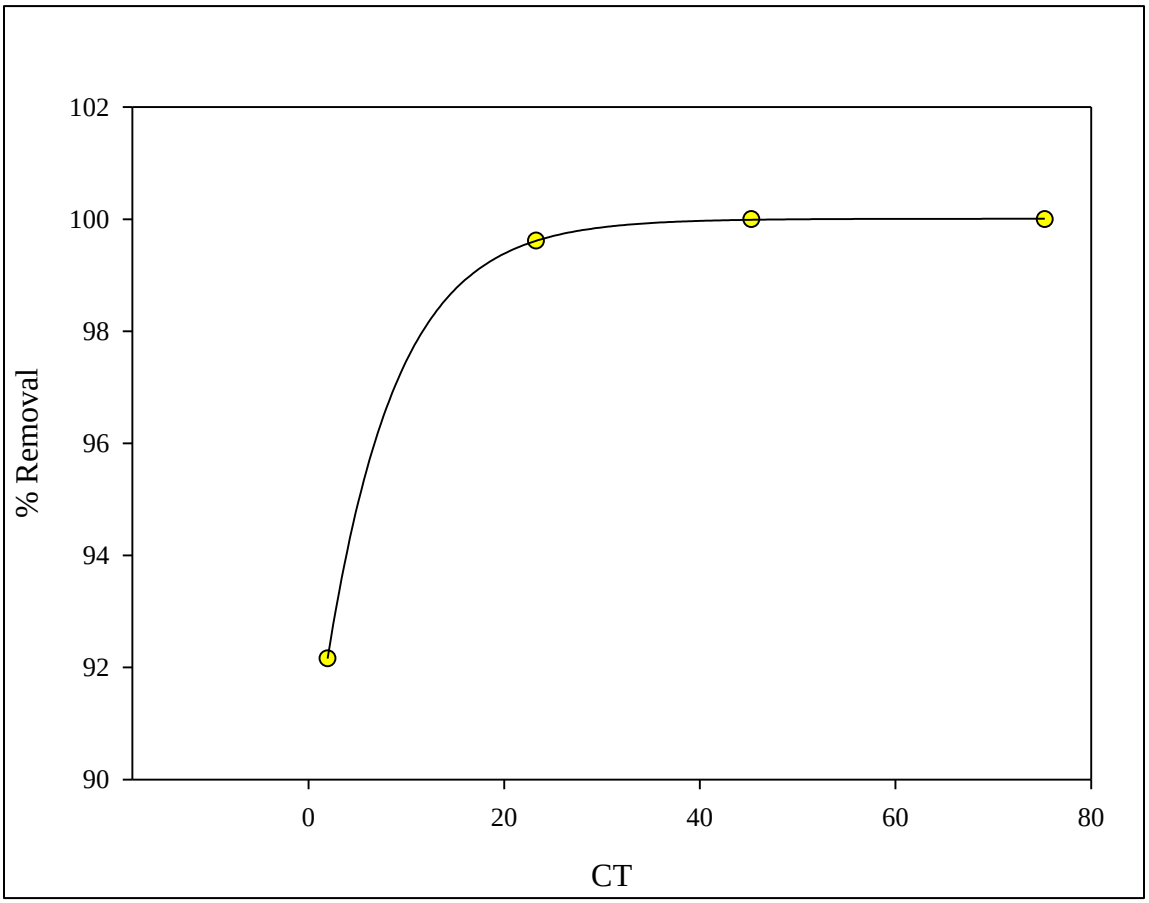

Figure 59 *B. subtilis* removal by disinfection.

Table 27 Equation parameters and statistical results of disinfection.

	Coefficient	Std. Error	P	R^2
y_0	89.6879	0.0401	0.0003	1
a	10.3207	0.0364	0.0022	
b	0.1404	0.0019	0.0085	

The efficiency of the disinfection basin was evaluated by the calculation of the inactivation of *B. subtilis* by percent removals. Such values resulted in high percent removals, with 92 % (1.1

log removal) being the least removal achieved for the first sample taken at 1.95 mg-min/L (17.7 minutes). Higher percent removals were achieved with increasing CT (up to 100% removal) and, hence, were in accordance with the performed tracer study of the disinfection basin. Synergistic studies had been performed with ozone, UV, chlorine dioxide (ClO_2), H_2O_2 and free chlorine for the inactivation of the *B. subtilis* spores (Cho et al., 2011; Cho et al., 2006) (Table 28). Although their results showed a similar behavior between them, they still were lower than those from the current study. However, the current study was performed with a free chlorine stock solution considerably higher (5.6 to 560 times) than the aforementioned studies.

Table 28 *B. subtilis* inactivation by free chlorine stock solutions of 300 mg/L (Cho et al., 2006) and 0.1-3 mg/L (Cho et al., 2011).

Cho, 2006		Cho, 2011	
Log removal	CT (mg-min/L)	Log removal	CT (mg-min/L)
0	90	0.1	60
0.2	175	0.55	120
1	250	1.3	180
1.8	330	2.1	240
2.4	410	2.9	300
		3.6	360

Residual free chlorine measurements ranged from 0.11 to 0.41 mg/L (Figure 60). These residual concentrations were found to be approximately the same (average of 0.387 mg/L) except for the first sample that was taken before the HRT of the disinfection basin. Moreover, these measurements comply with the National Primary Drinking Water Primary Standards (MRDL = 4 mg/L) (USEPA, 2009).

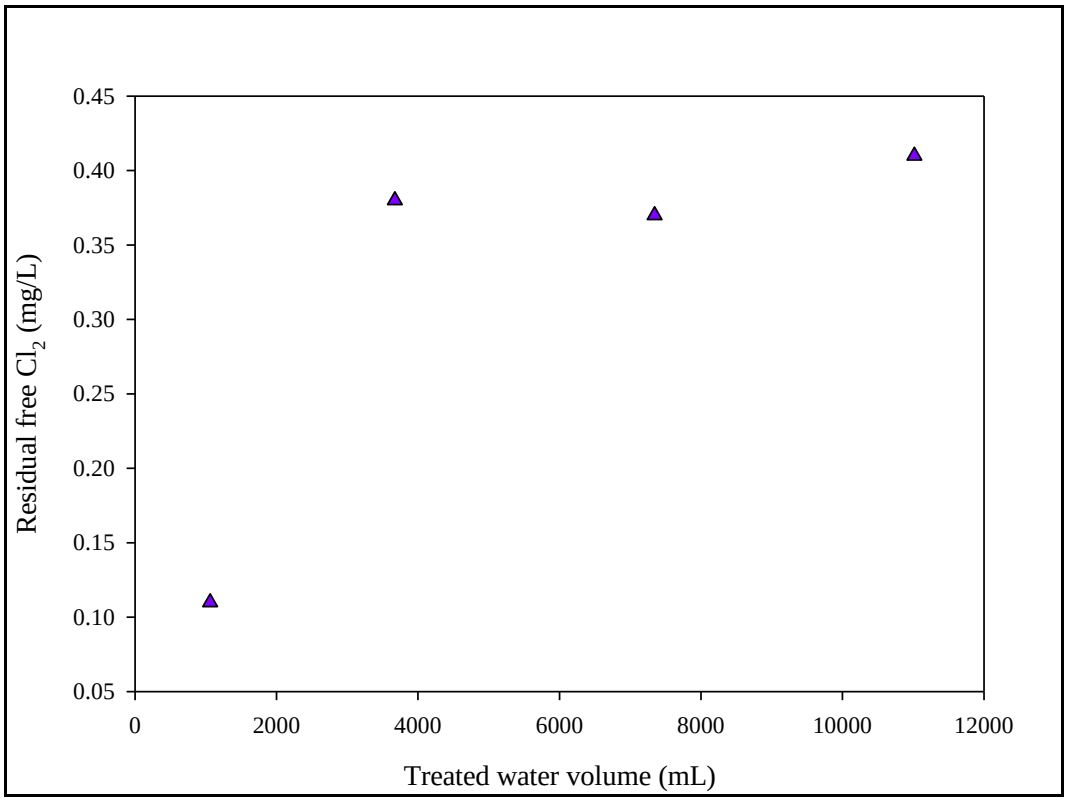

Figure 60 Residual free Cl_2 concentrations during disinfection.

Comparing residual chlorine concentrations of Hom model with the values obtained in the disinfection basin, it was noticed that the Hom model appeared to have a lower residual concentration than the disinfection basin. Moreover, differences in the initial concentrations were extremely different between two approaches. This difference might be due to difference in reactors: the Hom model used a batch reactor, whereas the disinfection basin behaved as a continuous flow reactor (CSTR). The Hom model approaches for different reactors and order reactions with their equivalent equations are presented in Table 29 (Fogler, 2006).

Table 29 Kinetic expressions.

Reactor type	Order of reaction	
	Zero order	First order
Batch	$kt = C_0 - C$	$kt = \ln C_0/C$
CSTR	$kt = C_0 - C$	$kt = (C_0 - C) - 1$

4.3.4.3 Effect of disinfection on spores

Batch experiments with varying doses of Cl_2 and contact times were performed to visualize the effect of the disinfection extent on the spores. Figure 61 shows the *B. subtilis* spores of the first batch experiment performed. Wet heat treatment influenced the size of the spore, as proved in the section 4.2.1, by decreasing them after submitted to the cold treatment. In contrast, the effect of increased Cl_2 doses on the spores was not clear.

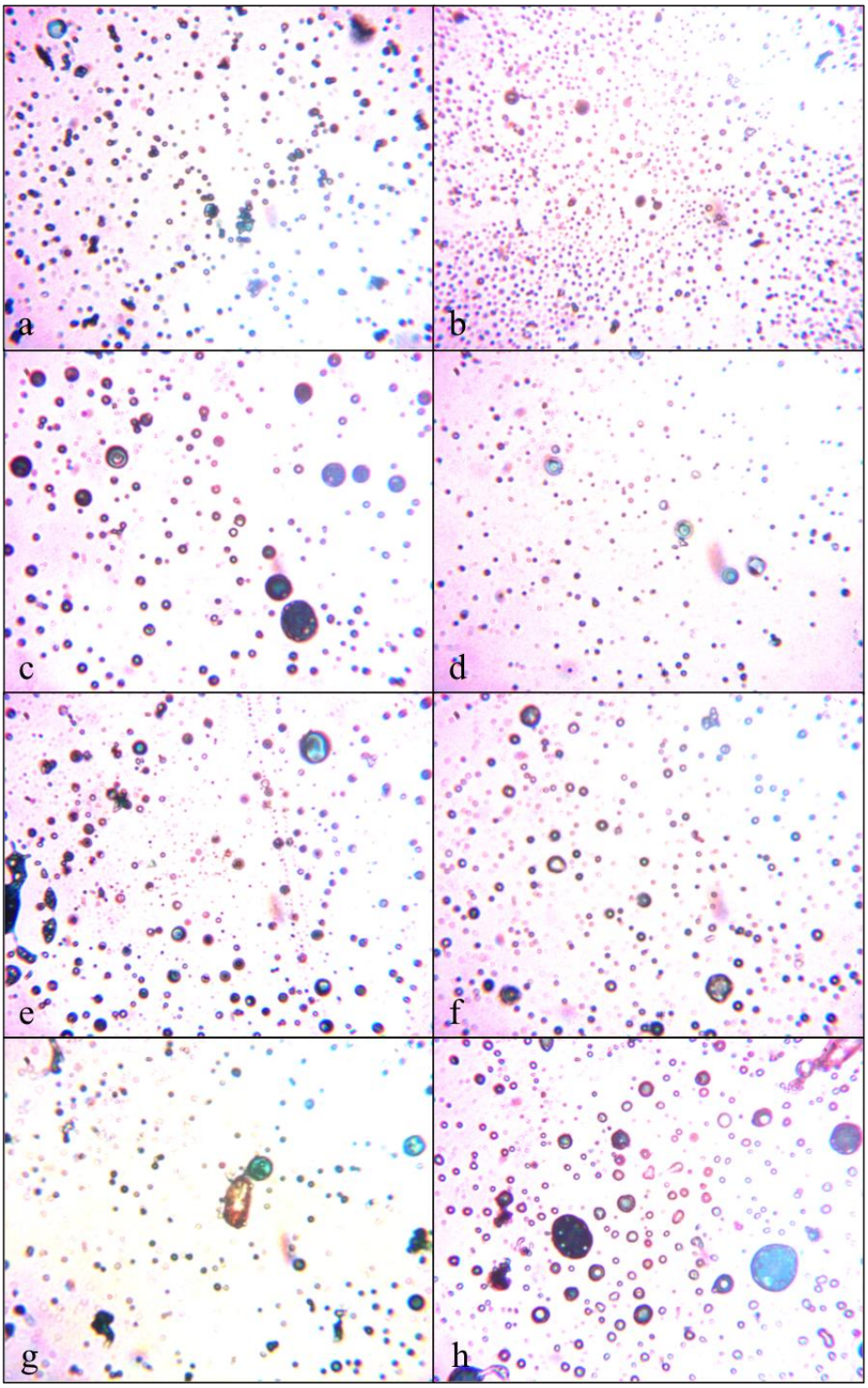

Figure 61 *B. subtilis* spores after 30 minutes contact time at initial Cl_2 concentration of (a) 0 mg/L after heat treatment, (b) 0 mg/L after cold treatment, (c) 2 mg/L after heat treatment, (d) 2 mg/L after cold treatment, (e) 5 mg/L after heat treatment, (f) 5 mg/L after cold treatment, (g) 10 mg/L after heat treatment and (h) 10 mg/l after cold treatment observed at 100x magnification.

Figure 62 and Figure 63 shows the results from the second batch experiment. In both Cl_2 doses, i.e. 10 and 20 mg/L, the size of spores increased with increasing contact times, supporting the experiment performed without disinfectant and presented previously in Figure 44. No significant difference in size was noticed between the two doses. *B. subtilis* number decreased with decreasing Cl_2 dose. This spore resistance to Cl_2 could be due to two major factors: the outer coat of the spore and the low permeability of the inner membrane (Setlow, 2006; Young and Setlow, 2003).

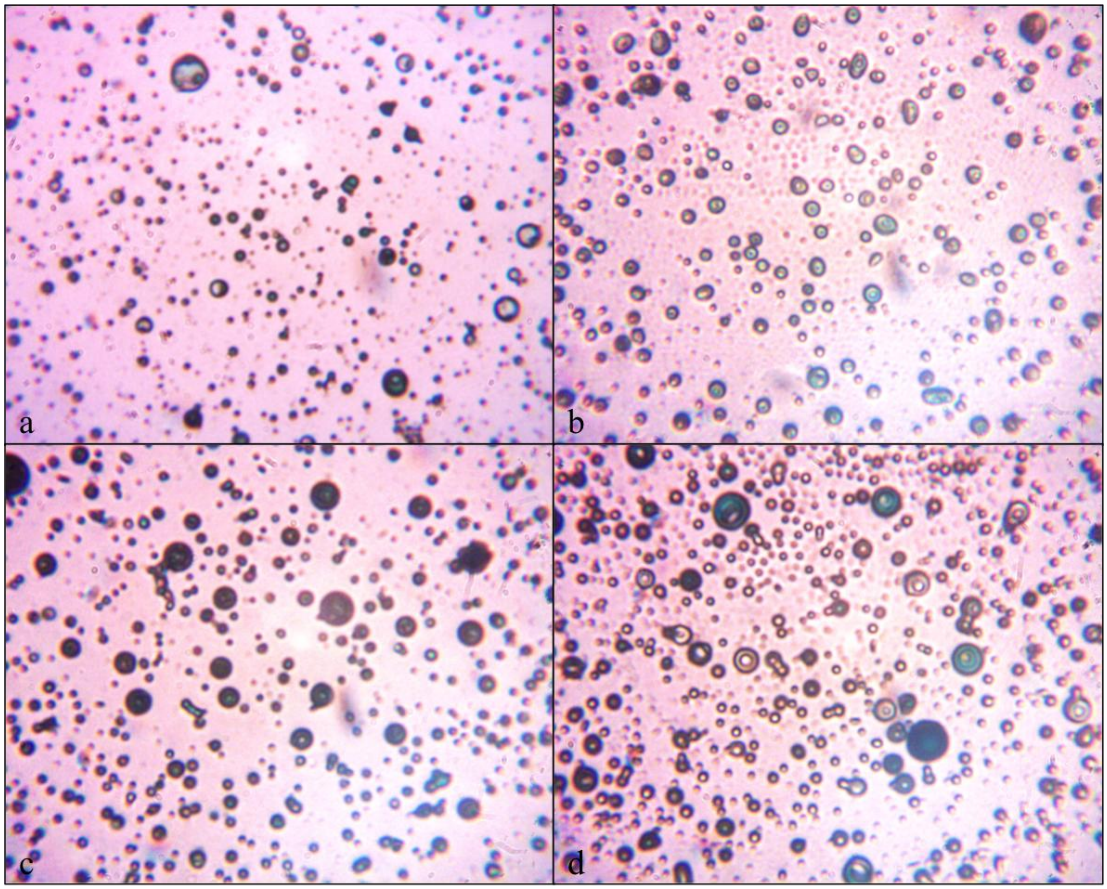

Figure 62 *B. subtilis* spores after 30 minutes contact time of 10 mg/L Cl_2 initial concentration at (a) 3 minutes, (b) 10 minutes, (c) 15 minutes and (d) 30 minutes of wet heat observed at 100x magnification.

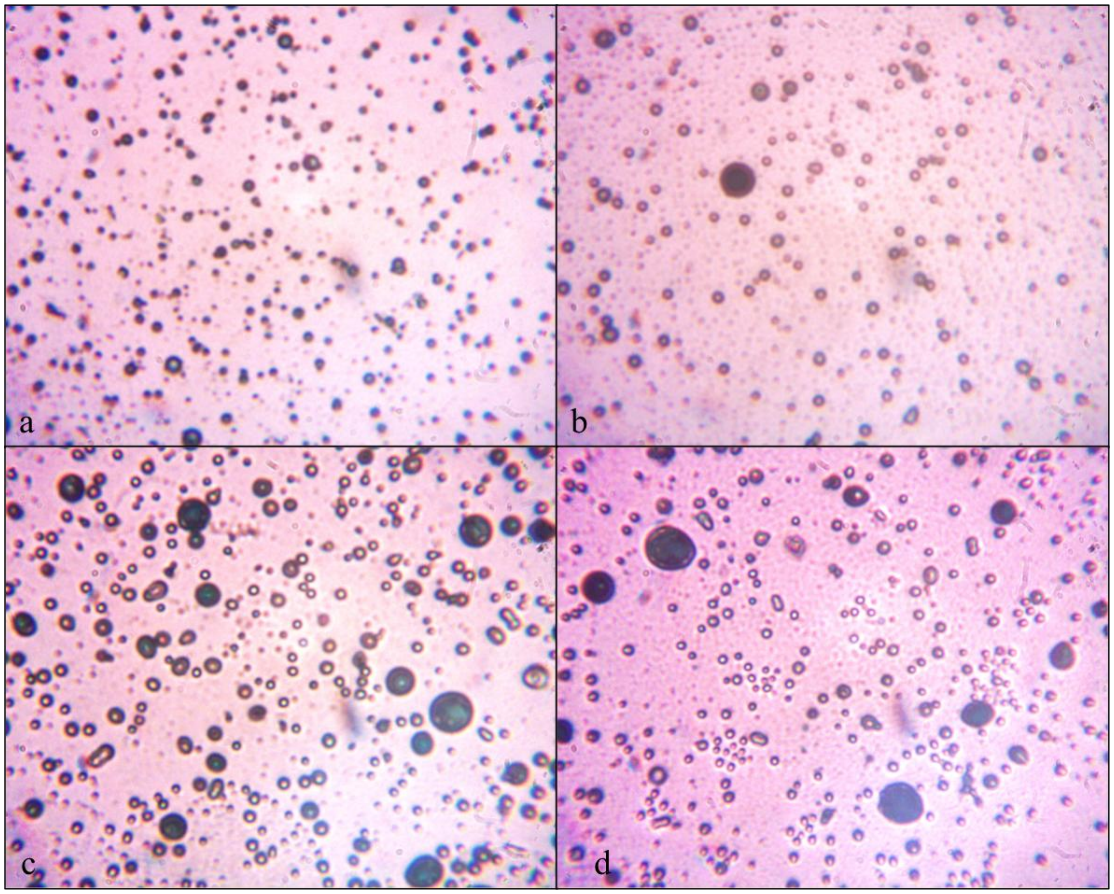

Figure 63 *B. subtilis* spores after 30 minutes contact time of 20 mg/L Cl_2 initial concentration at (a) 3 minutes, (b) 10 minutes, (c) 15 minutes and (d) 30 minutes of wet heat observed at 100x magnification.

B. subtilis was also submitted to 0 mg/L Cl_2 and 10 mg/L Cl_2 and observed under the SEM (third experiment). Results evidenced the effect of chlorine in the bacteria. As shown on Figure 64 where the bacteria were not exposed to any chlorine dose, *B. subtilis* was in its vegetative form (rod shape). Figure 65 confirmed the effect of chlorine on *B. subtilis* by inducing the bacteria to transform into its defensive form, spore (circular shape). Qualitatively, a decrease in numbers was observed, showing inactivation of *B. subtilis* by chlorination.

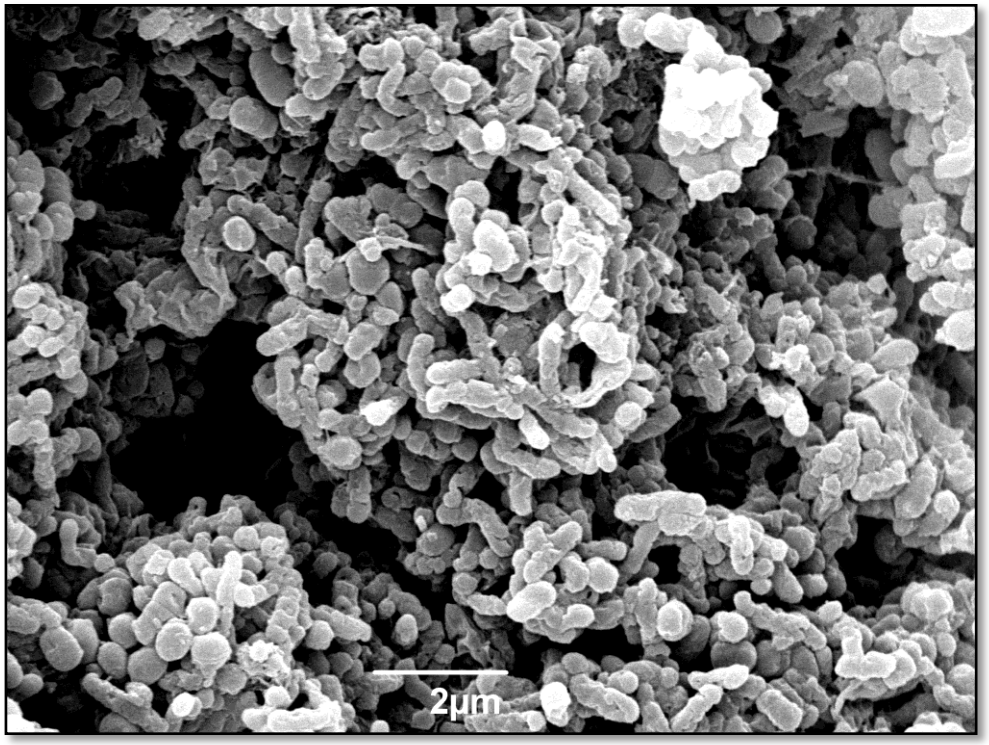

Figure 64 SEM image of *B. subtilis* after 30 minutes contact time of 0 mg/L Cl_2.

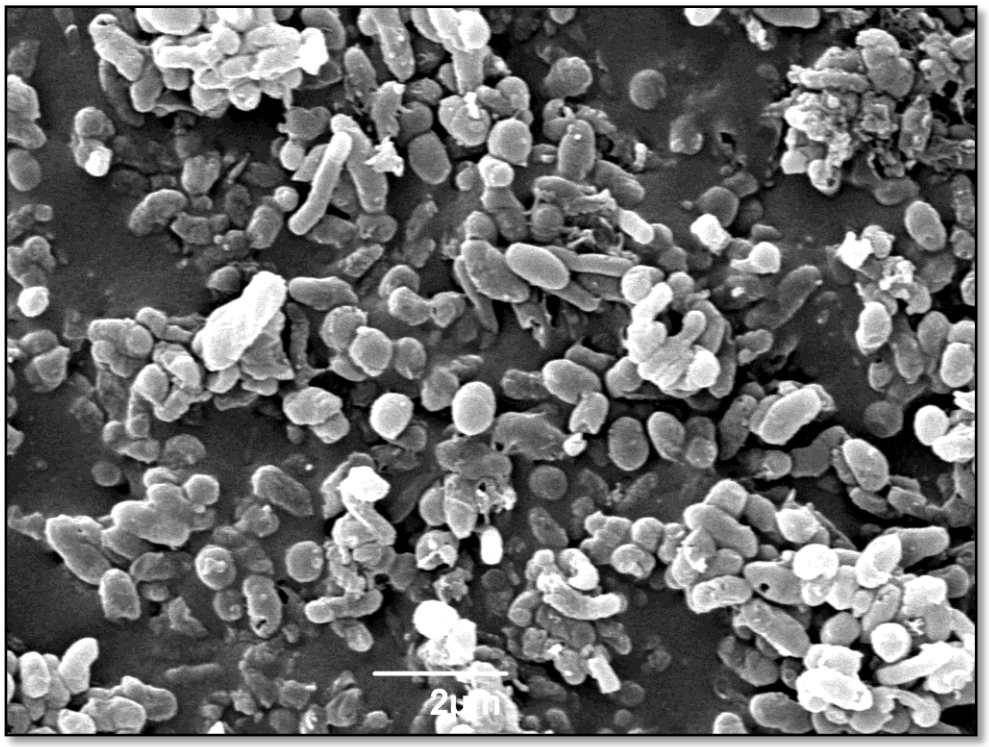

Figure 65 SEM images of *B. subtilis* after 30 minutes contact time of 10 mg/L Cl_2.

4.3.5 Treatment Train

4.3.5.1 Filtration follow by disinfection (short-term run)

System 1 was connected to the disinfection basin to evaluate the effectiveness of the treatment train during 65 pore volumes equivalent. Results from the filter effluent are presented in Figure 66. A 2-parameter Exponential Decay regression was used to fit the data using the following equation and with parameters shown in Table 30:

$$f = ae^{-bx}$$

Eq. 12 2-parameter Exponential Decay regression

where, a is the y-intercept; and b is the decay factor.

Removals of the bacteria were increased to reach the maximum of 1.2 log removal (93.6 % removal) at less than 10 pore volumes equivalent and then decreased to less than 0.2 log removal (37.5 % removal).

Results of *B. subtilis* removal after the disinfection treatment train are presented in Figure 67. A linear regression was used to fit the data, excluding the point before 3,674 mL of treated water and an equation with an R^2 of 0.43788 was obtained:

$$R = -0.0001005V + 1.5769$$

Eq. 13 *B. subtilis* log removal by disinfection (short-term run)

where, R is the *B. subtilis* log removal; and V is the treated water volume (mL)

Generally, an increase in *B. subtilis* removal up to 6,000 mL of treated water (CT~65 mg-min/L) was observed and then decreased. However, *B. subtilis* removals achieved after disinfection were lower than 1.5 log removal. The negative log removal of *B. subtilis* shown in

Figure 67 was because disinfection basin was initially filled with the Caín Alto River water spiked with *B. subtilis*. Therefore, the number of *B. subtilis* in the disinfection basin was higher than those in the influent t_{10}, corresponding to the approximately 1,000 mL treated water volume (CT = ~4.25 mg-min/L). Comparing with the results (100% removal) in the section 4.3.4.2, the CT values achieved were similar (excluding last sample that increased up to 96 mg-min/L) but log removals were slightly lower, reaching a maximum of 1.32 log removal (95 % removal). Likewise, log removal results of the previous synergistic studies (Table 28) were still lower even with higher CT's values (Cho et al., 2011; Cho et al., 2006).

Residual free Cl_2 were between 0.2 and 0.7 mg/L (Figure 68). Again, the lowest concentration was found before the HRT of the disinfection basin. Moreover, the residual free Cl_2 concentration increased to a maximum (0.66 mg/L) at 2 HRT and then started to decrease. However, all measurements were found to be lower than the MRDL.

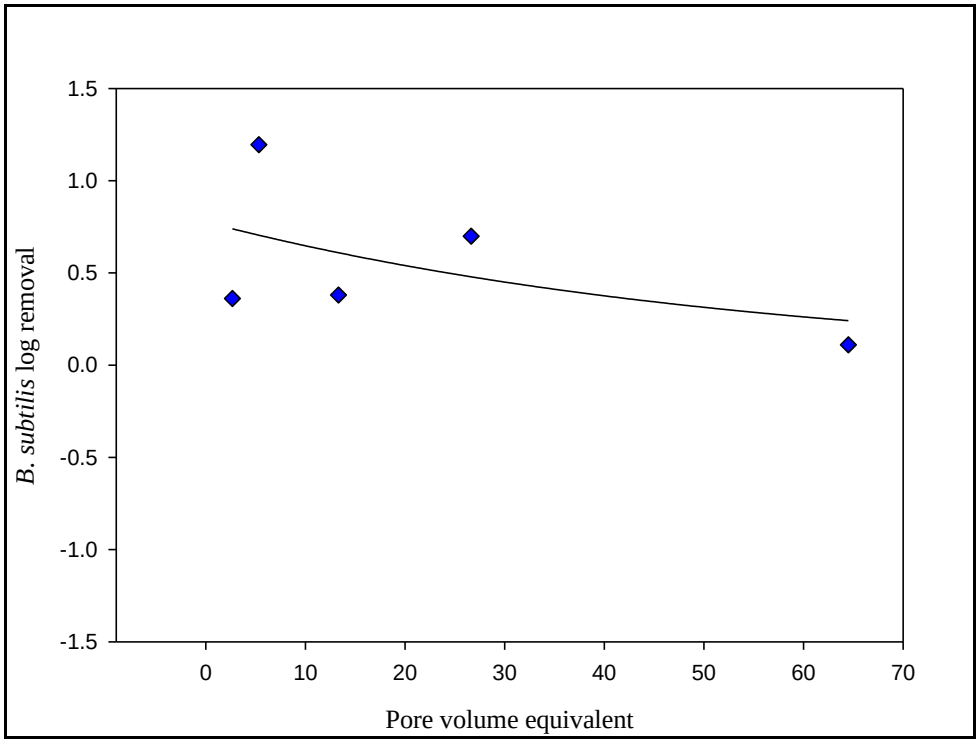

Figure 66 *B. subtilis* removal by filtration during treatment train (short term).

Table 30 Equation parameters and statistical results of filtration during treatment train (short term).

	Coefficient	Std. Error	P	R^2
a	0.7757	0.3223	0.0953	0.2792
b	0.0181	0.0245	0.5136	

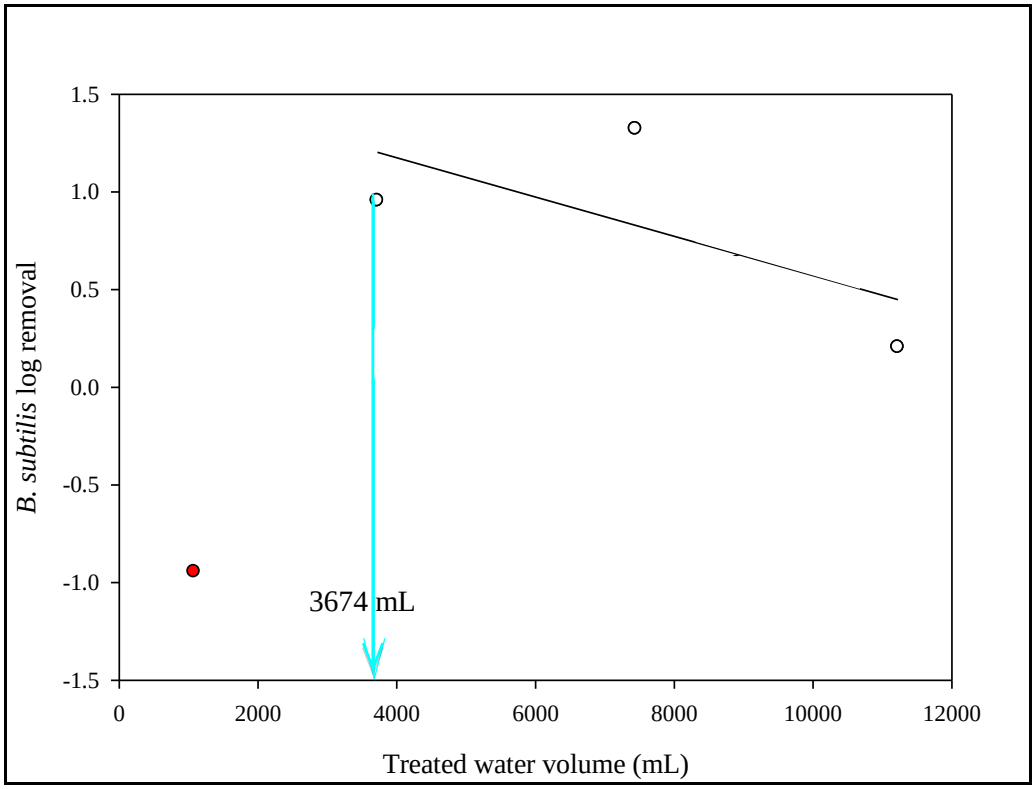

Figure 67 *B. subtilis* removal by disinfection during treatment train (short term).

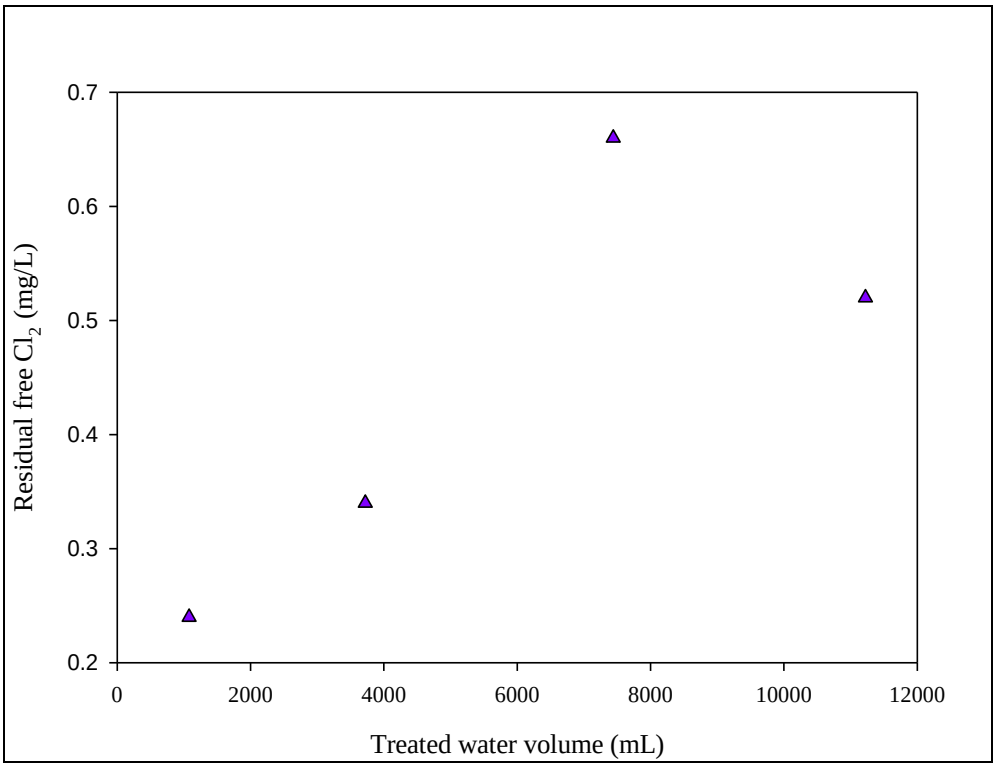

Figure 68 Residual free Cl_2 concentrations during disinfection in treatment train (short-term).

B. subtilis log removal of the treatment train was then found to be ranging from 0.2 to 2 log removal. A schematic of the filtration units with their respective log removal ranges by the unit and treatment train is shown in Figure 69.

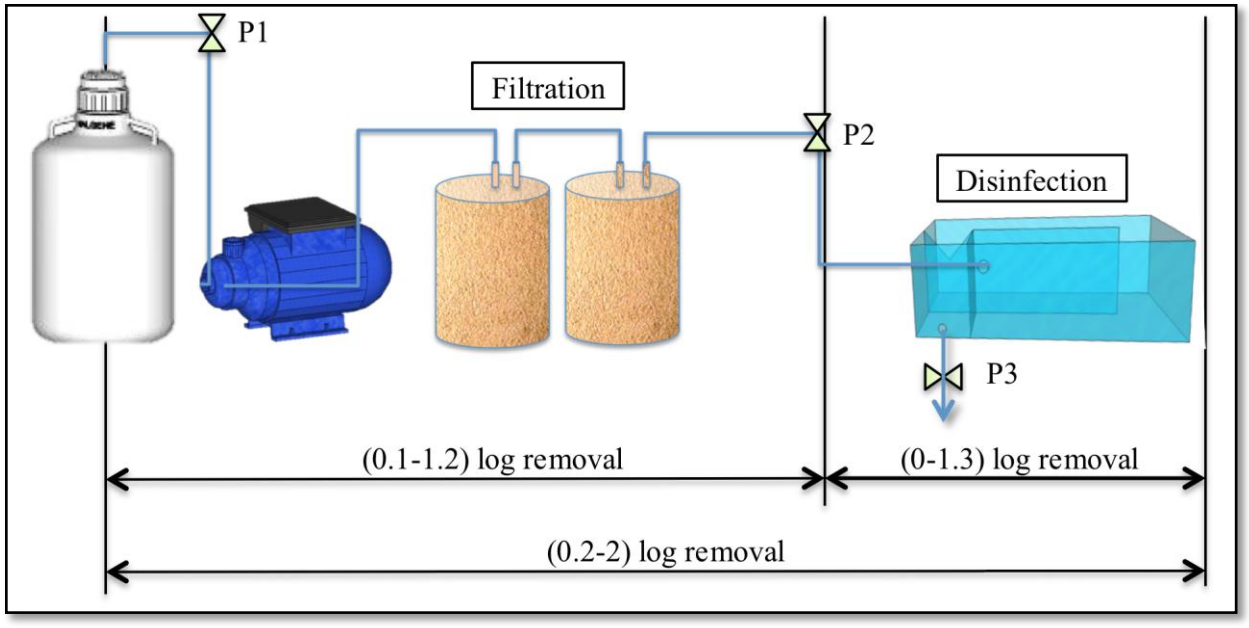

Figure 69 Treatment train schematic of *B. subtilis* removal by log-term (short term run).

4.3.5.2 Filtration followed by disinfection (long-term)

Treatment train was submitted to a long-term (>500 pore volume equivalent) experiment to evaluate the service life of the filters. From Figure 70 it can be seen that the filters reached an apparent saturation with respect to *B. subtilis* removal after 200 pore volumes. However, after 400 pore volumes the removal began to increase again.

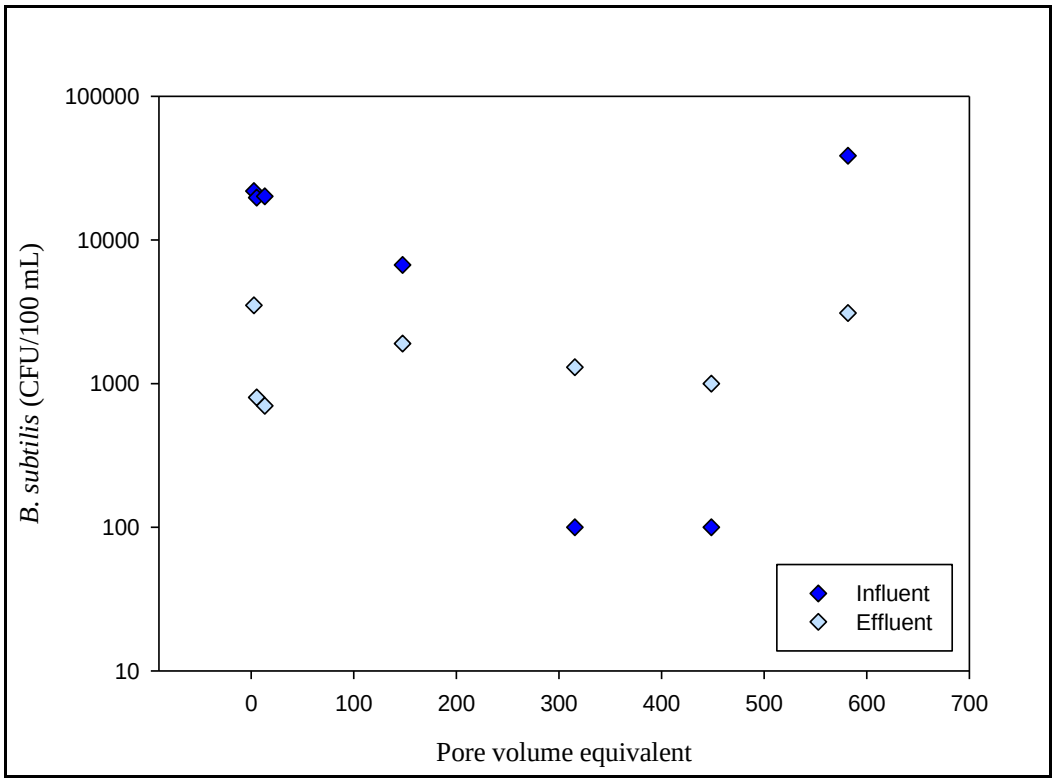

Figure 70 Influent and effluent *B. subtilis* numbers by filtration during treatment train (long term).

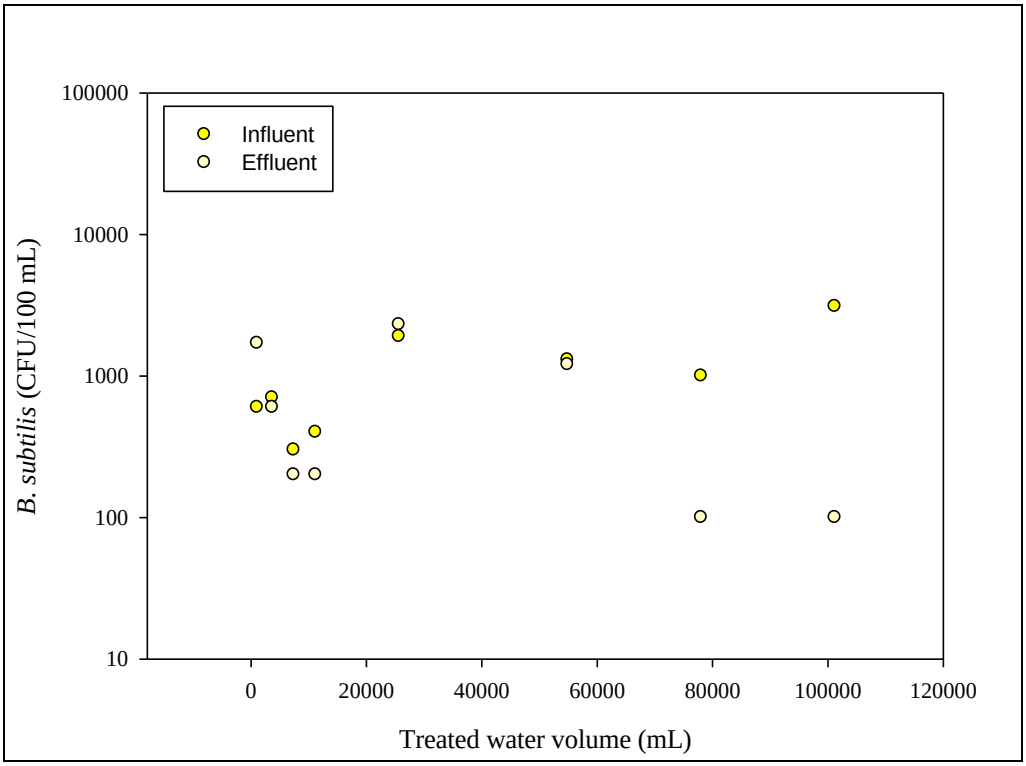

Figure 71 Influent and effluent *B. subtilis* numbers by disinfection during treatment train (long term).

Evaluation of the disinfection basin of the treatment train is shown in Figure 71. Similarly to the filters behavior, removal by the disinfection basin was increased up to a 50 % removal (0.30 log removal) at 11,224 mL of treated water (CT = 33.12 mg-min/L), then decreased to 0 and increased to a 96.7 % removal (1.49 log removal) at the end of experiment (CT = 3,136.45 mg-min/L). This behavior corresponded to the apparent saturation of the filter. As discussed previously, the disinfection basin was initially filled with the Caín Alto River water, which contained wild bacteria and *B. subtilis* solution. This made the disinfection basin to not completely inactivate the *B. subtilis*. In contrast to sections 4.3.4.2 and 4.3.5.1, Cho et al. (2011 & 2006) did achieve greater inactivation log removals of *B. subtilis* after 120 mg-min/L (Cho et al., 2011) and 250 mg-min/L (Cho et al., 2006) than this long-term treatment train study.

Residual free Cl_2 concentration measurements are shown in Figure 72. Behavior of these measurements were fitted with the Quadratic Polynomial regression:

$$f = y_0 + ax + bx^2$$

Eq. 14 Polynomial regression

Where, y_0 is y-intercept, residual free Cl_2 at 0 mL, $\left(\frac{mg}{L}\right)$; a is the linear coefficient; and b is the quadratic coefficient.

Parameters and statistical results of **Eq. 14** are presented in Table 31. Residual free Cl_2 concentrations were and increased exponentially from the initial 0.07 to 1.89 mg/L, lower than the MRDL. However, the overall inactivation of *B. subtilis* of ~0.2 log removal by disinfection was slightly higher than the overall disinfection assessed in the section 4.3.5.1, residual free Cl_2 were considerably higher with maximum value, more than 2 times higher than that in the previous section.

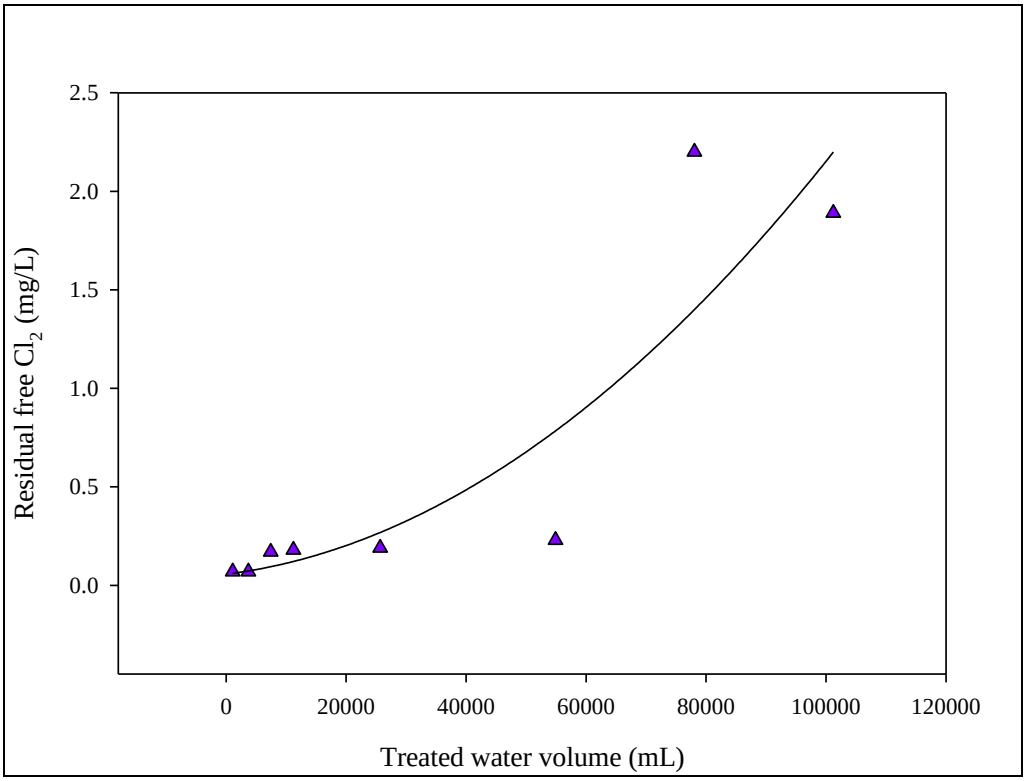

Figure 72 Residual free Cl_2 concentrations during disinfection in treatment train (long-term).

Table 31 Equation parameters and statistical results of residual free Cl_2 concentration during treatment train (long term).

	Coefficient	Std. Error	P	R^2
y_0	0.0562	0.2841	0.8509	0.8056
a	3.87E-06	1.88E-05	0.8446	
b	1.71E-10	1.89E-10	0.4064	

Overall assessment of treatment train of the long term run, in terms of log removals, is presented in Figure 73. *B. subtilis* log removals achieved in the treatment train were from 0 to 3.0. These results implied that complete inactivation of *G. lamblia* (3-log removal) with the same parameters used could be achieved. However, a greater inactivation of *Cryptosporidium* could be achieved since the USEPA specified a 2-log removal of *Cryptosporidium*.

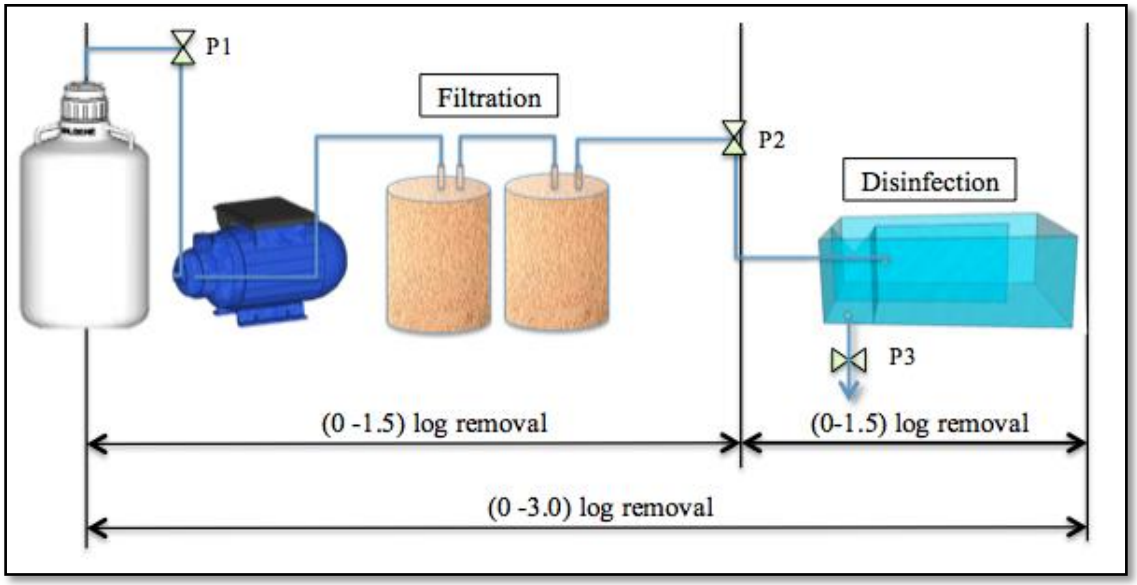

Figure 73 Treatment train schematic of *B. subtilis* removal by log-term (long term run).

4.3.5.3 Backwash

Filters were submitted to a backwash with the treated effluent form disinfection for over 120 pore volume equivalent (Figure 74). Results of the process are shown in Figure 75. The Cl_2 concentration in the backwash influent ranged from 4.64 to 4.84 mg/L. Results showed that it was necessary to flush the filters for at least 100 pore volume equivalent with the treated water to reach a pseudo-constant Cl_2 demand of 2.8 mg/L in the filter 1 effluent and of 1 mg/L in the filter 2 effluent. Since this run time was considerably long, the initial concentration of Cl_2 could be increased so as to decrease the pore volume equivalent necessary for the backwash. Difference in Cl_2 demand might be due to sand interaction with Cl_2 and to Cl_2 decomposition inside the filter. In an ideal case, both effluents from the filters should be equal. However, this was not the case in our system. In contrast, Jegatheesan et al. (2009) evaluated the effect of filtrations on chlorine demand on a drinking water treatment plant. Their findings showed no effect of fast and slow sand filtration on chlorine demand, i.e. Cl_2 demand remained at approximately 3.18 mg/L.

Moreover, self-decomposition of chlorine under closed conditions had also been encountered in electrolyzed oxidizing water (Len et al., 2002).

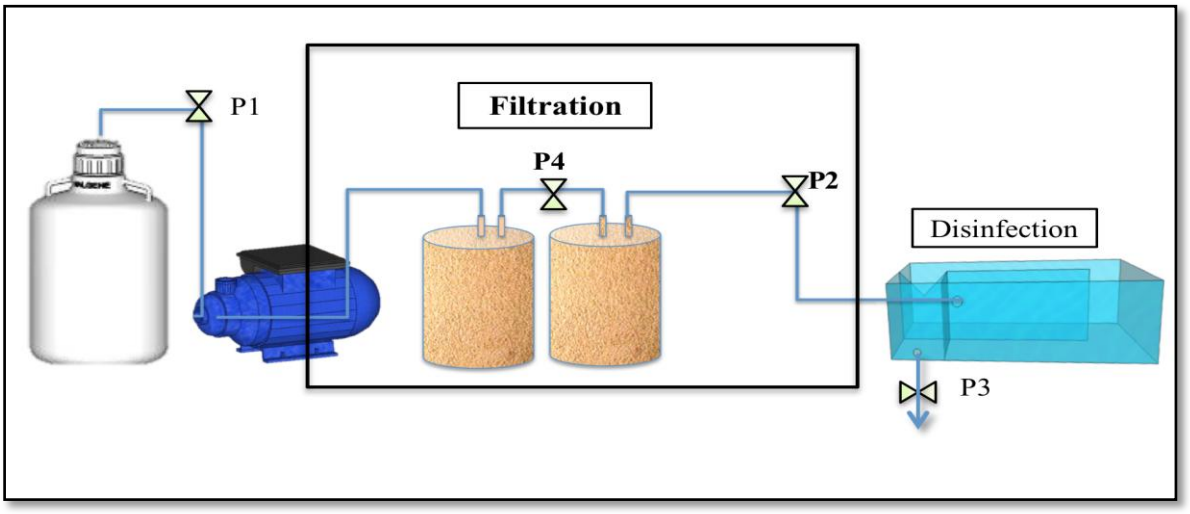

Figure 74 Schematic of filters backwash.

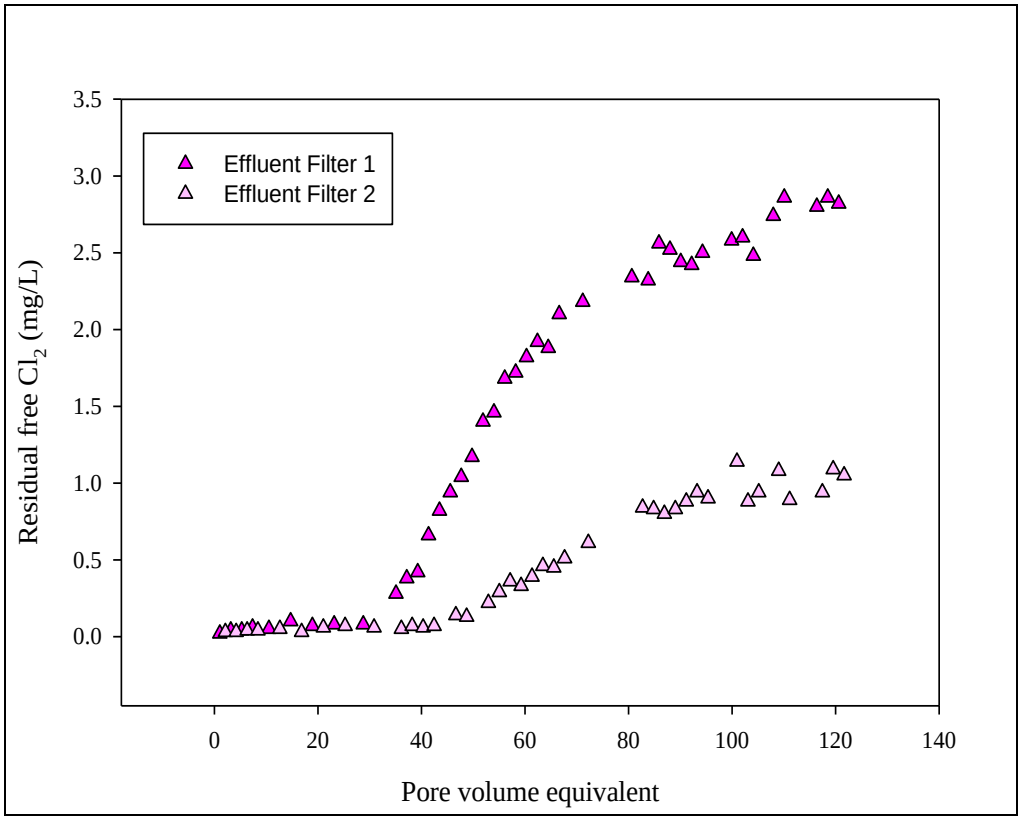

Figure 75 Filters backwash.

4.4 FIELD-SCALE SYSTEMS

The SEED unit was assessed for *B. subtilis* removal in three different drum combinations that were constructed with the same hydraulic characteristics. Physicochemical and bacteriological parameters were monitored for each sampling time, port and drum configuration.

4.4.1 Physicochemical and Bacteriological Parameters

Five different physicochemical parameters were measured at each port and sampling times (i.e. 0, 2, 4, 6 and 7 hours) unless otherwise specified. The first parameter measured was temperature (Figure 76) and showed no significant variation among the ports. Minor differences between the sampling times at the first two days and the third day were noticed. However, these differences might be due to the sampling times, i.e. experiments were performed at different times during the day and hence highest temperature were observed at ~15:00.

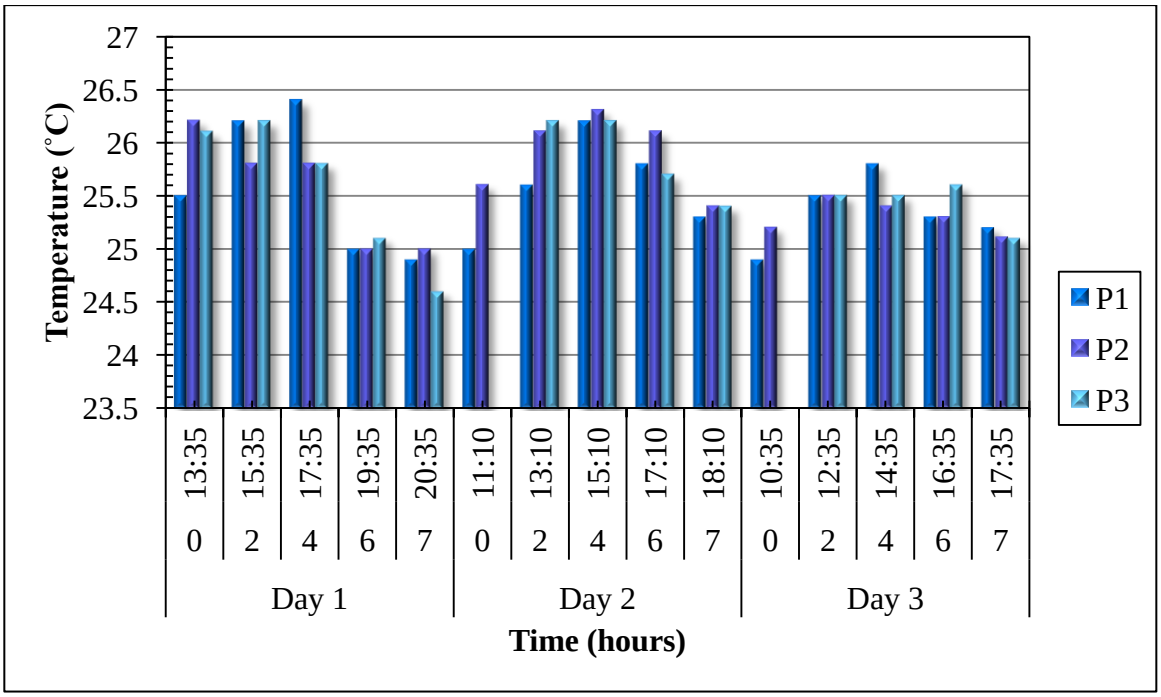

Figure 76 Temperature measurements at field-scale.

Moreover, a difference in pHs (Figure 77) was significant between the ports at the same sampling times. In general, a reduction in pH was noticed after filtration (P2) but then increased after chlorination (P3), except at the first three samples of Day 1. However, at treatment train, a pH reduction of approximately 0.2 units was noticed in almost each sampling time and days. Although a decrease in pH was achieved, the final measurement of the treatment train stayed between 8.4 and 8.5, which was in the range of the recommended Secondary Standards of pH (USEPA, 2009) but was slightly higher than the preferred value (< 8.0) suggested by WHO (2011).

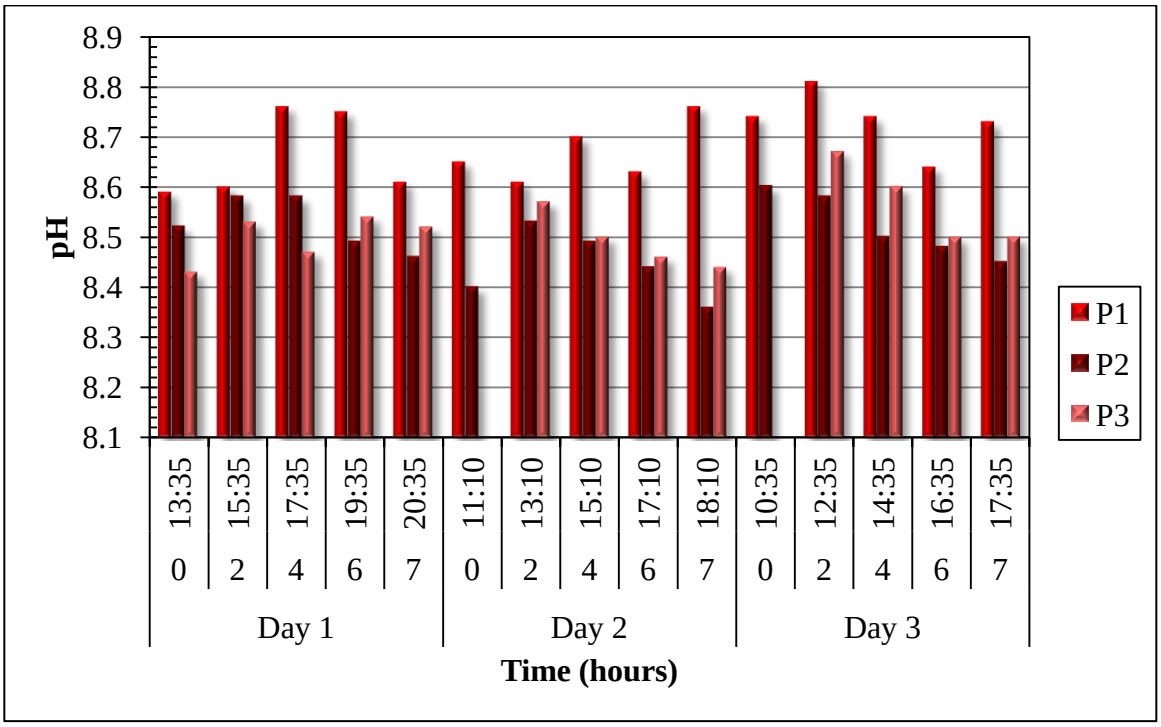

Figure 77 pH measurements at field-scale.

Conductivity was increased at P3 in all samples at the three experiments (Figure 78). No specific trend was noticed at P2. At P1 and P2 during Day 1, the values were in the range of 365 - 370 µS/cm. At Day 2, the values at P1 and P2 were slightly lower (350 - 360 µS/cm). A greater

variation was noticed during Day 3, measurements fluctuated from approximately 345 to 370 µS/cm.

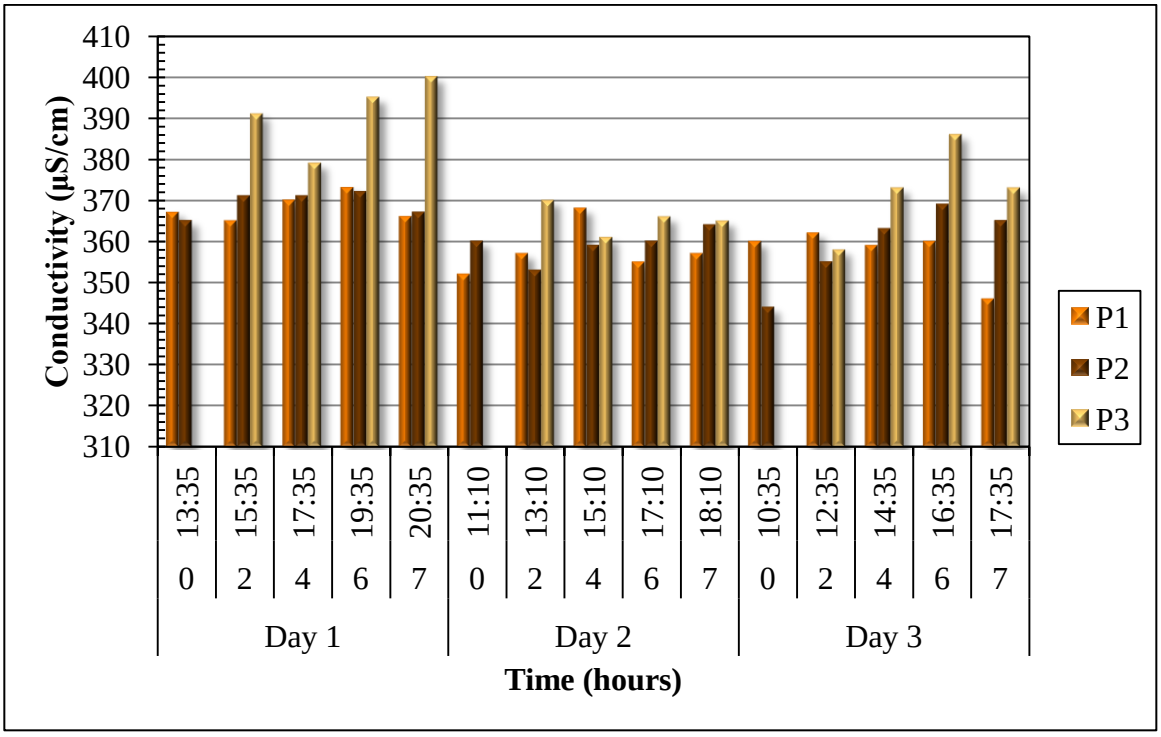

Figure 78 Conductivity measurements at field-scale.

Turbidity was increased through sampling times during the experiments (Figure 79). All turbidity levels were lower than 1 NTU at P1 but increased at P2 and P3. Increase in turbidity at P2 might be due to escape of colloidal sand particles from the filters. An increase in turbidity at P3 might be due to the type of chlorination technique used. It was observed that the chlorine tablet did not completely dissolve in the water, resulting in suspended debris in the system. This abrupt increase was only noticed during the first day of experiment. Hence, further field adjustments were made for the subsequent experiments to solve this issue. However, the final turbidity values were still slightly higher than 1 NTU and did not comply with the USEPA MCL regulation (USEPA, 2009).

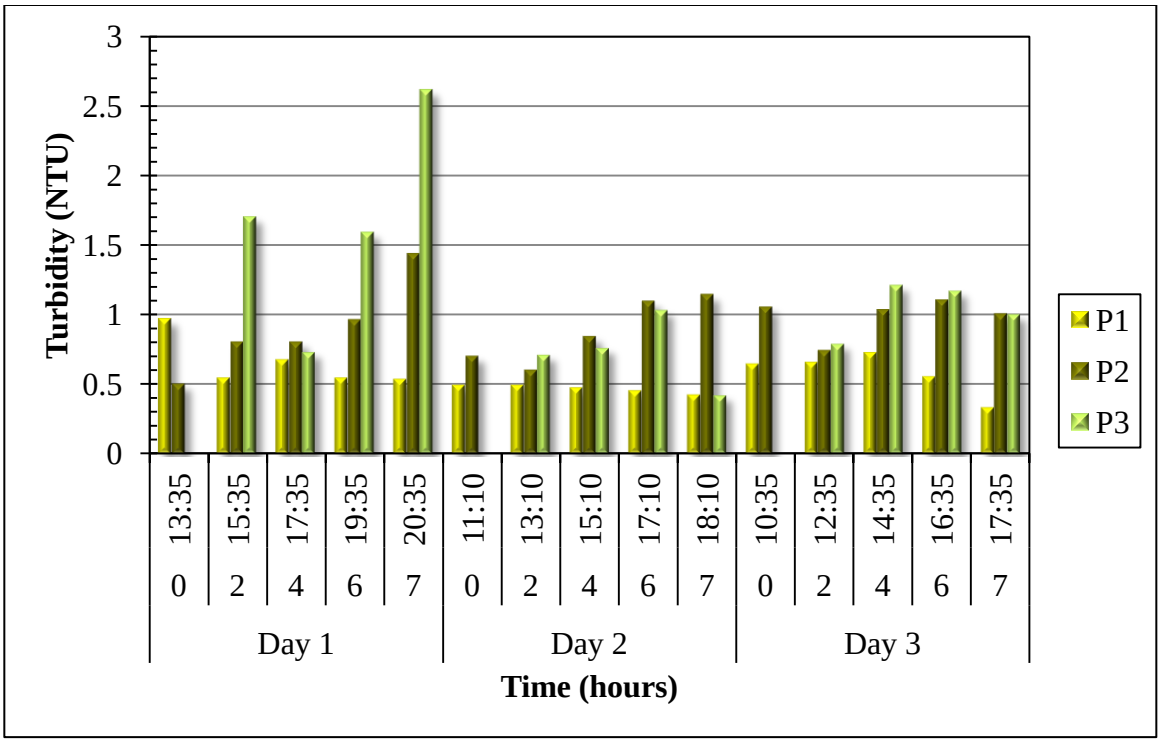

Figure 79 Turbidity measurements at field-scale.

TOC concentrations varied significantly through the three days (Figure 80). At Day 1, slight increases in TOC were observed through sampling times and in some instances through ports, ranging from ~13 mg/L to ~20 mg/L. In contrast, variations of TOC concentrations at Days 2 and 3 were abrupt with a low value of ~3 mg/L and a high value of ~30 mg/L. However, no specific trends within the days were observed. Dissimilarities in TOC concentrations at the influents among the three days were found. No similar reductions or increases neither by port nor by contact time were seen.

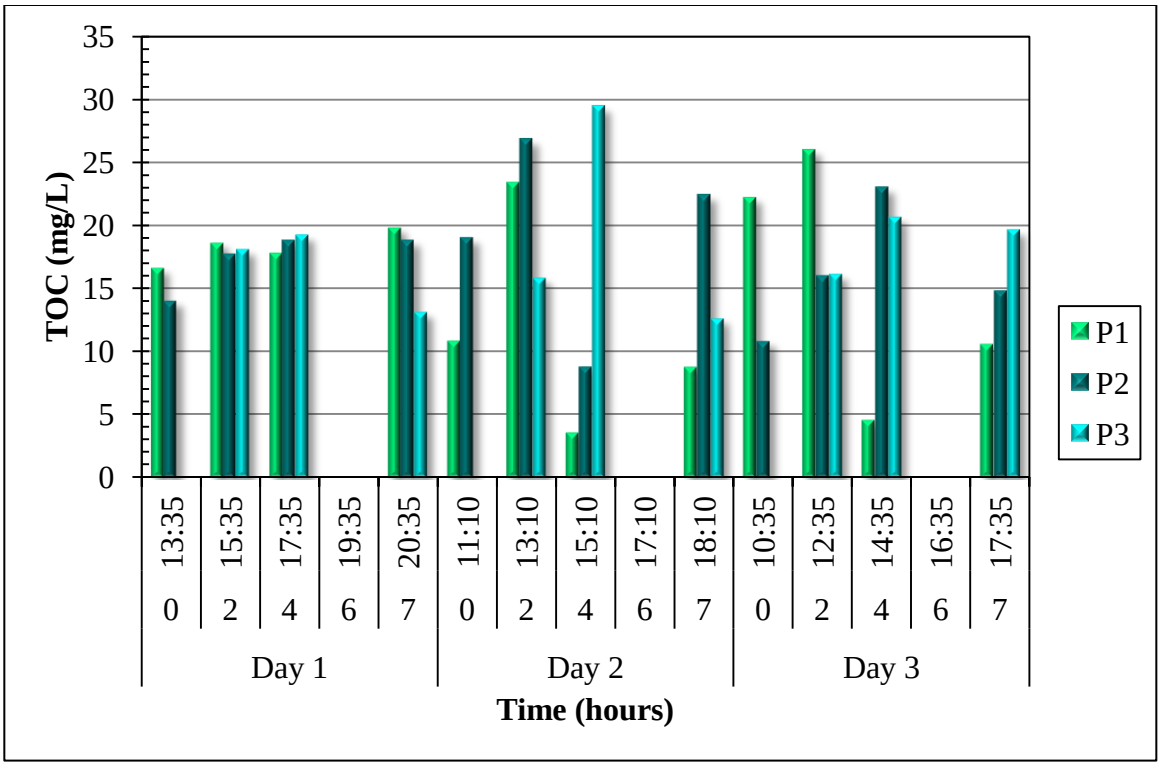

Figure 80 TOC measurements at field-scale.

Initial numbers of *B. subtilis* (P1) were lower than 500 CFU/100 mL through the three days ranging from 75 to 214 CFU/100 mL at Days 2 and 3 (Figure 81). Increases in numbers of *B. subtilis* at P2 and P3 were found in almost all samples and days. Particularly, at Day 3 a steeper increase of *B. subtilis* was observed with maximum values of 16,400 CFU/100 mL at P2 and 27,000 CFU/100 mL at P3. These high numbers of *B. subtilis* might indicate saturation of the system during the last day of assessment.

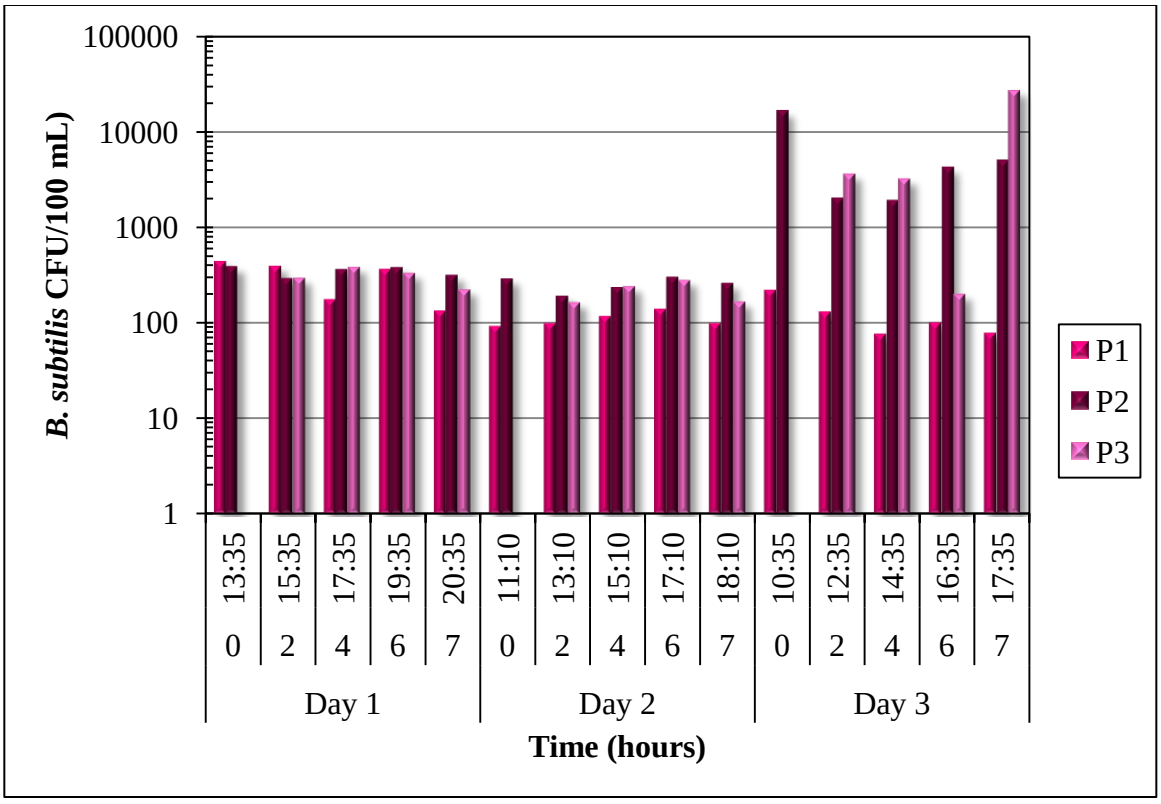

Figure 81 *B. subtilis* numbers at field-scale.

Statistical analyses were performed on the physicochemical and bacteriological parameters, including matrix plots, Pearson correlation coefficients and P-values. These analyses were done for each port and day using the Minitab. In general, a clear relationship between parameters could not be identified since none of the combinations perceived the same relation during the three days.

The first set of statistical analyses was applied to P1 at Day 1. The matrix plot (Figure 82) suggested a positive relation between pH and conductivity and a negative relation between TOC and turbidity. Pearson correlation coefficients and P-values (Table 32) evidenced the highly positive relation between pH and conductivity with values of 0.895 and 0.4, respectively. The high inverse relation between TOC and turbidity was found with the Pearson correlation

coefficient of -0.914 and P-value of 0.086. In addition, the Pearson correlation coefficient (-0.654) and P-value (0.346) suggested that TOC might be negatively correlated to *B. subtilis*. Finally, other Pearson correlation coefficients and P-values (0.432 and 0.467, respectively) suggested that turbidity might also be correlated to *B. subtilis*, although P-values were found to be >0.05.

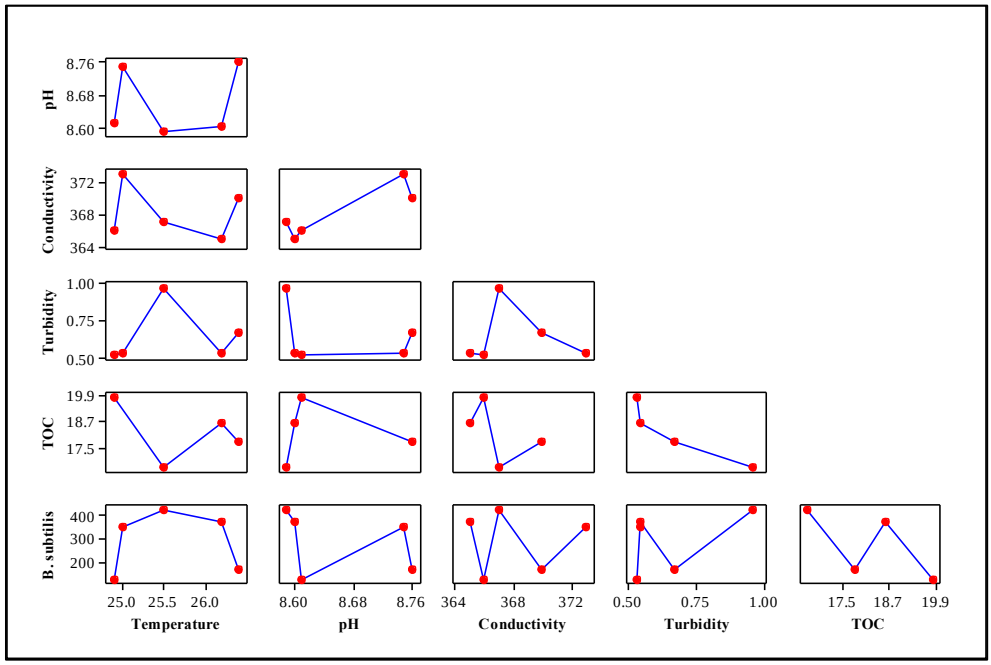

Figure 82 Matrix plot of P1 at Day 1 of SEED unit.

Table 32 Pearson correlation and P-values for P1 at Day 1 of SEED unit.

	Temperature	pH	Conductivity	Turbidity	TOC
pH	0.138				
	0.825				
Conductivity	-0.191	**0.895**			
	0.759	**0.04**			
Turbidity	0.138	-0.271	-0.103		
	0.825	0.659	0.869		
TOC	-0.376	-0.099	-0.413	**-0.914**	
	0.624	0.901	0.587	**0.086**	
B. subtilis	0.05	-0.288	-0.001	**0.432**	**-0.654**
	0.937	0.639	0.998	**0.467**	**0.346**

The matrix plot of the samples from P1 at Day 2 is shown in Figure 83. The plot suggests correlations between conductivity and temperature, turbidity and pH, TOC and pH, *B. subtilis* and TOC, and *B. subtilis* and temperature. Moreover, for the proper analysis, Pearson correlation coefficients and P-values were calculated and thus supported the matrix plot suggestions (Table 33). Outcomes from these calculations proved that conductivity was highly positively related to temperature with respective coefficients of 0.832 and 0.081 of Pearson correlation and P-value. In addition, it was shown that TOC was highly negatively related to pH with a Pearson correlation coefficient of -0.727. However, P-value (0.273) was high and, hence, did not support the relation between the parameters. Moreover, Pearson correlation (-0.739) indicated that turbidity was highly negatively related to pH but P-value (0.153) did not provide strong evidence of the relation. In terms of bacteriological parameters, *B. subtilis* might be negatively related to TOC as the Pearson correlation implied (-0.518). However, P-value (0.482) was higher than 0.05. In contrast, *B. subtilis* might be positively related to temperature with respective coefficients of Pearson correlation coefficient and P-value 0.692 and 0.195. Likewise, P-value was greater than 0.05 and thus provided a weak evidence.

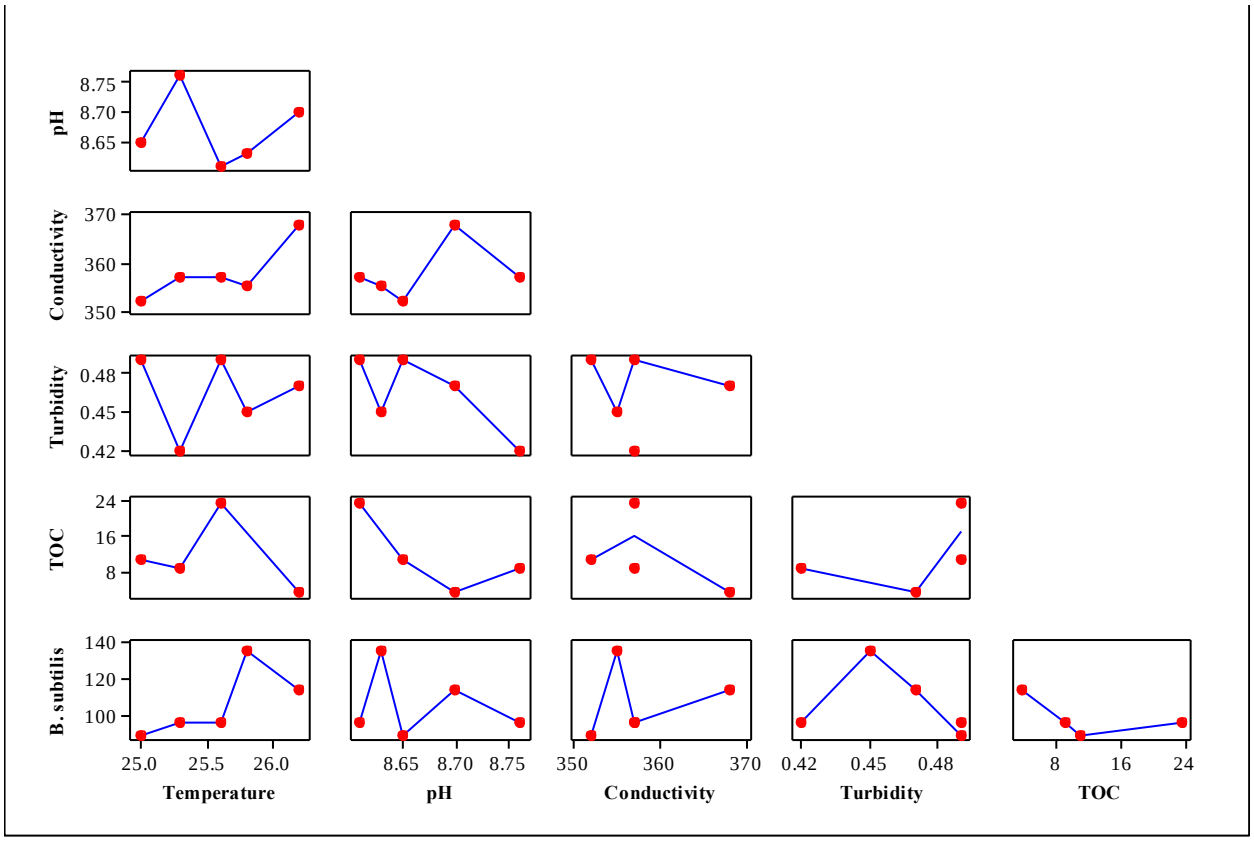

Figure 83 Matrix plot of P1 at Day 2 of SEED unit.

Table 33 Pearson correlation and P-values for P1 at Day 2 of SEED unit.

	Temperature	pH	Conductivity	Turbidity	TOC
pH	-0.045				
	0.943				
Conductivity	**0.832**	0.348			
	0.081	0.566			
Turbidity	-0.029	**-0.739**	-0.05		
	0.963	**0.153**	0.936		
TOC	-0.27	**-0.727**	-0.497	0.434	
	0.73	**0.273**	0.503	0.566	
B. subtilis	**0.692**	-0.195	0.254	-0.28	**-0.518**
	0.195	0.753	0.68	0.648	**0.482**

The matrix plot analysis for P1 at Day 3 suggested relations between turbidity and conductivity, and *B. subtilis* and TOC (Figure 84). Table 34 gave the Pearson correlation coefficients and P-values for the parameters assessed. The Pearson correlation coefficient, 0.888, proved that turbidity and conductivity were highly positively related. The P-value, 0.044, of the analysis strongly evidenced the relation. Likewise, other correlation was found between physicochemical parameters, pH might be positively related to TOC with a Pearson correlation number of 0.691. In terms of bacteriological parameters, statistical analysis showed that *B. subtilis* was highly positively related to TOC with a Pearson correlation coefficient of 0.725. Furthermore, *B. subtilis* might also be negatively related to temperature with a Pearson correlation coefficient of -0.696. Although, the Pearson correlation coefficient indicated correlation between the above parameters still P-values were greater than 0.05 indicating weak evidence of the relations.

It was expected that all three days would have had the same correlations between parameters since P1 was the influent to the SEED unit. However, a wide variation was achieved between days. One reason of this variation could be the diverse condition of the lines. Yet one trend was found during Day 1 and 2: the negative relation between *B. subtilis* and TOC.

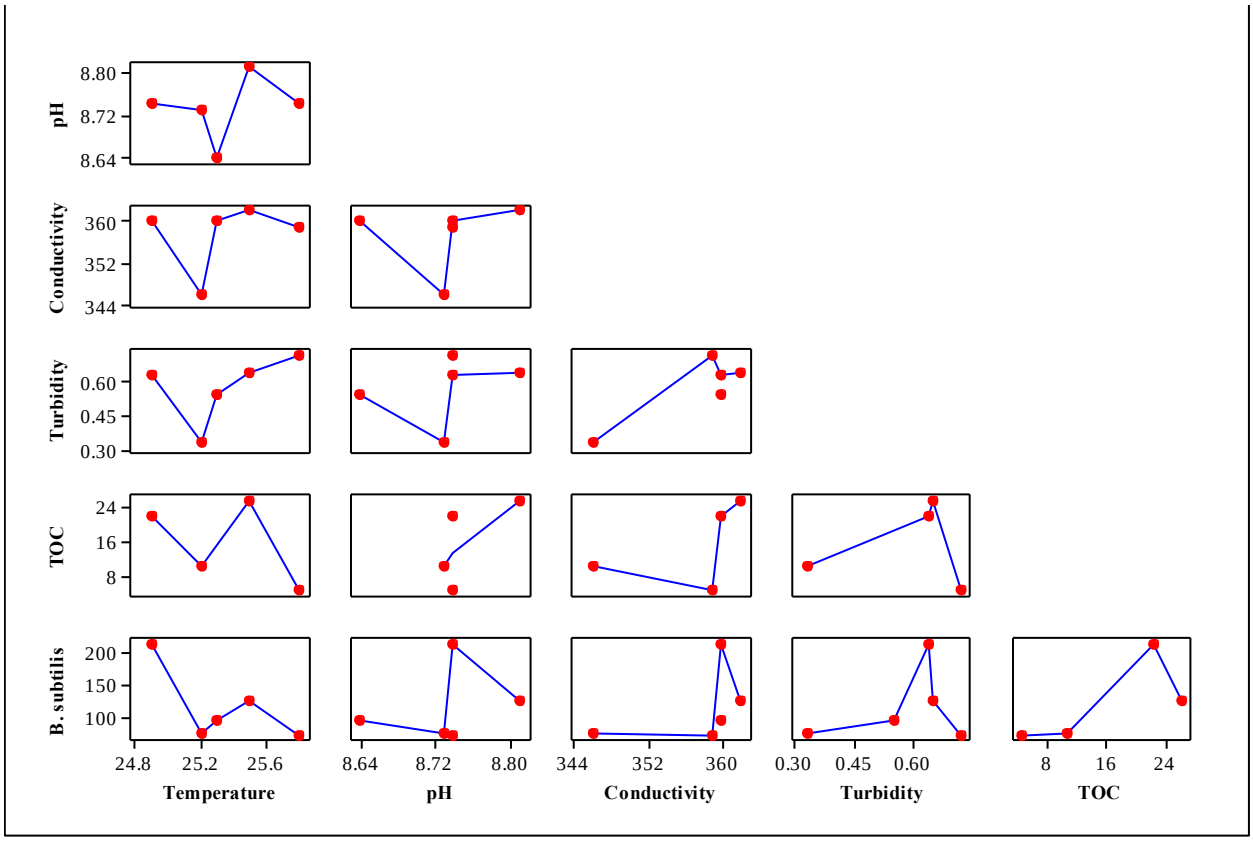

Figure 84 Matrix plot of P1 at Day 3 of SEED unit.

Table 34 Pearson correlation and P-values for P1 at Day 3 of SEED unit.

	Temperature	pH	Conductivity	Turbidity	TOC
pH	0.204				
	0.742				
Conductivity	0.209	0.112			
	0.735	0.857			
Turbidity	0.42	0.282	**0.888**		
	0.481	0.646	**0.044**		
TOC	-0.485	**0.691**	0.483	0.16	
	0.515	**0.309**	0.517	0.84	
B. subtilis	**-0.696**	0.224	0.431	0.324	**0.725**
	0.191	0.717	0.468	0.594	**0.275**

Figure 85 shows the matrix plot of P2 at Day 1. This analysis suggested relations between conductivity and temperature, *B. subtilis* and TOC, turbidity and conductivity, turbidity and pH, TOC and turbidity and *B. subtilis* and turbidity. The Minitab was used to calculate the Pearson correlation coefficients and P-values for a proper analysis (Table 35). Pearson correlation indicated that turbidity might be negatively related to: TOC with a coefficient of -0.62; and to *B. subtilis* with a coefficient of -0.621. Moreover, conductivity might be negatively related to temperature (Pearson correlation = -0.623). In contrast, turbidity might be positively related to: pH (Pearson correlation = 0.686) and to conductivity (Pearson correlation = 0.721). The only relation found in terms of bacteriological parameters was the highly positive relation between *B. subtilis* and TOC (Pearson correlation = 1). However, the correlations of the parameters had P-values greater than 0.05 (except for the correlation between *B. subtilis* and TOC).

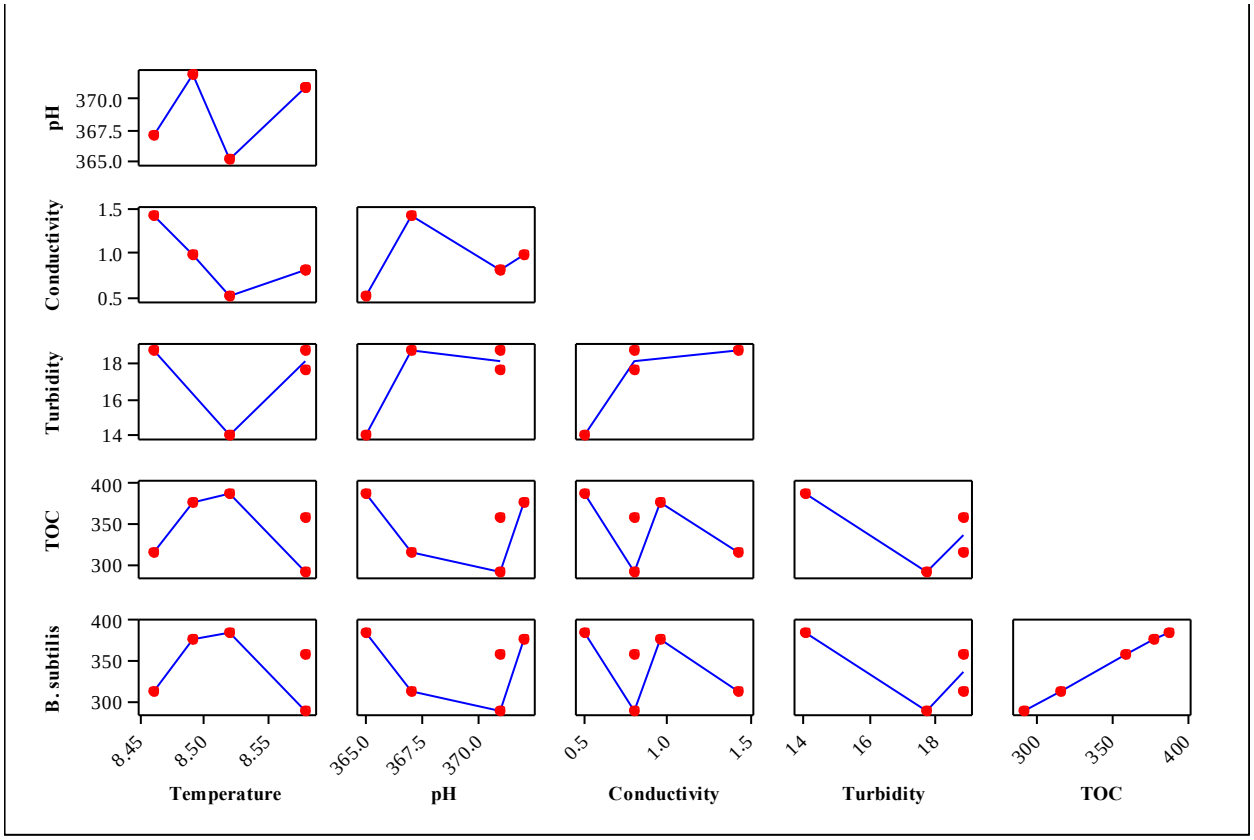

Figure 85 Matrix plot of P2 at Day 1 of SEED unit.

Table 35 Pearson correlation and P-values for P2 at Day 1 of SEED unit.

	Temperature	pH	Conductivity	Turbidity	TOC
pH	0.405				
	0.498				
Conductivity	**-0.623**	0.078			
	0.262	0.901			
Turbidity	0.057	**0.686**	**0.721**		
	0.943	**0.314**	**0.279**		
TOC	-0.175	-0.182	-0.478	**-0.621**	
	0.778	0.769	0.415	**0.379**	
B. subtilis	-0.175	-0.182	-0.478	**-0.621**	**1**
	0.778	0.769	0.415	**0.379**	*****

Samples of P2 at Day 2 were also statistically analyzed. The matrix plot of such samples suggested correlation between pH and temperature, conductivity and temperature, conductivity and pH, turbidity and conductivity, *B. subtilis* and conductivity and *B. subtilis* and turbidity (Figure 86). The Pearson correlation coefficients confirmed those relations and proved two more relations: *B. subtilis* and pH and pH and turbidity (Table 36). The Pearson correlation coefficient, and P-value showed that conductivity and: temperature might be negatively related (-0.63 and 0.255), pH were highly negatively related (-0.912 and 0.031), turbidity were highly positively related (0.804 and 0.101) and *B. subtilis* were positively related (0.7 and 0.188). Additionally, coefficients indicated that pH and: turbidity might be negatively related (-0.632 and 0.253), *B. subtilis* were highly negatively related (-0.711 and 0.178), temperature were highly positively related (0.868 and 0.056). The last relation found was between *B. subtilis* and turbidity. Statistics results indicated that they might be positively related (0.559 and 0.327).

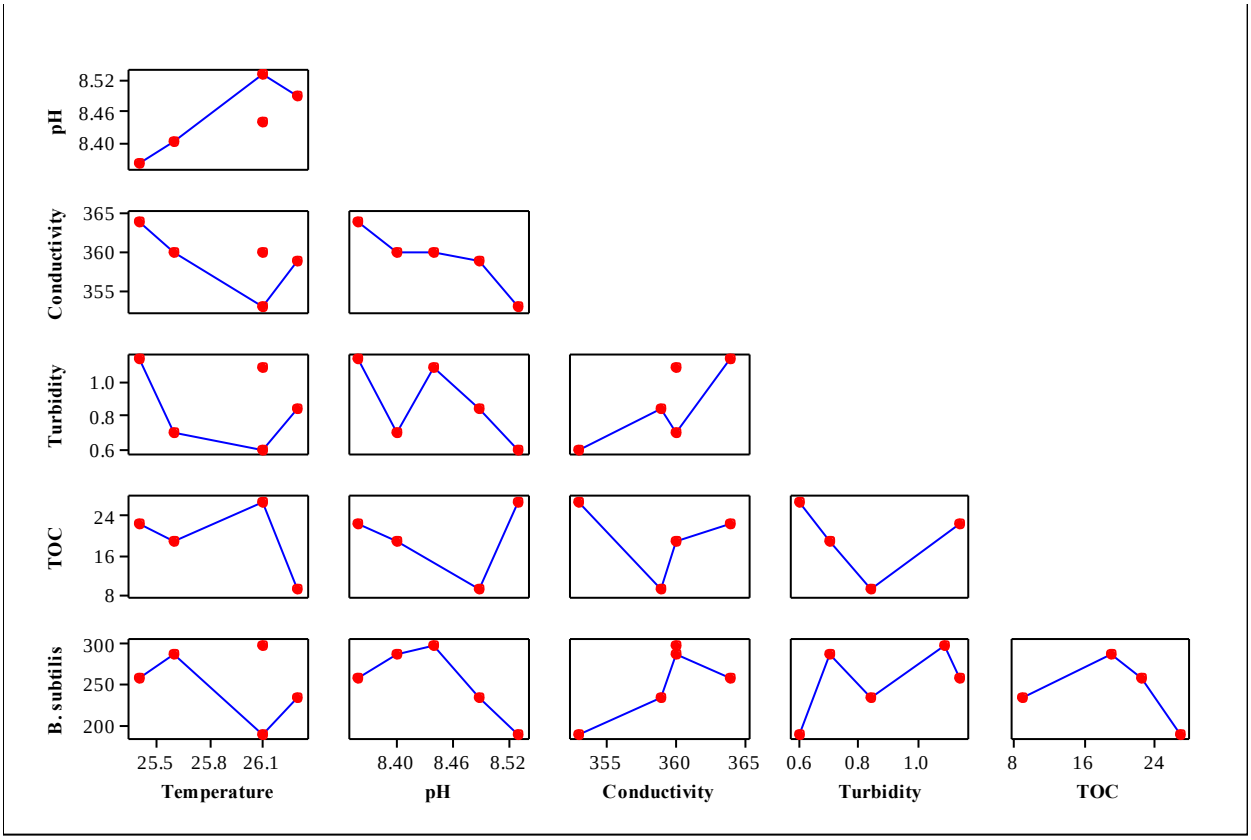

Figure 86 Matrix plot of P2 at Day 2 of SEED unit.

Table 36 Pearson correlation and P-values for P2 at Day 2 of SEED unit.

	Temperature	pH	Conductivity	Turbidity	TOC
pH	**0.868**				
	0.056				
Conductivity	**-0.63**	**-0.912**			
	0.255	**0.031**			
Turbidity	-0.294	**-0.632**	**0.804**		
	0.631	**0.253**	**0.101**		
TOC	-0.432	-0.047	-0.285	-0.154	
	0.568	0.953	0.715	0.846	
B. subtilis	-0.364	**-0.711**	**0.7**	**0.559**	-0.282
	0.547	**0.178**	**0.188**	**0.327**	0.718

The matrix plot of P2 at Day 3 suggested correlations between conductivity and pH, turbidity and temperature, TOC and *B. subtilis*, conductivity and *B. subtilis*, *B. subtilis* and pH (Figure 87). Table 37 shows the Pearson correlation coefficients and P-values of the parameters measured. High Pearson correlation coefficients (>0.7) were found for pH and conductivity (negative relation, -0.91), *B. subtilis* and conductivity (negative relation, -0.755) and *B. subtilis* and TOC (negative relation, -0.781). Medium Pearson correlation coefficients (in the range of ±0.5 to ±0.7) were obtained for turbidity and temperature (negative relation, -0.615), TOC and temperature (positive relation, 0.53), *B. subtilis* and temperature (-0.551), *B. subtilis* and pH (positive relation, 0.522), and TOC and conductivity (positive relation, 0.689).

Similar to P1, it was expected to find similar trends between P2 measurements within the three days. Although the drums were constructed in such a way that it could be assumed to have the same hydraulic properties, varied conditions of the media and lines caused dissimilar behavior within drums. However, two trends were found during Day 1 and 2: the negative relation between conductivity and temperature and the positive relation between turbidity and conductivity. Additionally, one trend was found during Day 2 and 3: the negative relation between conductivity and pH.

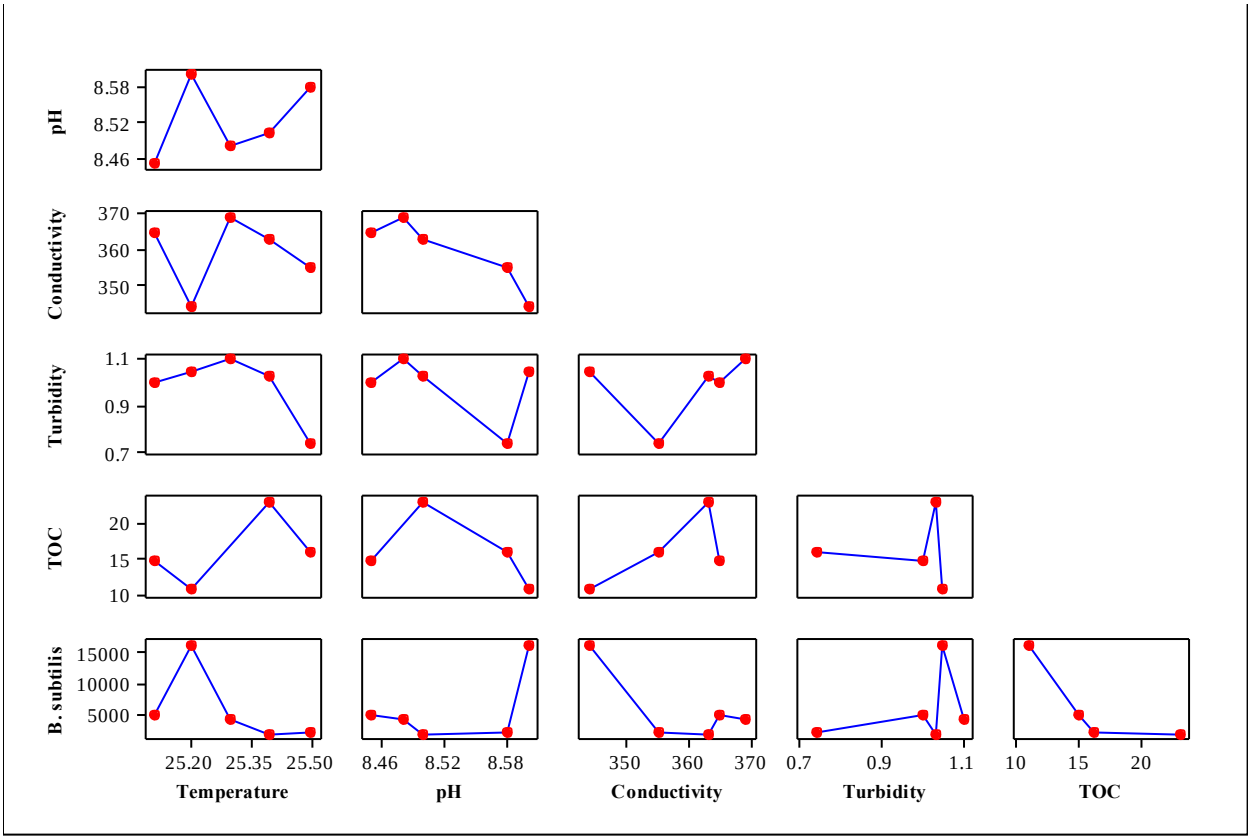

Figure 87 Matrix plot of P2 at Day 3 of SEED unit.

Table 37 Pearson correlation and P-values for P2 at Day 3 of SEED unit.

	Temperature	pH	Conductivity	Turbidity	TOC
pH	0.379				
	0.529				
Conductivity	-0.007	**-0.91**			
	0.991	**0.032**			
Turbidity	**-0.615**	-0.437	0.255		
	0.269	0.462	0.679		
TOC	**0.53**	-0.45	**0.689**	-0.01	
	0.47	0.55	**0.311**	0.99	
B. subtilis	**-0.551**	**0.522**	**-0.755**	0.367	**-0.781**
	0.335	**0.367**	**0.14**	0.543	**0.219**

Correlations were found between almost all parameters except for pH and temperature and pH and TOC of P3 at Day 1. These relations were suggested by the matrix plot (Figure 88) and were proved by the Pearson correlation coefficients and P-values (Table 38). Further, *B. subtilis* was highly correlated to conductivity (negative relation, Pearson correlation = -0.866), turbidity (negative relation, Pearson correlation = -0.983), and TOC (positive relation, Pearson correlation = 0.917). These statistical coefficients also indicated that *B. subtilis* might be related to temperature (positive relation, Pearson correlation = 0.552) and to pH (negatively, Pearson correlation = -0.543). In terms of physicochemical parameters, TOC was highly correlated to temperature (positively, 0.913), conductivity (negatively, Pearson correlation = -0.91) and to turbidity (negative relation, Pearson correlation = -0.935). Moreover, turbidity was highly positively related to conductivity (Pearson correlation = 0.94) and might be negatively related to temperature and pH with Pearson correlation coefficients of -0.655 and 0.634 respectively. Lastly, conductivity was highly positively related to pH (Pearson correlation = 0.82) and might be negatively related to temperature (Pearson correlation = -0.69). However, P-values were greater than 0.05 except for the relation between *B. subtilis* and turbidity (0.017).

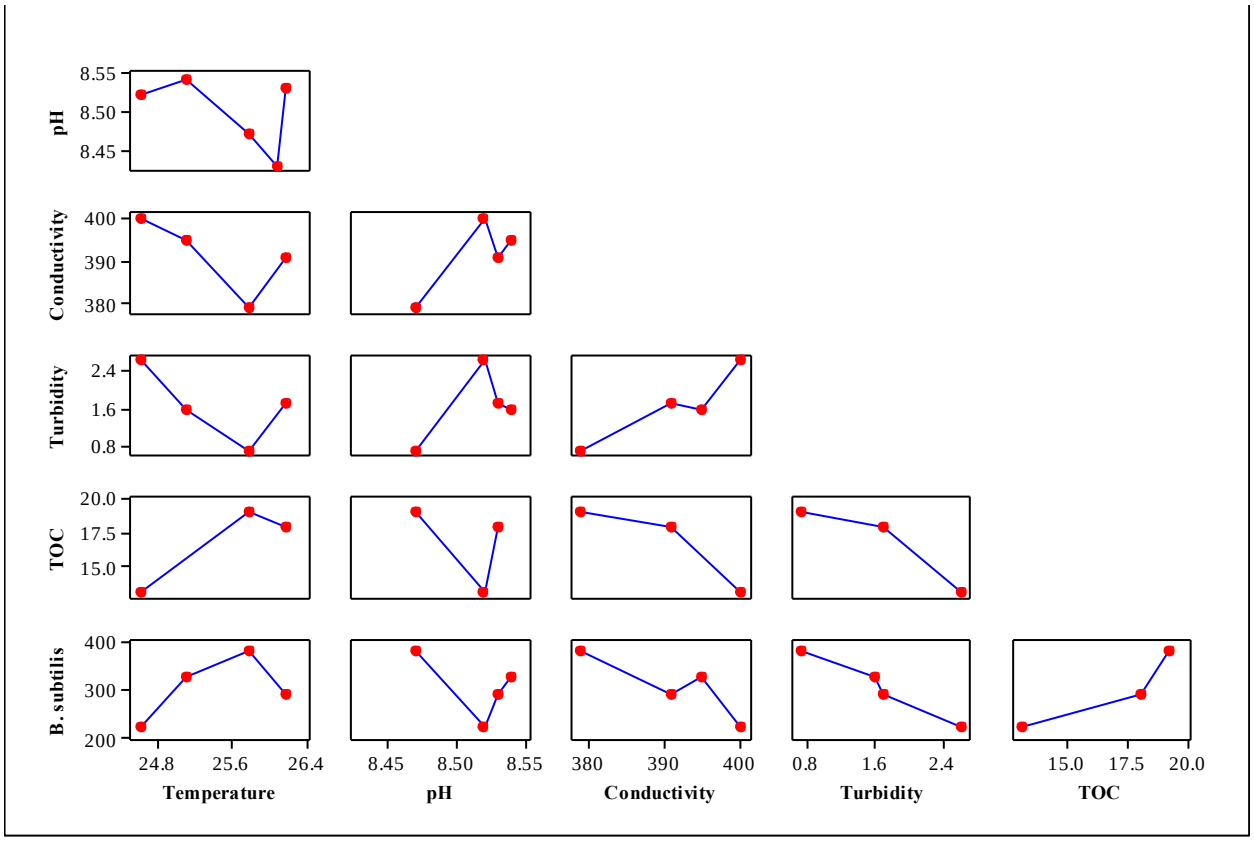

Figure 88 Matrix plot of P3 at Day 1 of SEED unit.

Table 38 Pearson correlation and P-values for P3 at Day 1 of SEED unit.

	Temperature	pH	Conductivity	Turbidity	TOC
pH	-0.495				
	0.397				
Conductivity	**-0.69**	**0.82**			
	0.31	**0.18**			
Turbidity	**-0.655**	**0.634**	**0.94**		
	0.345	**0.366**	**0.06**		
TOC	**0.913**	-0.19	**-0.91**	**-0.935**	
	0.268	0.653	**0.272**	**0.232**	
B. subtilis	**0.552**	**-0.543**	**-0.866**	**-0.983**	**0.917**
	0.448	**0.457**	**0.134**	**0.017**	**0.261**

The statistical analysis of P3 at Day 2 showed relation among pH and temperature, TOC and temperature, pH and conductivity, conductivity and TOC, turbidity and TOC, turbidity and *B. subtilis*, TOC and *B. subtilis* (Figure 89 and Table 39). The correlations found were positive, except for conductivity and TOC. Although Pearson correlations were high (> 0.7 for must of the above mentioned relations) and > 0.5 for others, P-values were > 0.05 for all of the correlations found, which indicated weak evidence of the relations.

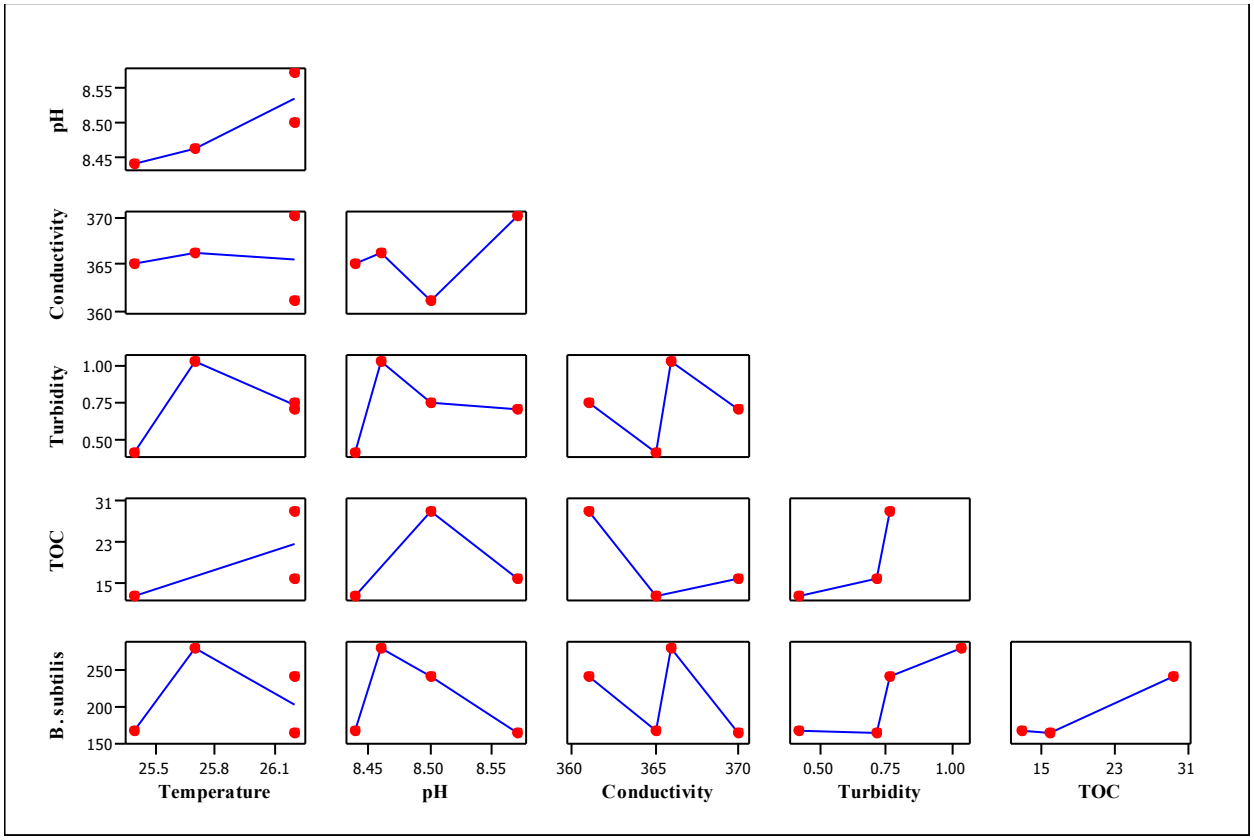

Figure 89 Matrix plot of P3 at Day 2 of SEED unit.

Table 39 Pearson correlation and P-values for P3 at Day 2 of SEED unit.

	Temperature	pH	Conductivity	Turbidity	TOC
pH	**0.857**				
	0.143				
Conductivity	0.034	**0.511**			
	0.966	**0.489**			
Turbidity	0.331	0.121	0.029		
	0.669	0.879	0.971		
TOC	**0.647**	0.136	**-0.719**	**0.745**	
	0.552	0.913	**0.489**	**0.465**	
B. subtilis	0.059	-0.333	-0.459	**0.847**	**0.979**
	0.941	0.667	0.541	**0.153**	**0.129**

In the case of the last samples assessed (P3 at Day 3), the matrix plot in Figure 90 implied correlations among pH and conductivity, conductivity and turbidity, turbidity and pH, TOC and conductivity, TOC and turbidity, TOC and pH and *B. subtilis* and temperature. The Pearson correlation coefficients (Table 40) proved that pH was highly negatively related to conductivity with a value of -0.847. However, P-value of such relation was > 0.05 (0.153) and thus indicated weak evidence. Additionally, conductivity was highly positively related to turbidity with a Pearson correlation coefficient of 0.829. Furthermore, turbidity might be negatively related to pH, having a Pearson correlation coefficient of -0.549. In terms of TOC, this parameter was highly positively related to conductivity, turbidity and might be negatively related to pH with a respective Pearson correlation coefficient of 0.977, 0.952 and -0.669, respectively. Finally, *B. subtilis* was highly negatively related to temperature with a Pearson correlation coefficient of -0.996 and P-value of 0.004. The P-values in all correlations found were higher than 0.05 (except for *B. subtilis* and temperature), and thus indicated weak evidence of the correlations.

No similar trends were found between parameters through the three days. However, other trends were found during Day 1 and 2. Such relations were the positive relations between TOC

and conductivity, conductivity and pH and the negative relations between and conductivity and between *B. subtilis* and conductivity. Through Day 2 and 3, one trend was found: the highly positive relation between TOC and turbidity. Likewise, through Day 1 and 3 the only trend found was the positive relation between turbidity and conductivity.

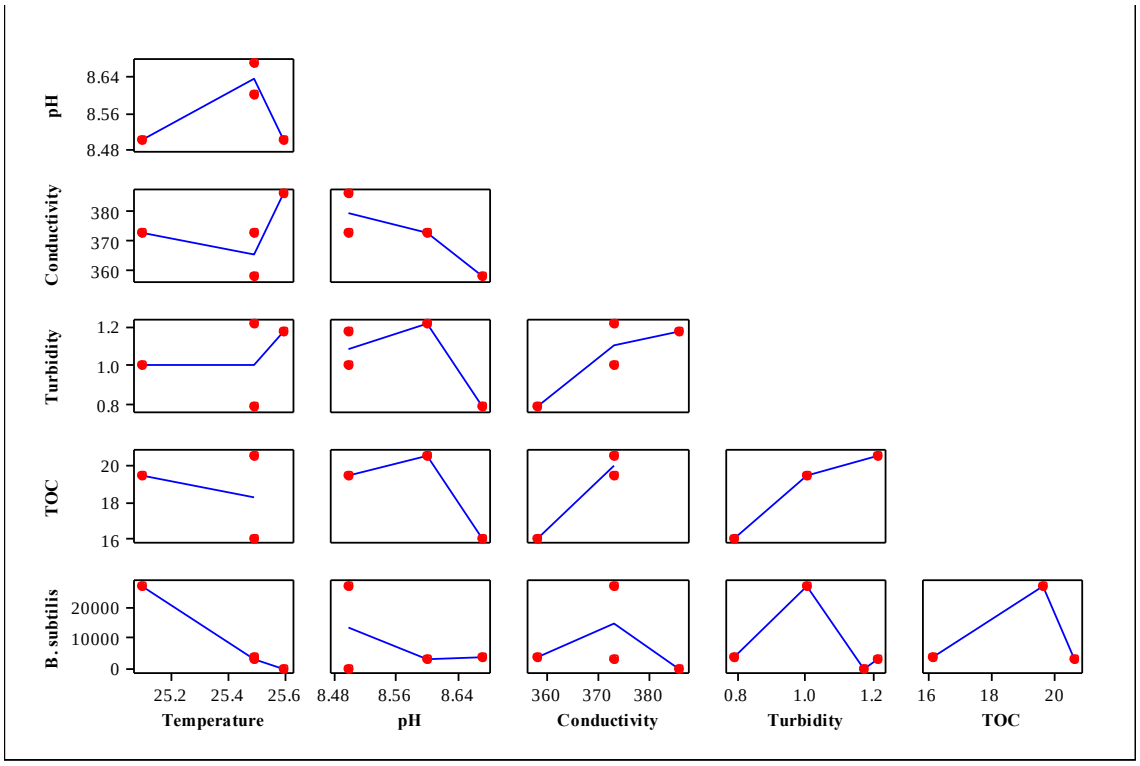

Figure 90 Matrix plot of P3 at Day 3 of SEED unit.

Table 40 Pearson correlation and P-values for P3 at Day 3 of SEED unit.

	Temperature	pH	Conductivity	Turbidity	TOC
pH	0.367				
	0.633				
Conductivity	0.151	**-0.847**			
	0.849	**0.153**			
Turbidity	0.234	**-0.549**	**0.829**		
	0.766	**0.451**	**0.171**		
TOC	-0.305	**-0.669**	**0.977**	**0.952**	
	0.802	**0.534**	**0.136**	**0.198**	
B. subtilis	**-0.996**	-0.44	-0.081	-0.21	0.291
	0.004	0.56	0.919	0.79	0.812

As discussed previously, the Pearson correlation coefficients and P-values were calculated for each parameter, port and day using the Minitab. It was expected to find similar trends between the three different combinations of drums since they were constructed with the same hydromechanical properties. Therefore, the three drums had analogous hydraulic properties. However, a clear relationship between parameters could not be identified since none of the combinations perceived the same relation during the three days.

4.4.2 SEED Unit

The percent removal of *B. subtilis* was calculated to assess the performance of the SEED unit. Each phase, i.e. filtration and chlorination, and treatment train for each day of experiment were assessed in this study. *B. subtilis* removal by filtration varied significantly through the three experiments with ranges of -140% to 24%, -95% to -167% and -1,463% to -6,394% at Day 1, 2 and 3, respectively (Figure 91). It was expected that ranges in removal were similar due to the same hydraulic properties of the drums. Even though ranges were not similar, yet they showed low or no removal. In contrast to this study, Swertfeger (1999) demonstrated a 2.4-log removal of endospores, >4-log removal of *Giardia* and a >2.5-log removal of *Cryptosporidium* using sand filters. Although both studies were performed using a rapid filtration, Swertfeger's studies were performed with influent water already treated with coagulation, flocculation and sedimentation (Swertfeger et al., 1999), whereas our study used influent water from the effluent of the gravel prefilter. However, initial turbidity measurements at both studies were approximately the same (≤2 NTU). Likewise, both studies were challenged with more than one microorganism and hence competition between them inside the filters was not seemed to cause the abrupt difference in filter effectiveness. Yet one major difference was found, which consisted

in filter's depth. Swertferger's filters were 10 ft long while our study used ~3 ft long filters. Configuration of drums in our study (filters were in series) was designed to overcome this issue but apparently more contact time was indispensable for a better performance of the filters.

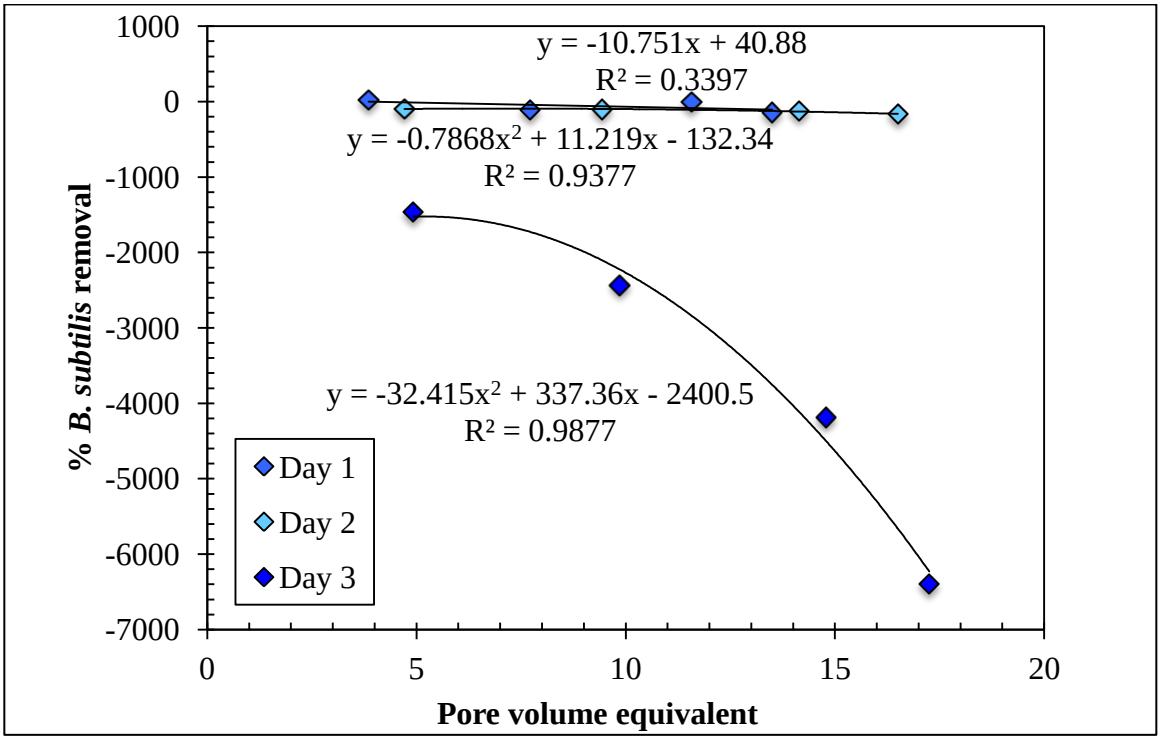

Figure 91 *B. subtilis* percent removal by filtration in the SEED unit.

Moreover, SEED unit was initially assembled in January 2008 (Figure 92). Due to lack of maintenance, the unit got corroded and nonfunctional (Figure 93). Hence, it was decided to replace the metal drums to polyethylene open head drums. Replacement was performed by taking out the sand from the metal drums, washed by hand the sand and lines (which were full of debris), transferred the full amount of sand to the new drums and assembled the equipment with the same previous configuration (Figure 94 and Figure 95). Even though sand was carefully washed, still one of the drums (B) seemed not being completely clean. However, during the SEED unit demonstration, the actual treatment system of the Río Piedras community was dealing

with a problem that did not allow the residents to have the normal quantity of water and kept the community with a water rationing. Therefore, a backwash could not be performed during the tests of this study. The lack of a backwash was detrimental for the assessment of the unit, which yielded non-favorable results, especially at Day 2 and 3 were drums combinations included drum B.

Figure 92 SEED unit in 2008.

Figure 93 SEED unit in 2012.

Figure 94 SEED unit replacement process.

Figure 95 SEED unit in 2014.

A similar trend was achieved during the three days in the second phase of the treatment train, chlorination. The trend behaved as a polynomial of second degree (Figure 96). During the first two days, chlorination inactivated *B. subtilis* in the same range (-3% to 36 % *B. subtilis* removal). In contrast, at Day 3 removal trend varied significantly through treated water volume with a lowest *B. subtilis* removal of -440 % at ~480 mL of treated water volumes. The other samples also achieved negative removals except at 414 mL treated water volume that reached 95% removal. Difference in removals might be due to different contact of water with the chlorine tablet since no constant chlorine concentration was achieved. However, Rice et al. (1996) demonstrated a 2-log reduction of aerobic spores of *Bacillus* genre after 65 minutes and CT of

114 mg-min/L and 3-log after 180 minutes and CT of 315 mg-min/L. The chlorination technique used in Rice study was different from our study and hence, difference in removals could have been expected.

Residual free Cl_2 through the three experiments showed a second polynomial degree trend (Figure 97). At Day 1, 2 and 3, residual free chorine concentration decreased, having its minimum of 1.75 mg/L at 270 gal, 0.4 mg/L at 395 gal and 0.2 mg/L at 300 gal of treated water volume, respectively, and then increased. It is important to recall that during testing, chlorine tablets in some instances were in more contact with water than in other samples. This was the reason of the high initial concentration (>4 mg/L) at Day 1 and 2 and of increased residual free chlorine concentration in some samples. Moreover, final concentrations measured, i.e. 3.35, 3.7 and 3 mg/L at Day 1, 2 and 3 respectively were within the WHO Guideline of Drinking Water Quality (>0.5mg/L) (WHO, 2011) and the USEPA MRDL (4 mg/L) (US EPA, 2009).

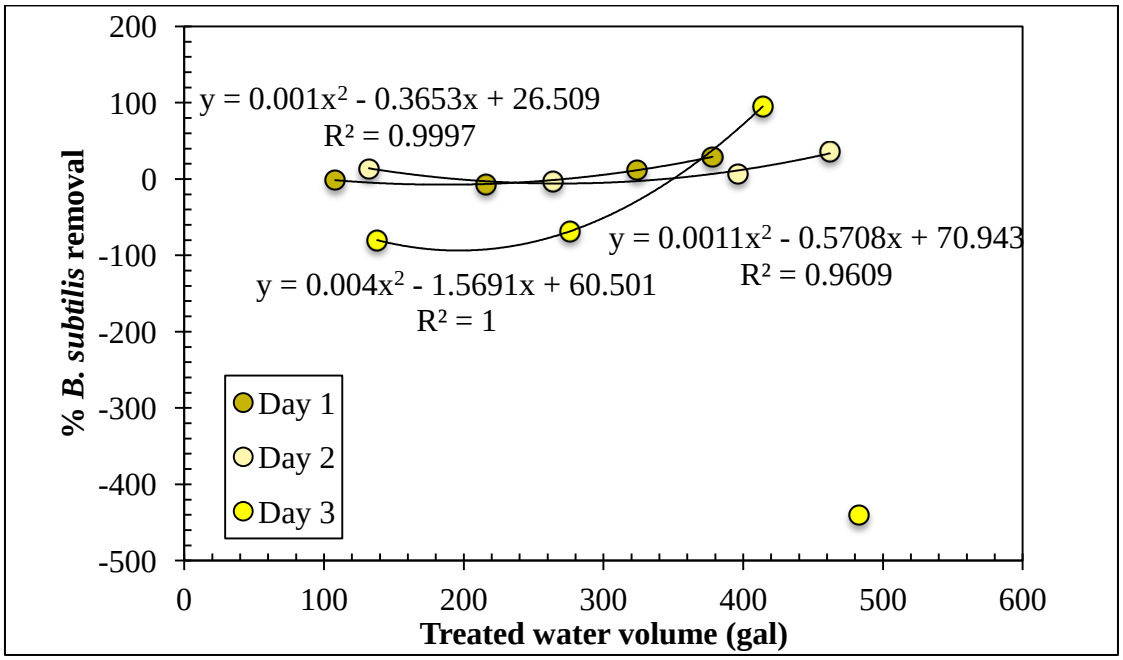

Figure 96 *B. subtilis* removal by disinfection in the SEED unit.

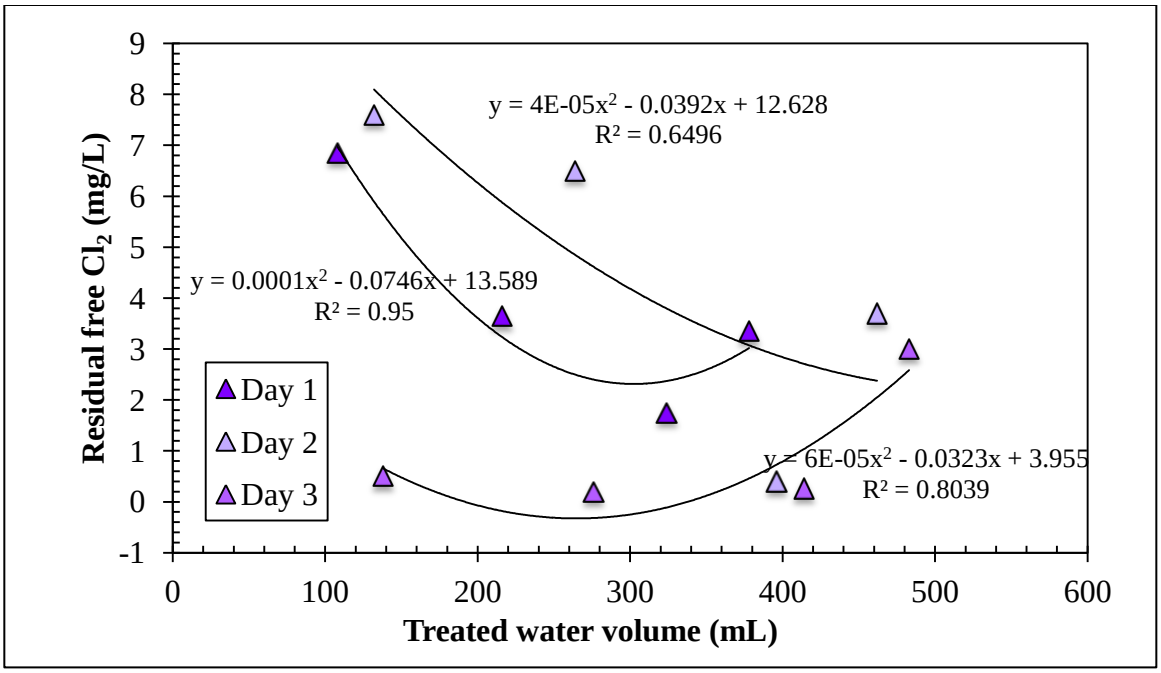

Figure 97 Residual free Cl_2 from field-scale system at Day 1, 2 and 3.

Treatment train assessment of the SEED unit efficiency results and percent removals by phase are presented in Figure 98 and Figure 99. Outcomes showed that the SEED unit in this configuration was not efficient for *B. subtilis* removal, since only very low removals were achieved and only a maximum of 23 % removal (0.11 log removal) was reached. Hence, assessment of the SEED unit, in this configuration, for the efficiency in removal and inactivation of *B. subtilis* did not serve for the prediction of occurrence of *Giardia* and *Cryptosporidium*, contrary to the suggestions of the study of Nieminski et al. (2000). Furthermore, these results showed no compliance with the SWTR. Moreover, several studies have proved the critically use of chemical pretreatment such as coagulants since serve as a multiple barrier and presented high log removals (Harrington et al., 2003; Al-Ani et al., 1986; Mosher et al., 1986; Logsdon et al., 1985). Therefore, the lack use of chemical coagulants as part of the unit treatment could have been detrimental for a better efficiency of the system.

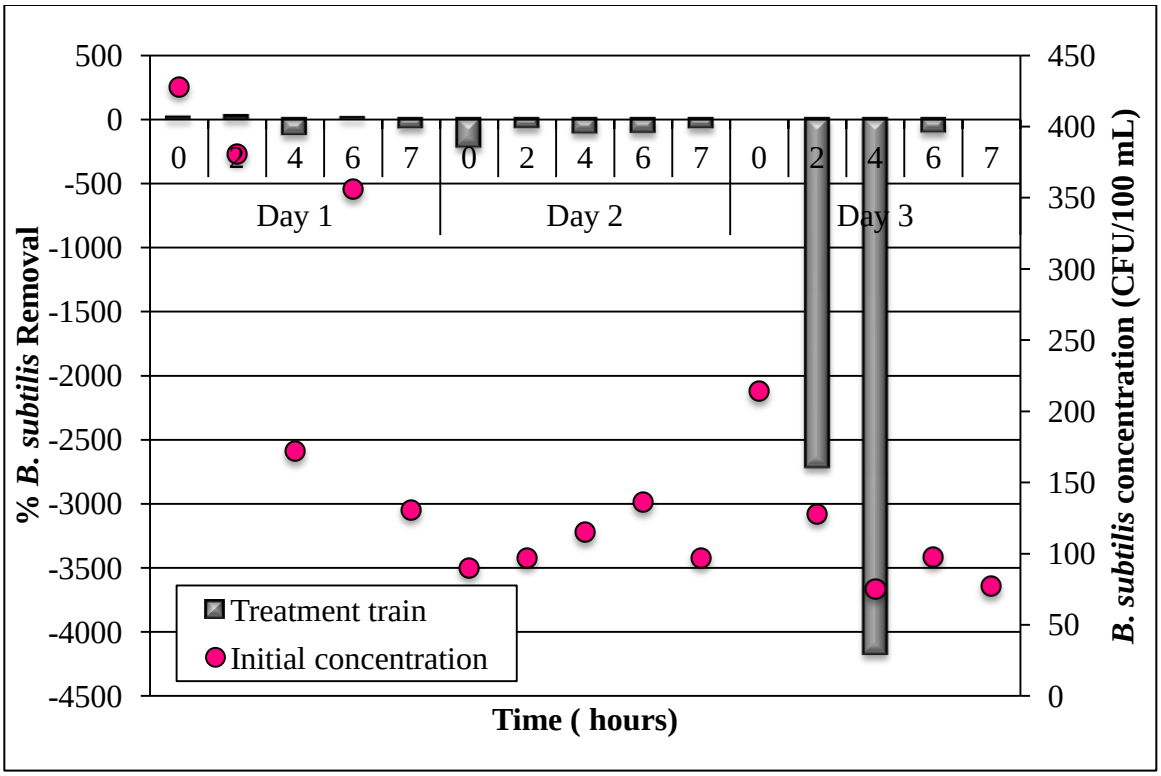

Figure 98 *B. subtilis* percent removal and initial concentration of treatment train (SEED unit).

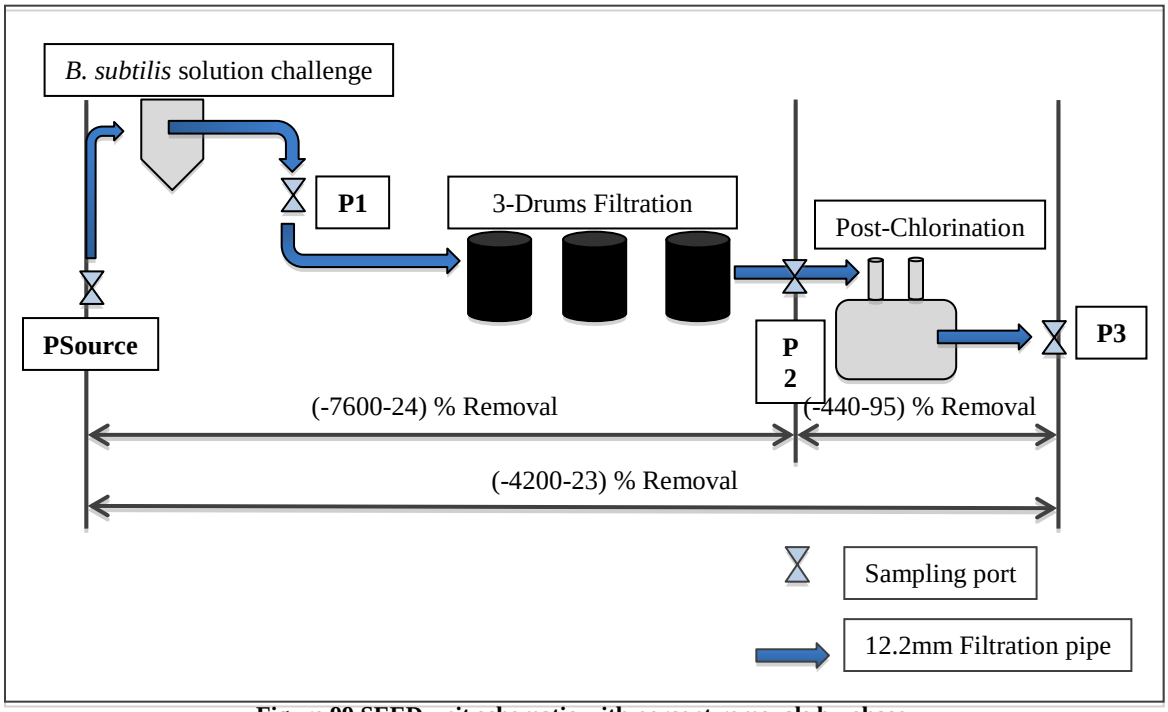

Figure 99 SEED unit schematic with percent removals by phase.

5. CONCLUSIONS AND RECOMMENDATIONS

Lab-scale and field-scale experiments were performed to evaluate the efficiency of the SEED unit in removing and inactivating *B. subtilis*. The following conclusions can be made based on the results of the lab-scale study:

- To improve performance of the filters, a better diffuser is vital.
- The filters needed to run at 60 mL/min achieving a maximum removal of 93.6% (1.2 log removal) at less than 10 pore volumes equivalent to behavior similar to field system.
- Individual assessment of filtration yielded a maximum removal of 1.5-log indicating the need for other pre- or post- treatments to comply with the requirements of *Giardia* (3-log) and *Cryptosporidium* (2-log) inactivation.
- To achieve a 3-log removal only by disinfection with the hydraulic properties of the disinfection basin, a residual chlorine concentration of 0.000262 mg/L could be remained and hence would not provide a mechanism for microbial control in the distribution system. Individual assessment of the disinfection basin inactivated 1.5-log of *B. subtilis*.
- The treatment train achieved a maximum of 3-log removal of *B. subtilis* implying that the system might effectively comply with the 2-log inactivation of *Cryptosporidium* and with the 3-log inactivation of *Giardia*.

From the results of the field-scale experiments with the SEED unit, the following conclusions were derived:

- Specific trends between physicochemical and bacteriological parameters were not found within the ports during the three days of experimentation with the SEED unit.

- Only at Day 1, SEED unit achieved 24% of removal by filtration and 35% by chlorination. Negative removals were obtained by filtration and chlorination during Day 2 and 3. Hence, the lack of a backwash of the SEED unit was detrimental for the system performance.
- No constant chlorine could be maintained using a tablet chlorinator during Days 1 and 2 of experimentation. Therefore, residual chlorine concentrations were greater than 4 mg/L Cl_2 at the initial samples.

Therefore, results showed that SEED unit in its actual configuration would not fully inactive *B. subtilis* in the removals specified by the standards of the USEPA for the removal of *Giardia* and *Cryptosporidium*.

Water quality of Caín Alto river water was monitored for one year and 4 months to determine its physicochemical and bacteriological characteristics. Fluctuations of measurements were expected especially during winter and summer. Furthermore, statistical analysis showed positive correlation between conductivity and TDS with a Pearson correlation of 0.953. Likewise, *B. subtilis* was positively correlated with turbidity (Pearson correlation of 0.720). Contrary, *B. subtilis* was negatively correlated with conductivity exhibiting a Pearson correlation of -0.556.

Further studies are needed in the following areas:

- Use the SEED unit connecting the three drums in series in order to increase the contact time of the bacteria through the filter media.
- Construct a hydraulic pump in the field to inject liquid chlorine instead of using a tablet chlorine to maintain a constant concentration.
- Evaluate the possible use of coagulants prior filtration.

- Assess the effect and recurrence of backwash on filter performance.

REFERENCES

Al-Ani, M.Y., Hendricks, D.W., Logsdon, G.S., Hibler, C.P. (1986). Removing *Giardia* cysts from low turbidity water by rapid rate filtration. Journal of the American Water Works Association 78, 66-73.

Aslan, S., Cakici, H. (2007). Biological denitrification of drinking water in a slow sand filter. Journal of Hazardous Materials 148, 253-258.

Barbeau, B., Boulos, L., Desjardins, R., Coallier, J., Prévost, M. (1999). Examining the use of aerobic spore-forming bacteria to assess the efficiency of chlorination. Water Research 33, 2941-2948.

Bradley, I., Straub, A., Maraccini, P., Markazi, S., Nguyen, T.H. (2011). Iron oxide amended biosand filters for virus removal. Water Research 45, 4501-4510.

Carcano, S. (2010). A model for cell growth in batch bioreactors. MS Thesis, Politecnico di Milano, Italy.

Centers for Disease Control (2012). Prevalence and trends data Puerto Rico Health status, 2012. Available at http://apps.nccd.cdc.gov/brfss/display.asp?cat=HS&yr=2012&qkey=8011&state=PR.

Chen, G., Driks, A., Tawfiq, K., Mallozzi, M., Patil, S. (2010). *Bacillus anthracis* and *Bacillus subtilis* spore surface properties and transport. Colloids and Surfaces B: Biointerfaces 76, 512-518.

Cho, M., Gandhi, V., Hwang, T., Lee, S., Kim, J. (2011). Investigating synergism during sequential inactivation of MS-2 phage and *Bacillus subtilis* spores with UV/H_2O_2 followed by free chlorine. Water Research 45, 1063-1070.

Cho, M., Kim, J., Yoon, J. (2006). Investigating synergism during inactivation of *Bacillus subtilis* spores with several disinfectants. Water Research 40, 2911-2920.

Cleary, S.A. (2005). Sustainable drinking water treatment for small communities using multistage slow sand filtration. MS Thesis, University of Waterloo, Canada.

Concepción, D., Falcón, J., Hwang, S., Sinha, R., Impelliteri, C. (2010). "Field testing of a small water purification system for non-PRASA communities", Proceedings of 2010 World Environmental & Water Resources Congress, Providence, RI, May 16-20, 2010.

Diao, M., Yao, M. (2009). Use of zero-valent iron nanoparticles in inactivating microbes. Water Research 43, 5243-5251.

Dow, S.M., Barbeau, B., von Gunten, U., Chandrakanth, M., Amy, G., Hernandez, M. (2006). The impact of selected water quality parameters on the inactivation of *Bacillus subtilis* spores by monochloramine and ozone. Water Research 40, 373-382.

Driks, A. (1999). *Bacillus subtilis* spore coat. Microbiology and Molecular Biology Reviews 63, 1-20.

Edzwal, J.K, Tobiason, J.E., Parento, L.M., Kelley, M.B., Gary, S., Dunn, H. J., Galant, P.B. (2000). *Giardia* and *Cryptosporidium* removals by clarification and filtration under challenge conditions. Journal of the American Water Works Association 92, 70-84.

Facile, N., Barbeau, B., Prévost, M., Koudjonou, B. (2000). Evaluating bacterial aerobic spores as a surrogate for *Giardia* and *Cryptosporidium* inactivation by ozone. Water Research 34, 3238-3246.

Fogler, H. S. (2006). Elements of Chemical Reaction Engineering. 4th edition. Prentice Hall.

Hamidin, N., Yu, Q.J., Connell, D.W. (2008). Human health risk assessment of chlorinated disinfection by-products in drinking water using probabilistic approach. Water Research 42, 3263-3274.

Han, S., Fitzpatrick, C.S.B., Wetherill, A. (2009). The impact of flow surges on rapid gravity filtration. Water Research 43, 1171-1178.

Harrington, G.W., Xagoraraki, I., Assavasilavasukul, P., Standridge, J.H. (2003). Effect of filtration conditions on removal of emerging water-borne pathogens. Journal of the American Water Works Association 95, 95-104.

Hecker, M., Rder, A., Fuchs, S., Pagels, M., Engelmann, S. (2009). Physiological proteomics and stress/starvation responses in *Bacillus subtilis* and *Staphylococcus aureus*. Research in Microbiology 160, 245-258.

Herrera, M. (2009). Development of a decision support tool to ensure safe drinking water in non-PRASA communities in Puerto Rico. MS Thesis, University of Puerto Rico at Mayaguez, PR.

Hijnen, W.A.M., Suylen, G.M.H., Bahlman, J.A., Brouwer-Hanzans, A., Medema, G.J. (2010). GAC adsorption filters as barriers for viruses, bacteria and protozoan (oo)cysts in water treatment. Water Research 44, 1224-1234.

Höper, D., Bernhardt J., Hecker, M. (2006). Salt stress adaptation of *Bacillus subtilis*: A physiological proteomics approach. Proteomics 6, 1550-1562.

Jarroll, E.L, Bingham, A.K., Meyer, E.A. (1981) Effect of chlorine on *Giardia lamblia* cyst viability. Applied and Environmental Microbiology 41, 483-487.

Jegatheesan, V., Kim, S.H., Joo, C.K., Baoyu, G. (2009). Evaluating the effects of granular and membrane filtrations on chlorine demand in drinking water. Journal of Environmental Sciences 21, 23-29.

Krasner, S.W., Weinberg, H.S., Richardson, S.D., Pastor, S.J., Chinn, R., Sclimenti, M.J., Onstad, G.D., Thruston, A.D. (2006). Occurrence of a new generation of disinfection byproducts. Environmental Science & Technology 40, 7175-7185.

Larson, M.A., Marinas, B.J. (2003). Inactivation of *Bacillus subtilis* spores with ozone and monochloramine. Water Research 37, 833-844.

Law, S.P., Melvin, M.M.A.L., Lamb, A.J. (2001). Visualization of the establishment of a heterotrophic biofilm within the schmutzdecke of a slow sand filter using scanning electron microscopy. Biofilm Journal 6. Online Journal: http://www.bioline.org.br/bf.

Len, S.V., hung, Y.C., Chung, D., Anderson, J.L., Erickson, M.C., Morita, K. (2002). Effects of storage conditions and pH on chlorine loss in electrolyzed oxidizing (EO) water. Journal of Agricultural and Food Chemistry 50, 209-212.

Liu, D., Teng, Z., Sansalone, J.J., Cartledge, F.K. (2001). Surface characteristics of sorptive-filtration storm water media. I: Low-density (ρ_s<1.0) oxide-coated buoyant media. Journal of Environmental Engineering 127, 868-878.

Logsdon, G.S., Thurman, V.C., Frindt, E.S., Stoecker, J.G. (1985). Evaluating sedimentation and various filter media for removal of Giardia cysts. Journal of the American Water Works Association 77, 61-66.

Mazoua, S., Chauveheid, E. (2005). Aerobic spore-forming bacteria for assessing quality of drinking water produced from surface water. Water Research 39, 5186-5198.

Mosher, R.R., Hendricks, D.W (1986). Rapid rate filtration of low turbidity water using field-scale pilot plant filters. Journal of the American Water Works Association 78, 42-51.

Muhammad, N., Sinha, R., Krishnan, E.R., Piao, H., Patterson, C.L., Cotruvo, J., Cumberland, S.L., Nero, V.P., Delandria, C. (2008). Evaluating surrogates for Cryptosporidium removal in point-of-use systems. Journal of American Water Works Association 100, 98-107.

Nakamura, L.K. (1989). Taxonomic relationship of black-pigmented *Bacillus subtilis* strains and a proposal for *Bacillus atrophaeus* sp. nov. International Journal of Systematic Bacteriology 39, 296-300.

National Archives and Records Administration (2011). Title 40 Protections of Environment Parts 136 to 149. Office of Federal Register.

Nieminski, E.C., Bellamy, W.D., Moss, L.R. (2000). Using surrogates to improve plant performance. Journal of the American Water Works Association 92, 67-78.

Nieto, J.I. (2012). Virus Inactivation by Homogeneous and Heterogeneous Fenton-like Processes. Sc D Thesis, École Polytechnique Fédérale de Lausanne, Switzerland.

Nuzzo, J. (2006). The biological threat to U.S. water supplies: Toward a national water security policy. Biosecurity and Bioterrorism: Biodefense Strategy, Practice, and Science 4, 147-159.

Pecson, B.M., Decrey, L., Kohn, T. (2012). Photoinactivation of virus on iron-oxide coated sand: Enhancing inactivation in sunlit waters. Water Research 46, 1763-1770.

Rennecker, J.L., Mariñas, B.J., Owens, J.H., Rice, E.W. (1999). Inactivation of *Cryptosporidium parvum* oocysts with ozone. Water Research 33, 2481-2488.

Reynolds, T.D., Richards, P.A. (1996) Unit Operations and Processes in Environmental Engineering. 2nd Edition. Cengage Learning.

Rice, E.W., Fox, K.R., Miltner, R.J., Lytle, D.A., Johnson, C.H. (1996). Evaluating plant performance with endospores. Journal of the American Water Works Association 88, 122-130.

Richardson, S.D., Plewa, M.J., Wagner, E.D., Schoeny, R., DeMarini, D.M. (2007). Occurrence, genotoxicity, and carcinogenicity of regulated and emerging disinfection by-products in drinking water: A review and roadmap for research. Reviews in Mutation Research 636, 178-242.

Setlow, P. (2006). Spores of *Bacillus subtilis*: their resistance to and killing by radiation, heat and chemicals. Journal of Applied Microbiology 101, 514-525.

Shi, C., Wei, J., Jin, Y., Kniel, K.E., Chiu, P.C. (2012). Removal of viruses and bacteriophages from drinking water using zero-valent iron. Separation and Purification Technology 84, 72-78.

Swertfeger, J., Metz, D.H., DeMarco, J., Braghetta, A., Jacangelo, J. G. (1999). Effect of filter media on cyst and oocyst removal. Journal of the American Water Works Association 91, 90-100.

Tchobanoglous, G., Burton, F.L., Stensel, D. (2003) Wastewater Engineering: Treatment and Reuse/ Metcalf & Eddy, Inc. 4th edition. McGraw-Hill.

Toenniessen, G.H., Johnson, J.D. (1970). Heat shocked *Bacillus subtilis* spores as an indicator of virus disinfection. Journal of the American Water Works Association, 589-593.

Upadhyayula, V.K.K., Deng, S., Smith, G.B., Mitchell, M.C. (2009). Adsorption of *Bacillus subtilis* on single-walled carbon nanotube aggregates, activated carbon and NanoCeram™. Water Research 43, 148-156.

USGS. (2014). USGS 50131990 Rio Guanajibo at Hwy 119 at San German, PR. Available at http://waterdata.usgs.gov/nwis/dv?cb_00060=on&format=gif_default&period=&begin_date=2012-08-01&end_date=2013-12-31&site_no=50131990&referred_module=sw

USEPA. (2009). National Primary Drinking Water Regulations. Retrieved on May 13, 2013, webpage.

USEPA. (2006). 40 CFR Parts 9, 141 and 142, National Primary Drinking Water Regulations: Long Term 2 Enhanced Surface Water Treatment Rule. Federal Register, 71.

USEPA. (1989) 40 CFR Parts 141 and 142, Drinking water; National Primary Water Regulations; filtration, disinfection; turbidity, *Giardia lamblia*, viruses, *Legionella*, and heterotrophic bacteria; Final Rule. Federal Register 54.

Waller, L., Fox, N., Fox, K.F., Fox, A., Price, R.L. (2004). Ruthenium red staining for ultrastructural visualization of a glycoprotein layer surrounding the spore of *Bacillus anthracis* and *Bacillus subtilis*. Journal of Microbial Methods 58, 23-30.

Westphal, A. J., Price, P. B., Leighton, T. J., Wheeler, K. E. (2002). Kinetics of size changes of individual *Bacillus thuringiensis* spores in response to changes in relative humidity. Proceedings of the National Academy of Sciences of the United States of America 100, 3461-3466.

WHO/UNICEF. (2013). Ending Preventable Child Deaths from Pneumonia and Diarrhoea by 2025: The integrated Global Action Plan for Neumonia and Diarrhoea (GAPPD). World Health Organization and United Nations Children's Fund.

WHO. (2011). Guidelines for drinking-water quality. World Health Organization. 4th edition.

Young, S.B., Setlow. P. (2003). Mechanisms of killing of *Bacillus subtilis* spores by hypochlorite and chlorine dioxide. Journal of applied microbiology 95, 54-67.

APPENDIX

A. WATER QUALITY

The Caín Alto river water was monitored for over one year. Table 41 shows the measurements of the parameters. Table 42 shows the historical data of the nearest USGS station.

Table 41 Caín Alto River water quality monitoring.

Date	pH	Conductivity (µS/cm)	Turbidity (NTU)	TDS (ppm)	TOC (mg/L)	Temperature (˚C)	*E. coli*	TC	*B. subtilis*
Aug-12	8.54	265	0.85	156	12.50	27.8	5		
Sep-12	8.56	308	0.51	208	18.05	24.6	6	800	
Sep-12	8.49	333	0.55	236	19.55	24.6	3	180	
Sep-12	8.58	281	0.74	200	2.90	24.4	11	2860	
Oct-12	8.63	276		196		25.2			
Oct-12	8.64	293	0.57	210	1.50	24.7	11		
Oct-12	8.62	247	1.21	175	2.70	25.7	11	1050	
Oct-12	8.69	298	0.79	213	3.50	24.6	16	630	1070
Nov-12	8.71	281	0.69	177	1.10	24.7	19	710	1100
Dec-12	8.74	245	1.11	174	8.25	23.7	31	1320	900
Dec-12	8.72	320	0.68	227	1.65	22.0	1	21	1280
Jan-13	8.66	325	1.23	232	0.85	21.7	1	31	105
Jan-13	8.64	340	0.72	241	0.30	22.4	0	11	110
Mar-13	8.43	361	0.55	259	0.55	23.9	5	240	120
Apr-13	8.43	352	0.40	253	3.35	23.9	0	750	280
Apr-13	8.45	286	0.38	203	2.50	22.6	17	1290	260
Aug-13	8.46	305	1.88	221	15.65	26.0	13	1090	370
Sep-13	8.61	242	1.14	172	1.20	23.8	50	1180	210
Sep-13	8.60	319	0.80	228	1.60	24.5	16	870	220
Oct-13	8.72	323	0.55	229	1.60	24.8	15	420	150
Oct-13	8.72	336	0.60	238	1.70	25.1	12	200	160
Oct-13	8.72	323	0.55	229	1.60	24.8	15	1980	150
Nov-13	8.71	230	2.45	176	2.20	24.1	36	1560	10200
Nov-13	8.72	323	0.55	229	1.60	24.8	15	800	790
Dec-13	8.69	329	0.52	234	1.25	23.4	17	570	770
High	8.74	361	2.45	259	19.55	27.8	50	2860	10200
Low	8.43	230	0.38	156	0.30	21.7	0	11	105
Median	8.64	308	0.68	221	1.68	24.6	13	775	270
Average	8.62	301	0.87	212	4.78	24.3	14	888	1372

Note: *E. coli*, TC and *B. subtilis* are in CFU/100 mL.

Table 42 Historical water quality samples of USGS 50133600 Rio Guanajibo near San German, PR.

Sample Date time	Temperature, ˚C	Turbidity, NTU	Specific conductance, water unf, µS/cm at 25 ˚C	Dissolved oxygen, mg/L	COD, high level, water, unfltrd, mg/L	pH, water, unfltrd, field, standard units	Total coliforms, M-Endo, immed, col/100mL
3/13/00 14:45	25.9	1.3	761	6	10	8.1	
5/16/00 13:15	29.9	0.6	544	7.2	< 10	8.1	
9/8/00 15:20	30	1.5	488	8.1	< 10	8.2	
10/26/00 14:00	28.4	7	442	7	< 10	8.1	
2/5/01 10:40	24	4	680	6.2	< 10	7.9	
5/17/01 15:15	29.5	2.1	615	9	< 10	8	
9/20/01 13:30	25.5		255	8.1	80	7.5	
12/13/01 13:10	25.5		433	7.3	10	7.9	
3/5/02 13:10	27		635	8.2	< 10	7.9	
5/21/02 12:30	27.2		561	9.4	< 10	8	
12/3/02 17:00	28.8		539	7.4	< 10	7.6	
2/6/03 8:15	24.4		588	3.2	10	7.8	7200
4/15/03 15:15	29.4		647	6.2	20	7.8	52000
7/21/03 17:35	30.7		627	7.7	10	8	620
9/4/03 12:30	28		398	5.9	20	7.7	22000
11/18/03 12:00	26.8		515	7.4	10	7.9	38000
3/30/04 14:00	27.8		612	7.8	< 10	7.9	
5/27/04 14:40	29.3		520	7.3	< 10	7.8	5000
8/24/04 8:48	23.6		365	7.4	< 10	7.8	26000
11/17/04 8:40	23.1		514	6.8		7.9	20000
2/10/05 12:20	23.2		633	7.5		7.6	2000
5/10/05 14:15	27.6		403	6.7		8	8000
8/11/05 14:05	30.2		518	6.8		8	6000
11/2/05 11:00	26.3		536	7.1		7.9	460

2/1/06 10:15	23.6	640	5	7.7	763
5/3/06 8:25	25.2	493	6.2	7.9	E 8000
8/22/06 10:45	27.4	555	5.6	7.5	E 800
11/28/06 10:45	25.1	548	6.7	7.8	690
2/6/07 9:30	24.4	649	3.6	7.7	E 8000
5/10/07 10:05	26.8	567	4.7	7.8	E 1010
9/4/07 16:10	28.3	353	6.9	7.9	55000
11/28/07 9:05	23.5	536	6.7	7.8	3300
2/26/08 11:35	25	637	4.2	7.6	6800
5/7/08 8:50	25.1	478	6.8	7.8	5400
8/13/08 9:25	27	549	6.1	7.8	E 1500
11/18/08 16:15	27.4	534	7.8	8.2	3200
3/19/09 10:40	24.8	628	6.1	7.9	800
6/3/09 14:10	28.9	544	7.1	8	E 1100
8/11/09 9:10					
8/11/09 15:10	28.8	384	7.9	8.2	7600
8/11/09 15:11					
10/29/09 12:05	27	457	8.2	8.1	E 1900
2/25/10 12:50	27.5	537	7.5	8.1	2000
5/12/10 16:15	25.7	148	7.4	7.5	200000
9/1/10 8:45	25	345	6.2	7.9	24000
11/16/10 13:45	27.1	599	8.5	7.9	780
2/9/11 9:50	23.9	650	5.9	7.8	E 1500
18-May-11	25.1	521	7	7.9	3900
8/10/11 12:10	28.4	514	7.3	7.9	3600
11/3/11 9:15	24.3	421	7.6	7.9	E 10000
2/2/12 10:15	21.8	590	7.5	7.9	3000
2/2/12 10:15					

5/16/12 12:10	27.9		401	8.3		8.1	64000
8/8/12 14:50	26.9		455	7.2		7.9	20000
High	30.7	7	761	9.4	80	8.2	200000
Low	21.8	0.6	148	3.2	10	7.5	460
Median	26.9	1.8	536	7.1	10	7.9	5000
Average	26.5	2.8	521	6.9	21	7.9	16049

Note: E stands for estimation.

B. IRON LEACHING

Similarly to 3.2.3.1, additional experiments were performed at pH 10 to measure the iron leachate from IOCS. Figure 100 and Figure 101 contain the result of the assessments.

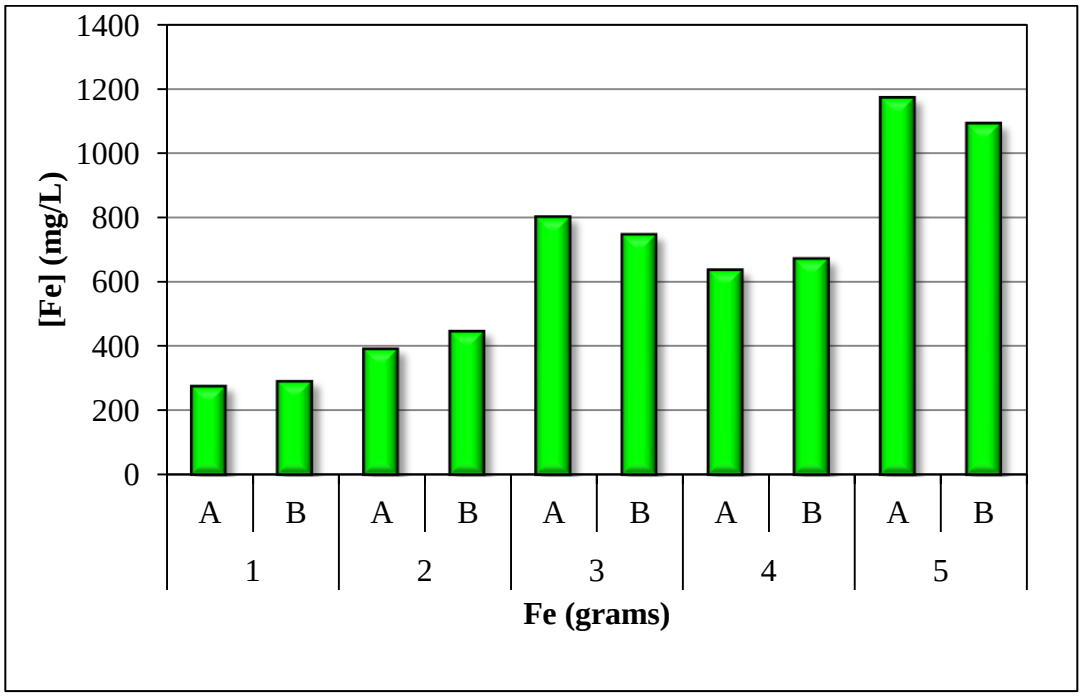

Figure 100 24-hour iron leaching from IOCS at pH 10.

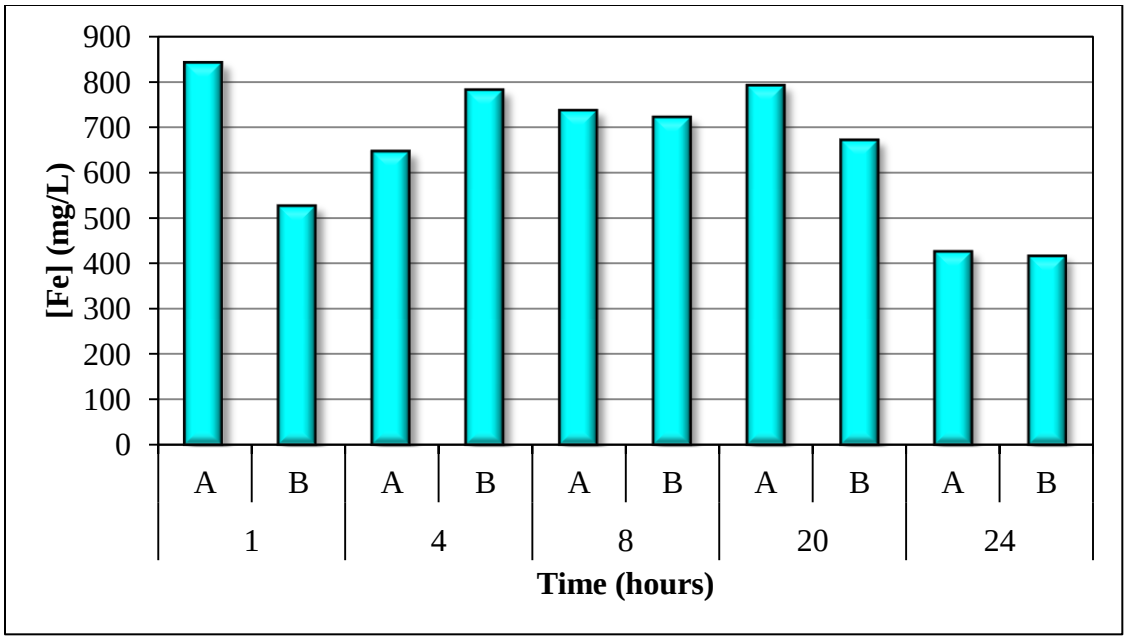

Figure 101 Iron leaching from 3 grams of IOCS at pH 10.

C. *B. SUBTILIS* SPORES

Peculiar images were taken from the experiments discussed in 4.3.4.3. Figure 102 and Figure 103 show the unidentified microorganisms observed after heat treatment at different exposure conditions.

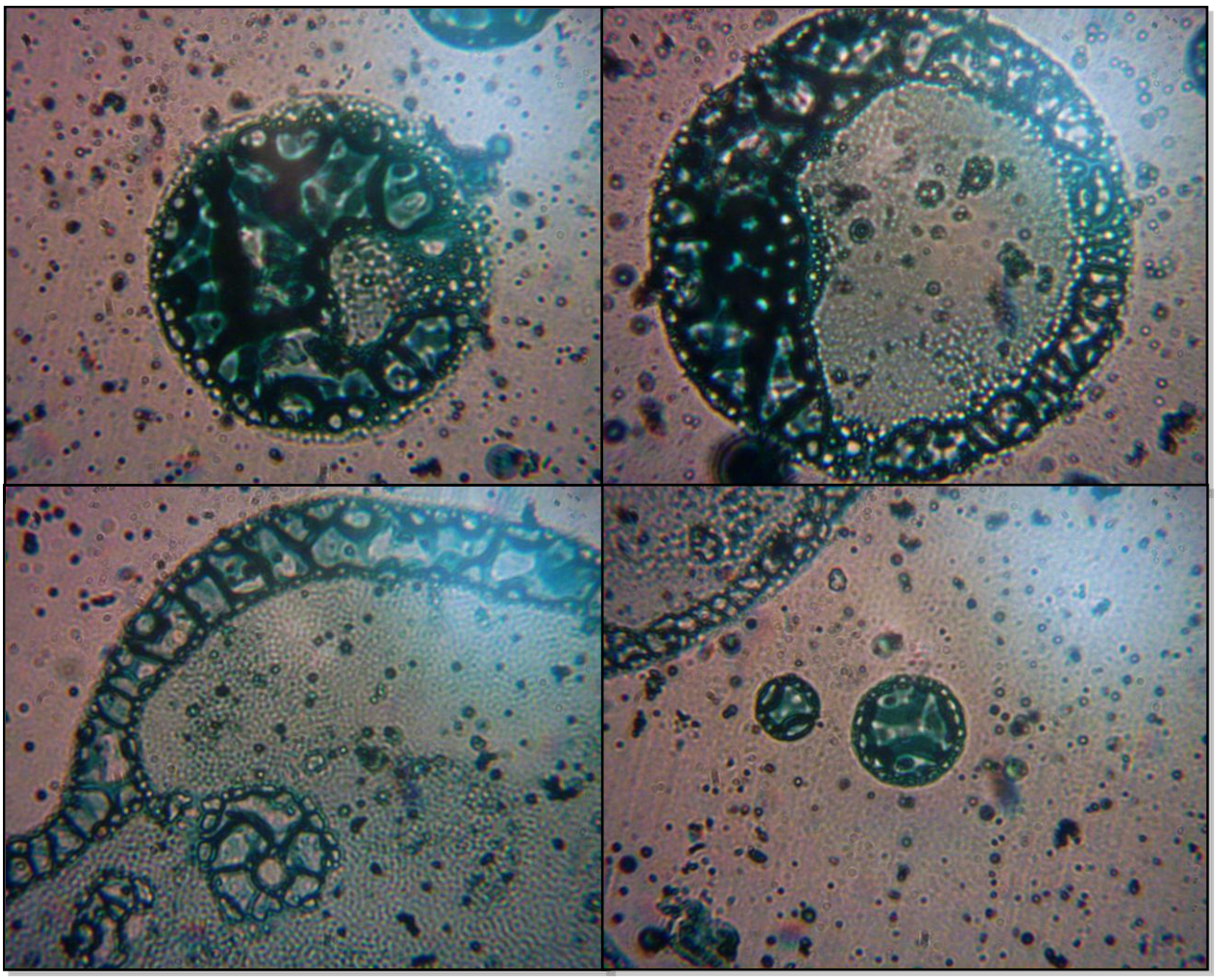

Figure 102 Unidentified microorganisms after 30 minutes contact time of 0 mg/L Cl_2 after heat treatment observed at 100x magnification.

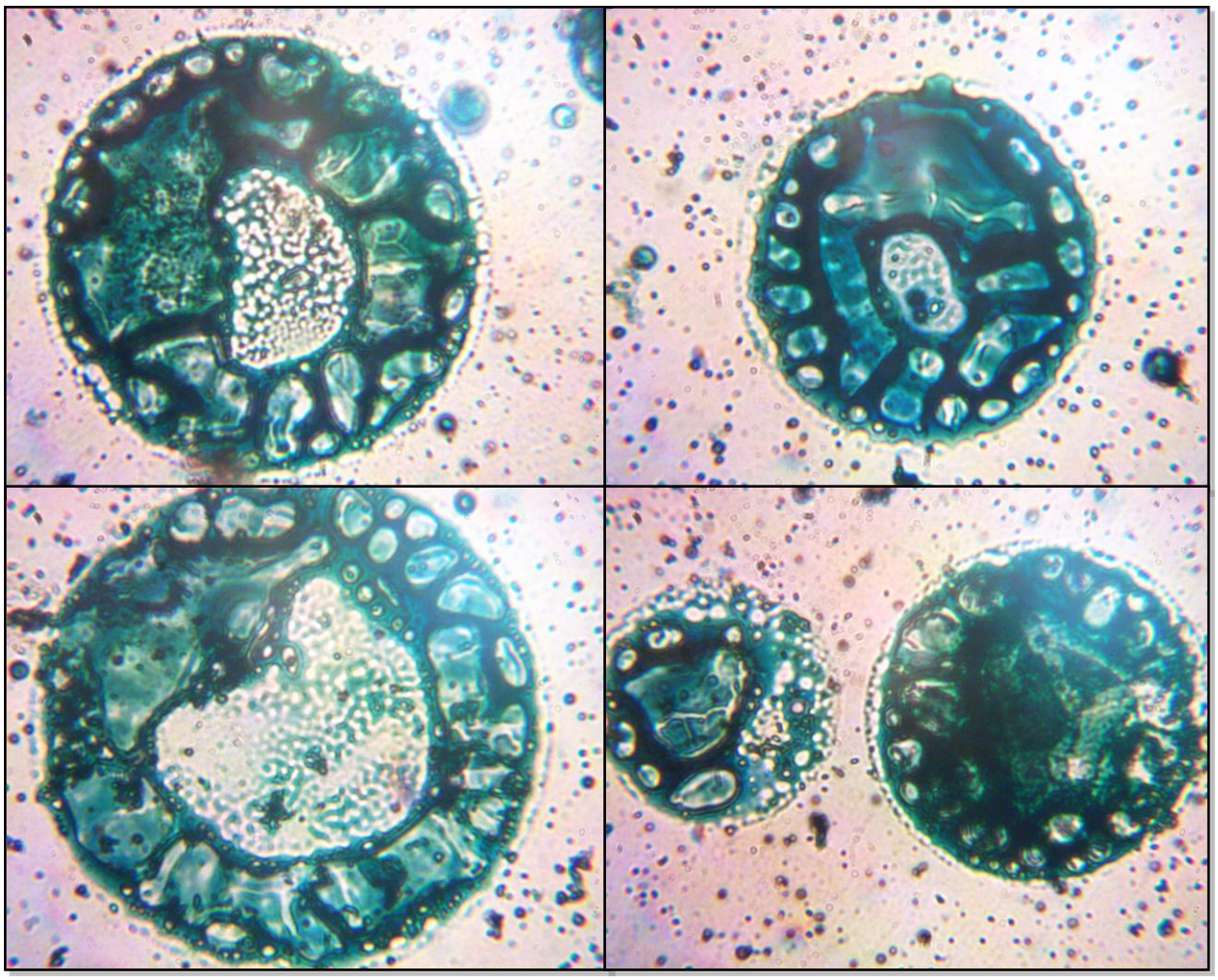

Figure 103 Unidentified microorganisms after 30 minutes contact time of 10 mg/L Cl_2 after heat treatment observed at 100x magnification.